uOttawa

L'Université canadienne
Canada's university

FACULTÉ DES ÉTUDES SUPÉRIEURES ET POSTDOCTORALES

uOttawa

L'Université canadienne
Canada's university

FACULTY OF GRADUATE AND POSTDOCTORAL STUDIES

Julien Brunet
AUTEUR DE LA THÈSE / AUTHOR OF THESIS

M.SC. (Biochemistry)
GRADE / DEGREE

School of Translation and Interpretation
FACULTÉ, ÉCOLE, DÉPARTEMENT / FACULTY, SCHOOL, DEPARTMENT

Signaling Pathways Involved in Connexin43 Expression and Cellular Sub-Localization in Human Astrocytoma

TITRE DE LA THÈSE / TITLE OF THESIS

L. Kleine
DIRECTEUR (DIRECTRICE) DE LA THÈSE / THESIS SUPERVISOR

CO-DIRECTEUR (CO-DIRECTRICE) DE LA THÈSE / THESIS CO-SUPERVISOR

EXAMINATEURS (EXAMINATRICES) DE LA THÈSE / THESIS EXAMINERS

M. Ekker

Z. Yao

Gary W. Slater
Le Doyen de la Faculté des études supérieures et postdoctorales / Dean of the Faculty of Graduate and Postdoctoral Studies

SIGNALING PATHWAYS INVOLVED IN CONNEXIN43 EXPRESSION AND CELLULAR SUB-LOCALIZATION IN HUMAN ASTROCYTOMA

Julien Brunet

Thesis submitted to the
Faculty of Graduate and Postdoctoral Studies
In partial fulfillment of the requirements
For the Master of Science

Department of Biochemistry, Microbiology and Immunology
University of Ottawa
Ottawa, Ontario, Canada

Your file Votre référence
ISBN: 978-0-494-61358-0
Our file Notre référence
ISBN: 978-0-494-61358-0

ABSTRACT

Gap junctions (GJ) are intercellular channels permitting bi-directional communication between adjacent cells. GJ function is associated with homeostasis while GJ deficiency results in uncontrolled proliferation. Most cancer cells are GJ deficient. Astrocytoma is the most common form of brain cancer in young adults and usually causes death within 9-12 months of diagnosis. Connexin 43 (Cx43) expression and sub-localization is usually impaired in human astrocytoma cells. Since phosphorylation by various protein kinases plays a crucial role in Cx43 trafficking, we investigated the signaling pathways involved in Cx43 sub-localization in the human astrocytoma cell lines, U-251 MG and U-87 MG. Cx43 was found to be present in both cell lines and was found to be phosphorylated on specific serine residues. Using antibodies against Ser-255 and Ser-262, Cx43 was shown to be nuclear; this is a novel observation in human astrocytoma. Interestingly Cx43 fragments of less than 43 kDa were shown to be mostly intranuclear when using antibodies against the phosphorylated forms of Cx43, suggesting a role for phosphorylation in the protein's turnover and sub-localization. Intercellular communication assays showed a lack of GJ function in U-251 cells; however, the presence of open hemichannels in U-87 MGs was observed. Protein kinase inhibitors including Bis I (PKC), PKAI (PKA) and PD98059 (ERK-MAPK) were tested on their ability to affect Cx43 expression and/or sub-localization. PD98059 treatment increased Cx43 expression in U-87 MG cells and partially restored normal membrane localization in U-251 MG. All three inhibitors either increased or decreased the presence of Cx43 fragments, depending on the phosphorylation site observed, suggesting a role for these pathways in Cx43 degradation. Morin, a natural flavonoid with anti-tumorigenic properties, was shown to increase Cx43 phosphorylation on Ser-262 but only in U-251 MG. This effect was exerted through the p38 MAPK pathway. Fractionation experiments showed that Cx43 is not present in caveolae, a structure which helps to compartmentalize signaling molecules with their protein targets. Our results suggest that it is worthwhile to continue in our attempts to restore function of Cx43 in human astrocytoma.

ACKNOWLEDGEMENTS

Thank you to my supervisor Dr. Léonard Kleine for your invaluable guidance and the many lessons learned. Thank you to the members of my Thesis Advisory Committee, Dr. Peter Liston, Dr. Luc Sabourin and Dr. Zemin Yao for your helpful advice. A sincere thank you to Dr. Jenny Phipps whose invaluable help and guidance made this project possible. Thank you to Ricardo Mojica for the shared laughs and being a good friend. Thank you to Dr. Saba Siddiqi for all the help and the delicious samosas that you brought at our special lunches. Thank you to Sharo, Loan, Marine, Wei and all the others from PharmaGap Inc. for your friendship. Special thanks to Dr. Robert Monette for the invaluable help regarding the confocal microscope. The help of Dr. Z. Yao and his lab (in particular Maroun) for the preparation of caveolae fractions was greatly appreciated.

TABLE OF CONTENTS

LIST OF ABBREVIATIONS

BCIP	5-bromo-4-chloro-3-indolyl phosphate
BisI	Bisindolylmaleimide I
BSA	Bovine serum albumin
Cav	Caveolin
Cx	Connexin
cAMP	Cyclic adenosine monophosphate
cGMP	Cyclic guanosine monophosphate
Da	Dalton
DMEM	Dulbeco's modified Eagle medium
EDTA	Ethylenediaminetetraacetic acid
EGF	Epidermal growth factor
ERK	Extracellular signal-regulated kinase
GAPDH	Glyceraldehyde-3-phosphate deshydrogenase
GBM	Glioblastoma multiforme
GJIC	Gap junction intercellular communication
GTP	Guanosine triphosphate
HEPES	*N*-2-Hydroxyethylpiperazine-*N'*-2-ethane-sulfonic acid
HRP	Horseradish peroxidase
MAP	Mitogen activated protein
MAPK	Mitogen activated protein kinase
MEK	MAP kinase or ERK kinase
MEM	Miminum essential medium

NBT	Nitroblue tetrazolium chloride
NP40	Nonidet P-40
PBS	Phosphate buffered saline
PDGF	Platelet derived growth factor
PKA	Protein kinase A
PKB	Protein kinase B
PKC	Protein kinase C
PMSF	Phenylmethylsulfonyl
PTEN	Phosphatase and tensin homolog deleted on chromosome10
RPM	Rotations per minute
RT-PCR	Reverse transcription polymerase chain reaction
SDS	Sodium dodecyl sulphate
SDS-PAGE	Sodium dodecyl sulphate poloyacrylamide gel electrophoresis
TBST	Tris-buffered saline with Tween-20
TPA	12-O-tetradecanoylphorbol-13-acetate

LIST OF FIGURES AND ILLUSTRATIONS

LIST OF TABLES

1.0 INTRODUCTION

During the course of evolution of single cells to multi-cellular organisms, new genes and functions were developed to assure coordinated regulation of cellular processes within these more complex entities. In multi-cellular organisms a delicate balance of regulatory and integrative mechanisms has to be achieved in order to maintain a relatively stable internal environment in the face of variations in the external conditions. This balance can be achieved by either sending a specific message to another cell or isolating a cell or group of cells from the rest of the community to maintain integrity (Mese *et al.*, 2007). This state of balance, termed homeostasis, is controlled by three major communication processes: 1) extracellular communication, 2) intracellular communication, and 3) intercellular communication. The integrated control of these communication routes permits an organism to proliferate, to differentiate, to undergo apoptosis (programmed cell death) and to adapt/respond to stimuli (Trosko and Ruck, 1998).

It has been suggested that the gain in ability of more complex organisms to regulate cell growth, differentiation and apoptosis is directly related to the appearance of intercellular communication. This notion is supported by several studies that have shown that this type of communication is severely impaired in cancers, which often exhibit behavior characteristic of a single-celled organism. Processes typical to these organisms such as uncontrolled cell proliferation, inability to terminally differentiate and an altered apoptosis rate are often found in cancerous cells (Trosko and Ruch, 1998). Besides growth control, intercellular communication plays an essential role in a variety of physiological processes including electrical coupling, tissue response to hormones,

differentiation and regulation of embryonic development. The role of intercellular communication in the regulation of embryonic development is especially important since it greatly varies during the different stages of cellular differentiation (Levin, 2007).

The diversity and the primordial character of these functions for the survival of an organism clearly demonstrate the importance of understanding the mechanisms involved in the control of intercellular signaling. Intercellular communication is mainly mediated through the gap junction communication channel, which has become one of the focal points of the research in the field with a particular emphasis on the regulatory aspects of gap junctional intercellular communication (GJIC). The insight gained from these studies can lead to the development of new therapeutic approaches to a variety of patho-physiological states caused by abnormal intercellular communication (Czyz, 2008).

1.1 The Gap Junction Communication Channel

1.1.1 Gap Junction Structure

Gap junctions form hydrophilic channels between closely adjoining cells linking their cytoplasms. It allows for direct two-way intercellular passage of molecules smaller than 1 kDa (Mese *et al.*, 2007). These channels are relatively non-specific and the observed selectivity is based mainly on molecular size. They allow for the bidirectional passive diffusion of small molecules and ions such as water, cAMP, sugars, nucleotides, amino acids, fatty acids, small peptides and drugs. Larger molecules such as proteins, complex lipids, polysaccharides, nucleic acids and other molecules are denied passage. Gap junctions are found in almost all multi-cellular organisms of the animal kingdom, both invertebrates and vertebrates, and in almost all tissues with the exception of a few

terminally differentiated cells such as differentiated erythrocytes, differentiated skeletal muscle and adipocytes (Kumar and Gilula, 1996).

An integral membrane protein called connexin is the main structural unit of the gap junction channel (Fig. 1, A). Connexins comprise a multi-gene family with at least twenty mammalian connexin genes discovered to date. The expression of a particular connexin type is strictly correlated with the cell type and tissue in which it is found. Several connexins can be expressed in a single cell. Gap junctions have a relatively simple molecular organization: they display a hierarchy of assembly with six connexin subunits forming an integral complex called a connexon or hemichannel (Fig 1, B). The connexons from the plasma membrane of the neighboring cells align and interact to form a gap junction channel (Fig 1, C). In turn, gap junctions cluster in specific regions of the membrane resulting in the formation of gap junction plaques (Fig 1, D) (Segretain and Falk, 2004).

All connexins appear to have the same topology in the plasma membrane with the polypeptide spanning the lipid bilayer four times, with both the N- and C- termini located in the cytoplasm. One of the four transmembrane domains, M3, is amphipatic in nature and contributes to the lining of the channel. The two extracellular loops (E1 and E2) (Fig 1, A) negotiate the docking of the two opposing connexons by facilitating the initial interactions between them. Each loop contains a characteristic arrangement of three cysteine residues that are thought to enhance the rigidity of these extracellular segments necessary for the docking of the two connexons and formation of a gap junction. The intracellular loop as well as the C-terminus exhibit the greatest variability among different connexins and therefore are believed to be important for regulation of the

Figure 1. The Structure of a gap junction.

Schematic model of a gap junction showing the arrangement of six connexin subunits to form a connexon, which contains the central channel connecting the cytoplasm of the two adjoining cells.

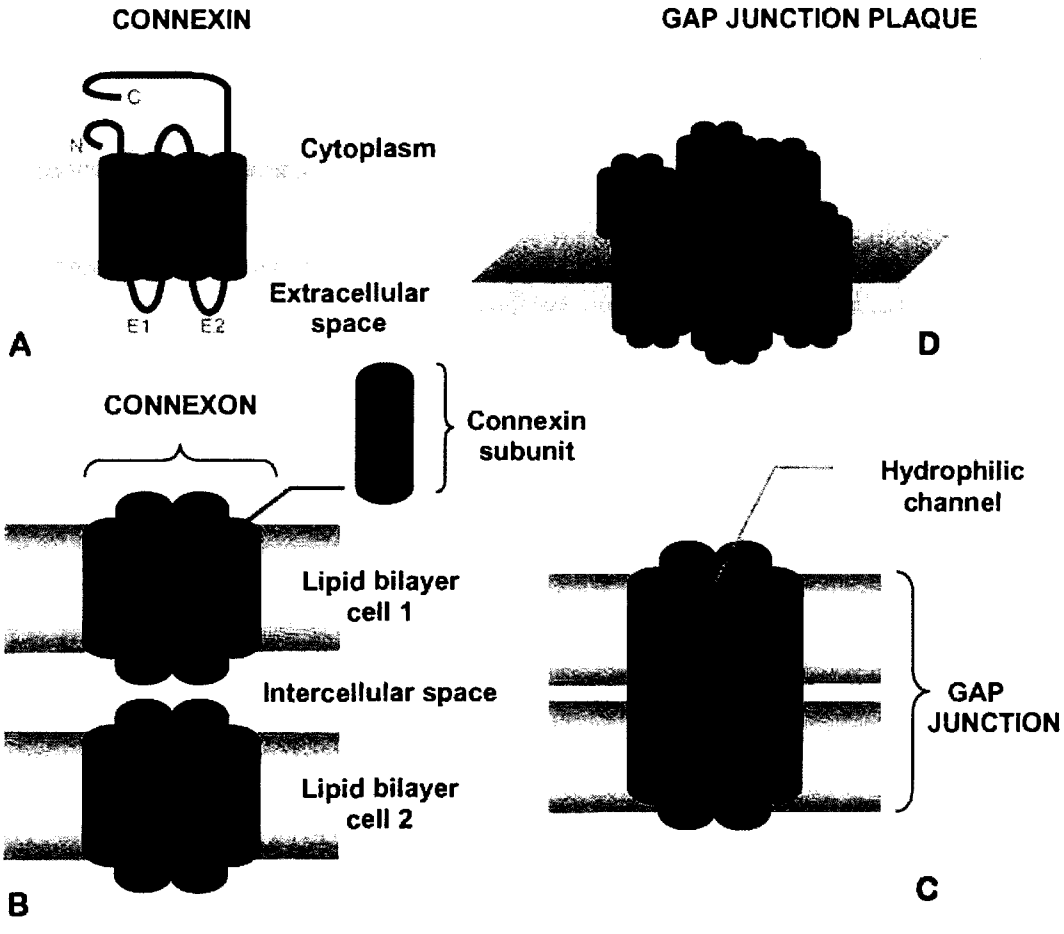
CONNEXIN
GAP JUNCTION PLAQUE
C
N
Cytoplasm
Extracellular space
E1
E2
A
D
CONNEXON
Connexin subunit
Hydrophilic channel
Lipid bilayer cell 1
Intercellular space
Lipid bilayer cell 2
GAP JUNCTION
B
C

protein (Kumar and Gilula, 1996). One exception however is Cx26 which lacks a functional C-terminus.

The X-ray crystallographic study of a recombinant gap junction membrane channel lacking its C-terminus has revealed that the outer diameter of a GJ within a membrane is of ~ 70 Å with the intercellular portion of the channel narrowing to ~ 50 Å (Unger *et al.*, 1999). The vertical cross-section of the interior of the channel disclosed that its diameter narrows down from ~ 40 Å to ~ 15 Å within its transmembrane region in proceeding from the cytoplasmic to the extracellular portion of the bilayer. The channel widens again to ~ 25 Å within its extracellular section. Taking into account the contributions from the amino acid side chains, the narrowest diameter of the GJ is about 5 Å (Unger *et al.*, 1999). When the channel is that narrow however, it is too small for 1000 Da molecules to go through; only ions are able to diffuse. This concept is at the basis of the electrical coupling in the heart (Desplantez *et al.*, 2007).

1.1.2 Assembly and Degradation

Similarly to other integral membrane proteins, "connexins are synthesized at the endoplasmic reticulum (ER) membrane in a typical process that involves a signal recognition particle, an integral signal anchor sequence, docking of the nascent-chain/ribosome complex to the translocon, and cotranslational integration of the connexin polypeptides into the ER membrane" (Falk, 2000). The final topological organization of the connexins is attained at the level of their ER membrane integration (Falk *et al.*, 1994; Ahmad *et al.*, 1999; Diez *et al.*, 1999) (Fig 2). The exact location at which connexin oligomerization takes place has not been clarified. Several studies have reported that

connexins are assembled into oligomers within specialized regions of the ER (George *et al.*, 1998, 1999), either the intermediate compartment or ER-Golgi intermediate compartment (Schweizer *et al.*, 1990). However, other studies in NRK and CHO cell lines suggested that oligomerization of endogenously expressed Cx43 takes place after exit from the ER in late Golgi membranes (Musil and Goodenough, 1993). These observations strongly suggest that the process is likely cell-type specific. Connexins traffic to the plasma membrane by a consecutive series of vesicle fusion and budding from the ER through the Golgi apparatus (Segretain and Falk, 2004; Musil and Goodenough, 1991) (Fig 2). While most connexins transfer to the plasma membrane following the classical secretory pathway, some connexins like Cx26 follow a Golgi independent pathway (Martin *et al.*, 2001). The process of targeting connexons to the plasma membrane is not currently understood but two general models have been proposed. The first involves the direct transport of the connexon to the GJ site whereas the other entails an indirect transport of the connexon by lateral movement within the plasma membrane towards the gap junction plaque site following its insertion at a distant location (Falk, 2000). During all of the intracellular transit, connexons are thought to remain in a closed configuration to maintain a strict ionic gradient between the lumenal and cytoplasmic environment (Martin and Evans, 2004). Once localized into the plasma membrane, the connexons from the neighboring cells dock with each other via interactions of their connexin subunit extracellular loop domains forming a complete GJ channel (Fig. 2). GJ channels in turn aggregate to form GJ plaques. The formation of plaques is assisted by calcium-dependent cell-adhesion molecules such as E-cadherins (Laird *et al.*, 1995; Laird 1996). The cytoskeletal proteins ZO-1 (Thomas *et al.*, 2002;

Figure 2. The Life Cycle of a Connexin.

Schematic representation of how a connexin is synthesized in the ER, trafficked to the plasma membrane via the Golgi, and internalized and subsequently degraded (borrowed from Laird, 2006).

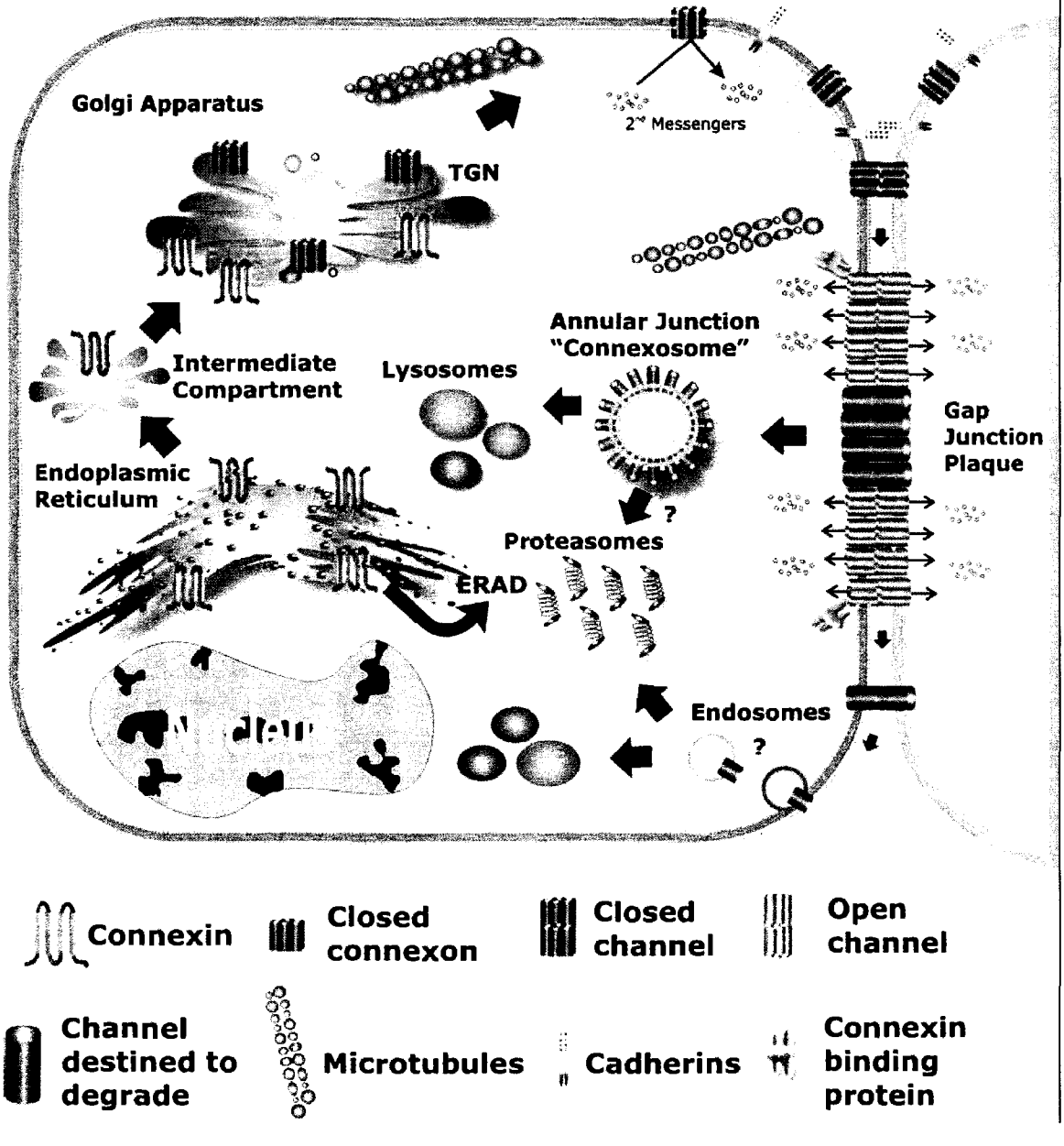
Golgi Apparatus
2nd Messengers
TGN
Annular Junction
"Connexosome"
Intermediate
Compartment
Lysosomes
Gap
Junction
Plaque
Endoplasmic
Reticulum
?
Proteasomes
ERAD
Endosomes
?
Connexin
Closed
connexon
Closed
channel
Open
channel
Channel
destined to
degrade
Microtubules
Cadherins
Connexin
binding
protein

Sorgen *et* al., 2004) and α-spectrin (Toyofuku *et al.*, 1998) have also been reported to play a role in this process in epithelia. It was shown however that in some cases connexons were delivered to the nonjunctional part of the plasma membrane and formed plaques before they could dock with connexons from neighboring cells (Lauf *et al.*, 2002). Analysis of living cells demonstrated that some gap junctions are relatively static in the plasma membrane whereas others are more fluid and cluster together (Jordan *et al.*, 1999).

The degradation and turnover of gap junctions are the least understood aspects of connexin processing within the cells. The turnover of connexins is relatively fast compared to other integral membrane proteins. It is probable that connexins exhibit a short half-life to react to physiological changes in their environment leading to an up- or down-regulation of gap junctions (Laird., 2006). Turnover rates have been reported to be in the range of 1-3 h for Cx43 and Cx45 in cultured cells or tissues (Beardslee *et al.*, 1998; Saffitz *et al.*, 2000) contrasted with 17-100 h for integral membrane proteins measured in hepatocytes (Chu and Doyle, 1985). The current evidence suggests that gap junctions are removed from the membrane by internalization of entire channels within large fragments of GJ plaques forming what is called annular junctions or "connexosomes" (Severs *et al.*, 1989; Laird, 2006). The subsequent degradation process involves both lysosomal as well as proteasomal pathways (Laing and Beyer, 1995; Laing *et al.*, 1997; Laird, 1996; Rahman *et al.*, 1993; Musil *et al.*, 2000). It was suggested however, that lysosomal and proteasomal degradation play distinct roles in the life cycle of connexin43, the most ubiquitous of all connexins. Both lysosomes and proteasomes play a role in the degradation of internalized gap junctions, but lysosomes have been

shown to degrade Cx43 delivered from the early secretory compartments before they reach the membrane (Qin *et al.*, 2003).

1.1.3 Gap Junction Function

As stated previously, gap junctions play an important role in tissue homeostasis in almost every organ of the human body. This homeostasis is attained by keeping a balance in secondary messengers, such as cAMP, cGMP and Ca^{2+}, from either side of the gap junction. When a cell receives a signal, be it a death signal for example, signaling pathways in that cell will be activated and/or inhibited resulting in a change of second messenger concentration. These messengers then diffuse to the adjacent cell where they act, for example, as co-factors of protein kinases. This way, signaling in cells within a tissue is equalized and the cells can act as a syncitium. This way a dying cell can propagate a death signal to neighboring cells that need to undergo apoptosis, or a cell can transfer a survival signal to adjacent cells following cellular stress.

There are three major signaling pathways involved in gap junction regulation and/or function: the PKA pathway, the PKC pathway and finally the ERK-MAPK pathway.

PKA is a kinase whose activation is dependent on cAMP. Ligands like hormones or neurotransmitters bind to specific receptors, like β-adrenergic receptors in the heart, GTP-binding protein (G_s) thus becomes activated leading to the activation of adenylyl cyclase and the production of cAMP (Lissandron and Zaccolo, 2006). The PKA kinase consists of two regulatory and two catalytic subunits that are linked together in a tetramer when the kinase is inactive. Upon binding of four cAMP molecules to the two regulatory

subunits the catalytic subunits are released and become active (Seino and Shibasaki, 2005). Once activated, PKA phosphorylates a variety of target proteins like the cAMP response element binding protein (CREB) which then translocates to the nucleus and regulates the transcription of cAMP regulated genes (Reddy, 2005).

Protein kinase C comprises a family of serine/threonine kinases categorized into three groups, classical (α, βI, βII, γ), novel (δ, ε, η, θ), and atypical isoforms (ζ, ι/λ), as based on domain structure and activator requirements (Mellor and Parker, 1998). The classical isoforms are activated by phorbol esters and are calcium dependent, while the novel isoforms are only activated by phorbol esters. The activity of the atypical isoforms is independent of both calcium and phorbol esters (Gutcher *et al.*, 2003; Breitkreutz *et al.*, 2007). The activation of the PKC isoforms result in a change in their cellular sub-localization following translocation to specific anchoring proteins. PKC can then phosphorylate a plethora of targets involved in cell proliferation, differentiation, transformation and apoptosis (Mackay and Twelves, 2007)

The mitogen-activated protein kinase (MAPK) pathway consists of a cascade of events comprised of three protein kinases that act as a signaling relay by protein phosphorylations (Roberts and Der, 2007). When a growth factor binds its specific receptor, for example EGF/EGFR, a protein called Ras is recruited to the membrane. Ras is then activated and leads to the serial phosphorylation and activation of the three protein kinases, namely Raf, MEK and ERK 1/2. Once phosphorylated ERK then translocates to the nucleus and activates different transcription factors involved mainly in cellular proliferation (Schulze *et al.*, 2004). The classical pathways as described above are however not static and their connections with other pathways and their changes in

disordered tissues have to be kept in mind since the connexins are also involved in these changes.

1.1.4 Non-Junctional Roles of Connexins

In recent years it has been suggested that connexins may play a role in processes that are gap junction independent (Plotkin *et al.*, 2002; Evans *et al.*, 2006). Confocal laser scanning microscopy experiments demonstrated that Cx43 was localized not only in junctional, but also in nonjunctional regions of the cell (Quist *et al.*, 2000). It has been observed that uncoupled connexons, or hemichannels, when in their open state would act as nonselective leak pathways and permit bidirectional flow of small molecules and ions between the cytoplasm and the extracellular space. This flow of ions would in turn create an osmotic gradient favoring water flow from the extracellular environment to the cytoplasm. This phenomenon is crucial since cell volume shares a close relationship with cell growth and metabolism, making it essential in mammalian cells (Quist *et al.*, 2000). Another important role of hemichannels is the propagation of calcium waves from cell to cell. ATP is released in the extracellular space through hemichannels which then bind to purinergic receptors on a neighboring cell thus leading to an increase in intracellular calcium concentrations. This calcium increase then activates more ATP-releasing channels leading to the propagation of the wave (Goodenough and Paul, 2003).

It has been shown in many studies that there was a correlation with connexin overexpression in transfected cells and a decrease in proliferation. It appears that this cell growth inhibition in some cases is observed without the establishment of intercellular channels or even hemichannels (Stout *et al.*, 2004). This channel independent inhibition

of growth is believed to happen through the down-regulation of certain key genes involved in cell growth (Qin *et al.*, 2002). One study showed that Cx43 inhibited expression of S phase kinase-associated protein 2 (Skp2), which is responsible for the ubiquitination of p27. Since p27 is an inhibitor of cell cycle proteins, an accumulation of p27 thus results in a decrease in cell growth (Zhang *et* al., 2003a; 2003b). It was also shown that the expression of only the C-terminal region of Cx43 was necessary to induce growth inhibition, suggesting this process is mediated by the carboxyl domain (Moorby and Patel, 2001; Stout *et al.*, 2004).

1.1.5 Gap Junctions and Their Role in Human Diseases

Gap junctions play an essential role in a number of diverse physiological processes. Charcot-Marie-Tooth (CMTX) disease was the first pathology associated with a connexin. This progressive neuropathy results from myelin disruption and axonal degeneration of peripheral nerves and is caused by a mutation in Cx32 (Deschenes *et al.*, 1997; Martin *et al.*, 2000). This connexin has a wide tissue distribution and is one of the major GJ proteins in the adult liver as well as in oligodendrocytes. The fact that a mutation in Cx32 results in only a mild neuropathy suggests that other connexin types can compensate for the loss of one or the other connexin in different tissues. Other diseases associated with mutations in various connexins include inherited dominant and recessive hearing loss (Cx26, Cx31, Cx30), dominant epidermal disease (Cx32, Cx30.3, Cx30), dominant skin disease caused by abnormalities in keratinization, cataracts (Cx46, Cx50) and abnormal cardiac development (Cx43) (Table 1) (Bennett, 1994; Kelsell *et al.*, 2001). Aberrant regulation of GJIC as well as several other alterations have been

implicated in several types of neoplasia (Andrade-Rozental *et al.*, 2000) where the pathology is a result of an altered function of gap junctions and not a mutation. The majority of tumors express less or no connexin, have fewer gap junctions and exhibit a decrease in GJIC (Cesen-Cummings *et al.*, 1998; Yamasaki, 1990).

Table 1. Human diseases associated with mutations in connexin genes (adapted from Kelsell *et al.*, 2001)

Connexin (gene)	Human disorder
Cx32	X-linked Charcot-Marie-Tooth Disease: neuropathy often associated with hearing loss
Cx26	Dominant and recessive non syndromic moderate-profound sensorineural hearing loss Dominant epidermal disease (palmoplantar keratoderma) and Vohwinkel's syndrome
Cx31	Recessive non-syndromic moderate-profound sensorineural hearing loss Dominant non-syndromic high frequency hearing loss Dominant skin disease (Erythrokeratoderma variabilis) Dominant sensorineural hearing loss and neuropathy
Cx30.3	Dominant skin disease (Erythrokeratoderma variabilis)
Cx30	Dominant hearing loss Clouston's dirotic ectodermal dysplasia: skin disease (palmoplantar keratoderma), hair loss, nail defects and often mental deficiency
Cx43	Association with visceroatrial heterotaxy
Cx46 **Cx50**	Dominant zonular pulverulent, cataract

1.2 Regulation of Gap Junctions

1.2.1 General Aspects of GJ Regulation

GJ regulation is a complex process that can be achieved by a broad range of mechanisms that can generally be categorized into two major groups. The first category includes all the processes that affect the formation and levels of GJs starting with Cx gene expression, translation, oligomerization to connexons, transport to the membrane, assembly in GJ and plaques, gating and finally degradation. The impaired GJIC caused by down-regulation of Cx in certain types of neoplasia is illustrative of this type of regulatory mechanism. The second group includes all the modes of regulation that do not alter the cellular levels of GJ but affect their functionality, which is directly related to the fluctuation of the channel between the "open" and "closed" states. This GJ gating can be affected by a variety of exogenous and endogenous factors including extracellular soluble factors (mitogens, hormones, anesthetics and drugs) and biomolecules (oncogenes, growth factors, tumor promoters) (Berthoud *et al.*, 2000; Evans and Boitano, 2001). These agents can exert their GJIC modulatory action either directly by introducing structural modifications to the channels, or indirectly for example by perturbing the lipidic environment in the proximity of the channel and thus affecting its conformation (Hossain and Boynton, 2000). The majority of GJIC modulators act by initiating complex signaling pathways leading to the activation of various kinases.

1.2.2 Regulation of Gap Junctions by Phosphorylation of Connexins

Most connexins, with the exception of Cx26, contain protein kinase "consensus phosphorylation sequences" and have been demonstrated to be phosphoproteins (Lampe and Lau, 2000). The majority of the phosphorylation events occur at the C-terminal cytoplasmic tail, which has been shown to be important for regulation. It is interesting to note that a Cx43 truncated mutant that lacks a C-terminal tail retains its ability to form functional channels in *Xenopus* oocytes or SKHep1 cells, albeit with altered permeability and electrophysiological properties compared with those of a wild type Cx43 channel (Fishman *et al.*, 1991; Dunham *et al.*, 1992). A Cx32 mutant that is truncated at its C-terminal tail has been linked to CMTX disease (Rabadan-Diehl *et al.*, 1994). The above examples emphasize the important regulatory role of the C-terminal domain in channel gating and in the rates of connexin transport, assembly and turnover.

A variety of protein kinase modulators have been applied to investigate the effects of phosphorylation on gap junction function, revealing that phosphorylation events are connexin and cell-type specific. However, some general trends have been observed across different connexins. For example, compounds such as cAMP, have been attributed to increase the rates of connexin transcription (Arnold *et al.*, 2005), increase in levels of connexin RNA or protein (Darrow *et al.*, 1996), changes in connexin phosphorylation status (Traub *et al.*, 1987), as well as changes in Cx43 transport (Atkinson *et al.*, 1995) and GJ conductance (Spray *et al.*, 1991; Jongsma *et al.*, 2000). On the other hand, agents that activate PKC such as phorbol esters generally diminish GJIC. Staurosporine, a protein kinase inhibitor, has been shown to increase GJIC in SKHep cells overexpressing Cx43, whereas okadaic acid, a phosphatase inhibitor has had

the opposite effect on GJIC (Moreno *et al.*, 1994). These studies taken together demonstrate that phosphorylation is an important regulatory mechanism for GJ function. However, the signaling pathways responsible for these observations seem to be cell phenotype specific and have not yet been fully deciphered.

1.2.3 Phosphorylation of Cx43

Cx43 is the most common connexin expressed across a broad range of tissues, but more predominantly in astrocytes and heart. The phosphorylation of Cx43 can have both an inhibitory and stimulatory effect on GJIC depending on the phosphorylation site. The primary sites of Cx43 phosphorylation are multiple serine residues (21 residues) on its C-terminal domain (Fig. 3). The extent of phosphorylation on threonine residues is significantly smaller (Kanemitsu *et al.*, 1997). The protein kinases PKC, MAP kinase and pp60src were shown to phosphorylate Cx43 (Lau *et al.*, 2000). Many other non-identified protein kinases could also be involved in Cx43 phosphorylation.

Cx43 extracted from untreated mammalian cells in culture and separated by SDS-PAGE can generally be resolved into several bands corresponding to the different isoforms. Typically observed are a nonphosphorylated (NP ~ 43 kDa) form that migrates faster on the gel and two slower bands that correspond to the most common phosphoisoforms (P1 and P2, ~45 kDa and ~47 kDa respectively), which have been shown to be phosphorylated mainly on serine residues (Musil and Goodenough, 1991).

Figure 3. A schematic representation of the primary structure of rat Cx43.

Phosphorylation sites in Cx43 targeted by V-src, MAP kinase and PKC are indicated. (borrowed from Lampe *et al.*, 2000).

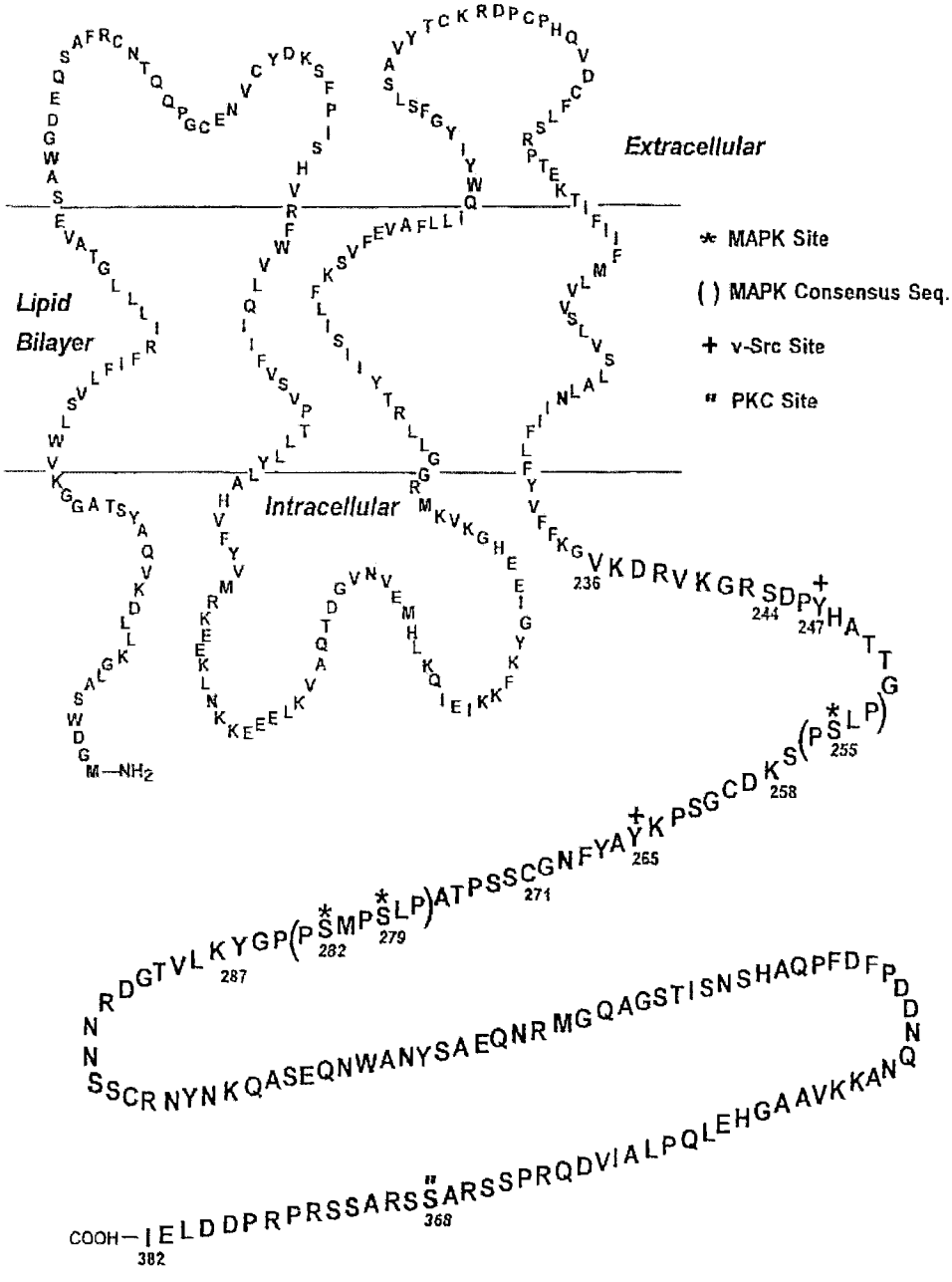
Extracellular
Lipid
Bilayer
Intracellular
* MAPK Site
( ) MAPK Consensus Seq.
+ v-Src Site
" PKC Site
M—NH2
COOH—I E L D D P R P R S S A R S S A R S S P R Q D V I A L P Q L E H G A A V K K A N Q
N S S C R N Y N K Q A S E Q N W A N Y S A E Q N R M G Q A G S T I S N S H A Q P F D F P D D N
R D G T V L K Y G P (P S M P S L P) A T P S S C G N F Y A Y K P S G C D K S (P S L P) T T G

However, neither the protein kinase(s) isoforms responsible for these phosphorylations nor their target sites in untreated cells have been identified.

It is very important to note however, that the kinases involved in the phosphorylation of connexins under basal conditions or physiological conditions are in general unknown, even for Cx43. This signifies that with some exceptions, the kinases known to be responsible for the phosphorylation of specific residues on connexins have only been identified through the stimulation of specific kinases with exogenously added activators (Cruciani and Mikalsen, 2002).

1.2.3.1 Phosphorylation of Cx43 During Its Life Cycle

Phosphorylation events have been associated with the sub-localization of Cx43 to the plasma membrane as well as with the aggregation of connexons into GJ plaques, pointing to the possible role of this post-translational modification in the regulation of Cx43 transport and/or the assembly or disassembly of GJs (Musil and Goodenough, 1991; Lampe and Lau, 2004). Phosphorylation has been demonstrated to occur as soon as 15 min after Cx43 synthesis in cultured fibroblast cells, clearly showing that it can occur before the protein's arrival at the membrane (Crow *et al.*, 1990). Phosphorylations have also been known to play a role in the mechanisms that modify the rate at which the connexon-containing vesicles are incorporated into the plasma membrane (Moreno, 2005). The fact that a nonphosphorylated form of Cx43 can be detected at the membrane suggests that either these early phosphorylations are transient in nature or that dephosphorylation occurs at the membrane (Musil and Goodenough, 1991). Although Cx43 does not have to be phosphorylated in order to be localized to the membrane, Cx43

present in GJ plaques has been found to be phosphorylated almost exclusively to its P2 isoform and selectively resistant to solubilization by Triton X-100 (Musil and Goodenough, 1991). It is not known however, if these phosphorylation(s) play a role in the formation and stabilization of GJs in plaques. Degradation has been linked to EGF stimulation where it induces hyperphosphorylation of Cx43 and its proteosome-dependent degradation (Leithe and Rivedal, 2004; Laird, 2005).

1.2.3.2 Phophorylation of Cx43 by PKC and PKA

The stimulation of PKC upon short exposure to phorbol esters such as TPA results in a marked decrease in GJIC, as indicated by a reduction in dye transfer in different cell types (Rivedal and Opsahl, 2001). PKC can phosphorylate Cx43 on Ser-368 and Ser-372 *in vitro* (Saez *et al.*, 1997; Lampe *et al.*, 2000). It has also been shown that Ser-368 is a major site of phosphorylation *in vivo* (Lampe *et al.*, 2000). The cells expressing the site-directed mutant Ser-368A were resistant to dye transfer inhibition by TPA. Examination of the channel conductance in cells treated with TPA has further supported the notion that the PKC-mediated phosphorylation of Ser-368 in Cx43 is involved in the mechanism of GJIC inhibition by TPA since the Ser-368A mutant (unlike wild-type Cx43) showed no decrease in the full open conductance state of GJ channels (Lampe *et al.*, 2000). TPA has been shown to increase Cx43 phosphorylation on Ser-262 as well (Solan and Lampe, 2005). PKA does not seem to phosophorylate Cx43 *in vitro*. Compounds that stimulate an increase in cAMP levels (leading to PKA activation) generally enhance Cx43 intracellular levels (Arnold *et al.*, 2005). This observation however, seems to be cell specific as some cell types do not change the phosphorylation

status of Cx43 upon cAMP treatment (TenBroek *et* al., 2001). Additionally, studies in which PKA or PKC were introduced into L929 cells transfected with either wild type or S364P mutant Cx43 cDNA have implied that both kinases may play a complex and possibly contrasting role in GJIC regulation (Britz-Cunnhingham *et al.*, 1995).

1.2.3.3 Phosphorylation of Cx43 by MAP Kinase

Both EGF and PDGF receptor tyrosine kinase activation through ligand binding negatively affected GJIC causing a rapid inhibition of dye transfer and a significant increase in the phosphorylation of Cx43 (Kanemitsu and Lau, 1993; Hossain *et al.*, 1998). This induced phosphorylation occurred on serine residues and not on tyrosine, indicating that the receptor doesn't phosphorylate Cx43 directly (Warm-Cramer and Lau, 2004). The effect of EGF receptor on Cx43 GJIC was shown to rely on activation of MAP kinase but not to be related to PKC activity (Kanemistu and Lau, 1993). MAP kinase seems to phosphorylate Cx43 directly in EGF-treated cells by targeting Ser-255, Ser-279 and Ser-282 residues (Warn-Cramer *et al.*, 1996; 1998). A triple mutant of these three residues formed functional gap junctions but was not affected by MAP kinase in response to EGF-stimulation (Warn-Cramer *et al.*, 1998). Evidence supporting the role of MAP kinase in the regulation of GJIC also comes from experiments in which purified MAP kinase was demonstrated to phosphorylate Cx43 channels reconstituted into liposomes and to induce a decrease in their conductance (Kim, *et al.*, 1999).

The inhibition of GJIC by activation of the PDGF receptor involves more complex mechanisms and is less understood. The process appears to depend on both

PKC and MAPK activity and may be regulated by other signaling pathways in addition to Cx43 phosphorylation (Hossain *et al.*, 1998; 1999a; 1999b).

In summary, the following aspects of the role of the Cx phosphorylation in the regulation of GJIC have been established (Lampe and Lau, 2000):

1. After the arrival of a connexon at the plasma membrane, Cx phosphorylation is not always necessary for the formation of a functional GJ channel,
2. phosphorylation of specific serine residues reduces GJIC, implicating the "gating" of GJ channels,
3. phosphorylation may facilitate protein-protein interactions important for Cx regulation,
4. phosphorylation is important for Cx processing. i.e. trafficking, assembly and/or turnover.

1.3 Gap Junctions and Cancer

In the 21st century cancer and anti-cancer therapies remain one of the most important problems in medicine. There are three main events that contribute to carcinogenesis: 1) inhibition of apoptosis, 2) activation of mitogenic pathways and 3) disruption of intercellular communication resulting in a loss of growth control by surrounding cells (Salameh and Dhein, 2005). Loewenstein was the first one to stipulate in 1966 that GJIC was associated in growth control and that cancer cells lose their ability to communicate with the neighboring cells via gap junctions (Loewenstein, 1966). Phipps *et al.* (Phipps *et al.*, 1990; Phipps *et al.*, 1997) were the first to demonstrate that intercellular communication disruption in cancer cells resulted in a loss of growth control by the surrounding cells. In later years it was indeed determined that many transformed cells and tumors are characterized by reduced GJIC (Loewenstein and Rose, 1992; Trosko and Ruch, 1998, Yamasaki, 1990). GJIC reduction can be the result of two phenomena: 1) a reduction in connexin expression or 2) an aberrant connexin sub-localization (Chipman *et al.*, 2002). As previously stated most cancer cells show a reduction or even an absence in connexin expression, even in precancerous lesions suggesting a role in tumor progression (Mesnil *et al.*, 2005; Salamah and Dhein, 2005). On the other hand, several studies have shown that connexins are expressed in tumor cells but they are abnormally localized and are sequestered in the cytoplasm (Mesnil *et al.*, 2005). In fact Arnold *et al.* have demonstrated that in the human neuroblastoma cell line IMR-32, Cx43 is sequestered around the nucleus (Arnold *et al.*, 2005).

Since many transformed cells have been shown to be GJIC deficient, researchers believed that the recovery of their gap junctional communication could lead to the

reestablishment of a normal phenotype (Mesnil, 2002). Indeed Cx43 was shown to decrease cell proliferation in vitro (Goldberg *et al.*, 2000) as well as inhibit tumorogenicity, leading to the notion that connexins behaved like tumor suppressors (Zhu *et al.*, 1991; Naus *et al.*, 1992; Rose *et al.*, 1993; Roger *et al.*, 2004). Chemicals such as tolbutamide have also been shown to increase Cx43 expression in rat glioma cells and blunt their proliferation (Sanchez-Alvarez *et al.*, 2001). In glioblastoma however, transfection of Cx43 did trigger a tumoral suppression *in vitro* but it was not associated with a gain of intercellular communication, since Cx43 remained cytoplasmic (Mesnil, 2004). This further supports a non-junctional role for connexins in a cell. Cx43 transfection has also been shown to render the cells more susceptible to apoptosis by decreasing the expression of bcl-2, an anti-apoptotic protein (Huang *et al.*, 2001).

1.4 Astrocytoma

Astrocytoma is the most common form of brain cancer (Nakase and Naus, 2004). In general, astrocytoma is a space-occupying mass in the brain that causes a high intra-cranial pressure, vessel occlusion and brain edema. The tumors are resistant to most forms of therapies and cause death within 9-12 months of diagnosis (Lokker *et al.*, 2002; Reardon, *et al.*, 2006). These tumors have evolved into the most aggressive and invasive of all human cancers (Gurney and Kadan-Lottick, 2001).

The World Health Organization (WHO) has divided astrocytomas into four categories of increasing malignancy: pilocytic astrocytoma (Grade I), astrocytoma (Grade II), anaplastic astrocytoma (Grade III) and glioblastoma multiforme (GBM) (Grade IV). GBMs are the most common and malignant form of astrocytoma and are associated with

a very poor prognosis especially in young individuals between 25 and 35 years of age (Besson and Yong, 2001). All GBMs arise from the malignant transformation of normal astrocytes (Soroceanu *et al.*, 2001). They are divided into two categories, primary and secondary GBM. Primary GBMs arise *de novo* after a short clinical history whereas secondary GBMs arise from pre-existing lower grade astrocytomas (Reardon *et al.*, 2006). Primary GBMs account for 95% of cases whereas the secondary form represents 5% and mainly affects younger individuals.

1.4.1 Signaling Abnormalities in Astrocytoma

Astrocytoma, like most tumors, present different oncogenic defects in their signal transduction pathways that lead to alterations in cell proliferation, survival as well as apoptosis. Those defects are observed in low-grade astrocytoma but they become more abundant in higher-grade tumors (Maher *et al.*, 2001).

One of the most common abnormality in astrocytoma is the PDGF autocrine signaling pathway characterized by the co-expression of PDGF and its receptor. The constitutive activation of the PDGF receptor leads to an activation of the MAPK pathway and subsequently to a signal of cellular proliferation. The co-expression of the ligand and its receptor is found in all stages of astrocytoma including the initial stages. These observations are consistent with PDGF being an initiating event in astrocytoma progression (Lokker *et al.*, 2002).

Another pathway in which the receptor is constitutively activated is the EGF pathway. There is an intragenic deletion between exons 2-7 of the EGF receptor gene that leads to constitutive activation of the MAPK pathway (Reardon *et al.*, 2006). It is

thought to induce glial cell transformation through increased proliferation and inhibition of apoptosis (Hulleman and Helin, 2005).

Another genetic defect in astrocytoma is the loss of the tumor suppressor gene, the phosphatase and tensin homolog deleted on chromosome 10 (PTEN). PTEN is a phosphatase and negative regulator of the PI3K signaling pathway which is a pathway involved in cell survival, inhibition of apoptosis and tissue neovascularization (Jagannathan *et al.*, 2006). Absence of PTEN results in an up-regulation of AKT in the PI3K pathway that leads to the survival of the tumor cell via the AKT/PKB kinases (Besson and Yong, 2001).

It has been shown that several PKC isozymes are involved in the proliferation and invasion of astrocytoma and glioblastoma. More precisely, the PKC alpha isoform is expressed at high levels in some tumor cells and is critical for the sustained growth and maintenance of tumorigenicity of malignant glia (Ahmad *et al.*, 1994). Targeting of PKCα has been achieved through antisense strategies. Cells overexpressing the antisense for PKCα were shown to have a reduced proliferation rate. This observation suggests that the inhibition of PKC isoforms is an important target for arresting the growth of astrocytoma.

1.4.2 Cx43 and Astrocytoma

The main cell type that shows extensive and high gap junctional coupling in the brain is the astrocyte. The main role of astrocytes is to support neurons in a metabolic and trophic manner. The main connexin expressed in astrocytes is Cx43 (Nakase and Naus, 2004). As stated previously, cancer cells usually express lower connexin levels. In

astrocytoma, only high-grade tumors show a decrease in Cx43 levels. An inverse correlation has been established between Cx43 expression and astrocytoma malignancy *in vitro* (Soroceanu *et al.*, 2001). Grade 1 and 2 astrocytoma express normal astrocytic levels of Cx43 (Mesnil *et al*, 2005) whereas Grade IV GBMs show a minimal expression of the protein (Shinoura *et al.*, 1996; Mesnil *et al.*, 2005). This inverse correlation between Cx43 and tumor malignancy further supports the notion that a lack of gap-junctional communication contributes to tumor formation and evolution towards an invasive phenotype.

1.5 Caveolae and Cx43

Caveolae were originally described in the mid 1950s as nonclathrin-coated flask-shaped membrane invaginations of 50-100 nm in diameter (Smart *et al.*, 1995). Caveolae are rich in cholesterol and sphingolipids and can exist as single entities or as clusters (Krajewska and Maslowska, 2003). Caveolae are most abundant in terminally differentiated cells and are anchored by the actin cytoskeleton. Caveolae are mainly composed of proteins called caveolins. There are three caveolin isoforms in humans: cav-1, cav-2 and cav-3. Cav-1 and -2 are usually co-expressed in terminally differentiated cells such as epithelial and endothelial cells, adipocytes, fibroblasts, smooth muscle cells (Krajewska and Maslowska, 2003) as well as primary astrocytes (Zschocke *et al.*, 2004). Cav-3 has been shown to be mainly muscle specific.

Several functions have been proposed for caveolae, such as clathrin-independent endocytosis, potocytosis (the uptake of small molecules into cells), cholesterol transport and regulation of signal transduction (Krajewska and Maslowska, 2003). Caveolae

contain various receptors, intracellular signaling molecules and proteins such as growth factor receptors, G-proteins, adenylate cyclase, PKA and PKC. They ensure that the different signaling molecules are compartmentalized and can interact together. Thus in addition to their structural role, there is significant evidence for their involvement in the modulation of cell signaling.

As previously discussed, aberrations in signaling pathways have been shown to be associated with a variety of pathologies, including cancer. There is growing evidence that the altered expression of caveolins contributes to such diseases as cancer, muscular dystrophy and Alzheimer's dementia. In fact, Cx43 has been shown to be directly targetted to caveolae and specifically interact with caveolin-1 (Schubert *et al.*, 2002; Lin *et al.*, 2003). Interestingly, it was shown that caveolin-1 was down-regulated in several high-grade tumors in different cell lines (Zhang *et al.*, 2006; Burgermeister *et al.*, 2007).

1.6 RATIONALE AND OBJECTIVES

Compromised GJIC has been clearly shown to play a role in the pathophysiology of cancer. The GJ channel is the main mediator of intercellular communication and, as such, is a potential target for therapeutic intervention. In several types of tumor cells, Cx43 is abnormally localized and is absent from the plasma membrane. Although the regulatory mechanisms of this abnormal localization are unclear, it is hypothesized that it involves phosphorylation of the connexin since phosphorylation has been known to play a role in connexin transport to the membrane. The benefits of deciphering the signaling pathways responsible for this aberrant localization are clear.

The goal of this study is to establish the Cx43 expression and phosphorylation profiles in two astrocytoma cell lines of varying malignancy and to try to identify the signaling pathways involved in the Cx43 sub-localization. We utilize a pharmacological approach using selective protein kinase inhibitors and characterize the effect on Cx43 expression and localization. The deciphering of these pathways could help us to elucidate how GJIC could be restored in astrocytoma or if the aberrant localization of the connexin confers a new function thus giving us insights on pharmacological therapies.

The objectives of this study can be summarized as follows:

1. to establish the expression and phosphorylation profiles of Cx43 as well as GJIC function in two astrocytoma cell lines;
2. to determine the signaling pathways involved in the sub-localization of Cx43 in astrocytoma; and
3. to determine the correlation between Cx43 and caveolin-1 expression/localization.

2.0 MATERIALS AND METHODS

2.1 Cell Lines and Culture Conditions

U-251 MG (IFO50288) and U-87 MG (ATCC#: HTB-14) human astrocytoma cells were used for the experiments. U-251 MG cells were grown in Minimum Essential Medium (MEM, Gibco) supplemented with 10% (v/v) fetal bovine serum (HyClone), streptomycin (HyClone, 100 μg/ml) and penicillin (HyClone, 100 U/ml), nucleosides (Sigma; adenosine 0.8g/L, guanidine 0.85g/L, cytidine 0.73g/L, uridine 0.73g/L and thymidine 0.24g/L), 1% (v/v) sodium pyruvate (HyClone), 1% (v/v) non-essential amino acids (HyClone), gentamicin (Wisent, 0.24 μg/ml) and sodium bicarbonate (Wisent, 2.2g/L). Cells were grown in T75 flasks (Falcon) at 37°C in 95% atmospheric air / 5% CO_2. The cell culture was maintained by subculturing the cells every third day according to the following procedure. The medium was removed and the 85-90% confluent cells were washed with Ca^{2+}- and Mg^{2+}- free phosphate buffered saline (PBS; 137 mM NaCl, 2.7 mM KCl, 4.3 mM Na_2PO_4, 1.4 mM KH_2HPO_4, pH 7.2; Sigma) followed by subsequent dissociation of the cells from the substrate with 0.15% trypsin-EDTA (HyClone). The cells were then resuspended in medium and centrifuged at low-speed in a centrifuge (Baxter Megafuge 1.0 R, Heraeus Instruments) for 5 minutes at 4°C at 150 g. The supernatant was discarded and the cell pellet was resuspended in fresh medium. The cells were then counted in the presence of trypan blue using a hemocytometer and $1x10^6$ cells were seeded in T75 flasks (Falcon).

U-87 MG cells were grown in Dulbeco's Modified Eagle's Medium (DMEM, Gibco) supplemented with 10% (v/v) fetal bovine serum, streptomycin (100 μg/ml) and penicillin (100 U/ml), nucleosides (adenosine 0.8g/L, guanidine 0.85g/L, cytidine

0.73g/L, uridine 0.73g/L and thymidine 0.24g/L), 1% (v/v) sodium pyruvate, 4% (v/v) non-essential amino acids, gentamicin (0.24 μg/ml), sodium bicarbonate (3.7g/L) and 2.2 g/L of HEPES (Sigma). Cells were grown in the same conditions using the same technique as previously described.

2.2 Cell Treatments

Cells were treated with protein kinase inhibitors at a final concentration of 5 μM Bisindolylmaleimide I (BisI) (LC Laboratories), 2 μM Protein Kinase A Inhibitor (PKAI) (Calbiochem), 50 μM PD98059 (Calbiochem), or 10 μM SB203580 (Calbiochem). In addition, cells were treated with the flavanoid Morin (Sigma) at a final concentration of 40 μM. The regular medium, MEM or DMEM with HEPES was replaced with medium supplemented with one of the aforementioned compounds. Cells were incubated at 37°C for 24 hours.

2.3 Estimation of Cell Population

Cells were seeded at a concentration of 5 x 10^5 on 58 cm^2 Starstdet culture plates containing 10 ml of the appropriate culture media. Cells were counted every day for a period of 4 days by following the same procedure as for subculturing. The experiment was done in triplicate. Reverse-phase micrographs of the cell culture were taken each day with a DAGE-MTI camera with the assistance of Image Pro 4.5 software.

2.4 Antibodies

Table 2. Antibodies used for the experiments described in the thesis.

Antibody	Supplier	Application Dilution	
		Immunocytochemistry	Immunoblotting
Cx43 (H-150) rabbit	Santa Cruz	1:200	1:1000
phosphoCx43 (Ser-255) rabbit	Santa Cruz	1:200	1:1000
phosphoCx43 (Ser-262) rabbit	Santa Cruz	1:200	1:1000
phosphoCx43 (Ser-279/282) goat	Santa Cruz	1:200	1:1000
phosphoCx43 (Ser-368) rabbit	Santa Cruz	1:200	1:1000
caveolin-1 (7C8) mouse IgG1	BD Biosciences	1:200	1:1000
β-tubulin (H-235) rabbit	Santa Cruz	-	1:1000
AlexaFluor 488nm goat anti-rabbit IgG	Molecular Probes	1:500	-
AlexaFluor 488nm donkey anti-goat IgG	Molecular Probes	1:500	-
AlexaFluor 488nm goat anti-mouse IgG	Molecular Probes	1:500	-
Goat anti-rabbit alkaline phosphatase IgG (H+L)	Jackson ImmunoResearch Laboratories, Inc.	-	1:5000
Donkey anti-goat alkaline phosphatase IgG (H+L)	Jackson ImmunoResearch Laboratories, Inc.	-	1:5000
Goat anti-rabbit IgG-HRP	Santa Cruz	-	1:5000
Donkey anti-goat IgG-HRP	Santa Cruz	-	1:5000

2.5 Immunofluorescence Microscopy

The following antibodies were used (all antibodies are from Santa Cruz): anti-Cx43 (H150) rabbit polyclonal antibody, anti-phosphoCx43 (Ser-255) rabbit polyclonal antibody, anti-phosphoCx43 (Ser262) rabbit polyclonal antibody, anti-phospho (Ser279/282) goat polyclonal antibody, anti-phospho (Ser368) rabbit polyclonal antibody.

For immunofluorescence microscopy, 5 x 10^4 cells were seeded on glass coverslips (Bellco Glass) and grown for the appropriate time. Cells were then washed twice with PBS and fixed for 30 minutes in 4% paraformaldehyde (Sigma) at room temperature. Following two PBS rinses, cells were permeabilized with 0.1% Triton X-100 (Sigma) for 10 minutes and then blocked for 1 hour with 1% BSA (HyClone) in PBS. The fixed cells were then incubated with the appropriate primary antibody at a dilution of 1/200 in 1% BSA overnight at 4°C. Cells were then washed twice with PBS and incubated with the Alexa 488 fluorescein-conjugated secondary antibodies at a dilution of 1/500 for 1 hour at room temperature. Two PBS washes were made to remove excess antibodies. Cells were observed with a Coulter microscope set with epifluorescence and the corresponding fluorochrome filters. Pictures were taken with a DAGE-MTI camera with the assistance of Image Pro 4.5 software.

2.6 Total Protein Extraction

Subconfluent cultures in 100 mm tissue culture plates were washed twice with Ca^{2+} - and Mg^{2+} - free PBS and lysed by the addition of 0.3 ml of RIPA buffer (PBS, 1% NP40, 0.5% sodium deoxycholate, 0.1% SDS, pH 7.2) with freshly added protease inhibitors (0.57 mM Phenylmethylsulfonyl (PMSF), 1 U/ml aprotinin, 1 U/ml leupeptin, 1mM

sodium orthovanadate; all inhibitors were from Sigma) and incubated on ice for 5 minutes. Cells were then scraped and passed 10 times through a 26-gauge syringe needle to shear the DNA. The cell lysate was incubated 30 min on ice and centrifuged 30 min at 10 000 g at 4°C in a microcentrifuge. Protein concentration was determined by the Bradford method using a protein assay kit (Bio-Rad Laboratories).

2.7 Nuclear Isolation and Extraction

Nuclei were isolated from cells grown in 15 cm petri dishes by incubation with 600 μL of hypotonic buffer (10 mM HEPES buffer (pH 8.0), 0.5 mM KCl, 2 mM $MgCl_2$) containing 9.9 μg/mL leupeptin, 1 μg/mL aprotonin, and 100 μg/mL PMSF and sodium orthovanadate for 10 minutes on ice. Cells were then scraped, vortexed for 5 minutes and centrifuged at 850 g for 5 minutes. The supernatant was collected and labeled as the cytoplasmic fraction. The nuclei pellet was lysed with 500 μL of nuclear lysis buffer (20 mM Tris (pH 7.5), 50 mM NaCl, 0.5% Nonidet P40, 0.5% sodium deoxycholate, 0.5% SDS, 1 mM EDTA) containing 9.9 μg/mL leupeptin, 1 μg/mL aprotonin, and 100 μg/mL PMSF and sodium orthovanadate, syringed 10 times through a 26 gauge needle, and centrifuged for 30 minutes at 10 000 g. The supernatant was collected and labeled as the nuclear fraction. Protein concentration was determined by the Bradford method using a protein assay kit (Bio-Rad Laboratories).

2.8 Immunoblotting

50 μg of proteins, quantified as mentioned above were boiled for 90 seconds at 100°C. Samples were separated on 10% SDS acrylamide gel electrophoresis (SDS-

PAGE) and electro-transferred to nitrocellulose membranes (BioRad). Membranes were probed with the appropriate primary antibody as mentioned previously (1:1000) in 1% BSA in tris-buffered saline with Tween 20 (TBST) overnight on a shaker at 4°C. Membranes were washed in TBST and probed with alkaline phosphatase-conjugated secondary antibodies (1:5000) for 1 hr at room temperature. Colorimetric detection was done by BCIP/NBT (Sigma) and chemiluminescence was performed using the Luminol detection kit (Santa Cruz). The intensity of the bands was quantified using the GelPro system (Media Cybernetics). Loading controls were standardized using β-tubulin.

2.9 RT-PCR

Sub-confluent cells were grown in 100 mm Petri dishes and their RNA was extracted using Trizol according to the manufacturer's protocol (Invitrogen). 4 μg of RNA was treated with RQ1 RNase-free DNase (Sigma) to remove excess DNA from the sample. RNA samples were submitted to reverse-transcription using random hexamer primers and MuLV Reverse Transcriptase according to the manufacture's protocol (New England Biolabs). PCR was performed using specifically designed primers for human Cx43 and human GAPDH was used as a loading control (Table 3).

Table 3. Primer sequences for the detection of human Cx43 and human GAPDH in RT-PCR.

Gene	Sequence (5′→3′)	PCR product size (bp)	Annealing temperature (°C)
Human Cx43	F : CGCCTATGTCTCCTCCTG R : TGCTGACGACCGAGACGA	275	52.5
Human GAPDH	F : GGGAAACTGTGGCGTGAT R : AGCGTCAAAGGTGGAGGA	315	56.5

PCR was performed using JumpStart AccuTaq LA DNA polymerase using the manufacturers' procedure. An initial denaturation step was performed at 94°C for 7 minutes, followed by 35 cycles of the following steps: 94°C for 30 seconds, the corresponding annealing temperature (52.5°C for Cx43 and 56.5°C for GAPDH) for 1 minute and 72°C for 1 minute. There was a final extension step at 72°C for the last 7 minutes. cDNA samples were then subjected to a 2% agarose gel horizontal electrophoresis and the bands were visualized using UV light.

2.10 Scrape Loading Dye Transfer Assay

GJIC in both cell lines was assayed using the scrape loading procedure with a membrane impermeable dye. Cells were washed twice with Ca^{2+}- and Mg^{2+}- free PBS and approximately 70 µl of Lucifer Yellow (Sigma, 0.1% dye in PBS) was loaded intracellularly by scraping on a monolayer of cells grown on glass coverslips with a 26-gauge needle. The dye solution was left on the coverslip for 3 minutes at room temperature. The solution was then removed by washing four times with PBS. The cells were then examined with an inverted epifluorescence microscope (Olympus) equipped with an appropriate filter. The level of GJIC was determined by examining the extent of Lucifer Yellow transfer into neighboring cells. The pictures were taken with the DAGE-MTI camera with the assistance of Image Pro 4.5 software.

2.11 Isolation of Lipid Rafts/Caveolae

Approximately 20 x 10^6 cells were washed three times with ice-cold PBS, scraped on ice and pooled. The cell suspension was then centrifuged at 1200 g at 4°C for 10 minutes and the supernatant was then discarded. The pellet was subsequently resuspended in 2 mL of MES buffer (25 mM MES (Sigma), 150 mM NaCl, pH 6.5) containing the previously mentioned protease inhibitors. Cells were then homogenized in a pre-chilled ballbearing homogenizer approximately 20 times. Cell homogenates were mixed with Triton X-100 (Sigma) to a final concentration of 1% (v/v) and incubated on ice for 30 minutes. An equal volume (2 mL) of sucrose solution (80% w/v, Sigma; prepared in MES buffer) was then added to the cell homogenates. The cell suspensions were then loaded into 12 mL ultracentrifuge tubes (for SW41 rotor, Beckman Instruments). The Triton X-100/80% sucrose cell lysates (4 mL) were then overlaid with 4 mL of 30% sucrose and 3.6 mL of 5% sucrose (in MES buffer). The tubes were then ultracentrifuged (Optima^{TM} L-100 XP ultracentrifuge--Beckman Coulter) at 189 000 g for 18h at 4°C. After centrifugation, 13 fractions of 900 µL each were collected from the top of the tube. 100 µL of each fraction was resuspended in loading buffer and subjected to SDS-PAGE electrotransfer as previously described (Zhang *et al.*, 2004). Membranes were probed with Cx43 primary antibody (H-150) as well as cav-1 (both from Santa Cruz).

2.12 Confocal Microscopy

5x 10^4 cells were seeded on glass coverslips and were fixed, permeabilized and labeled with the H-150 anti-Cx43 or anti-caveolin-1 antibodies, as previously described. An Alexa488 fluorescein-conjugated secondary antibody was used to probe the Cx43

and caveolin-1 antibodies and an Alexa647 wheat-germ agglutinin was used as a membrane marker (Molecular Probes). Coverslips were then mounted cells facing down on a glass microslide with VectaShield (Vector Labs) hardening media and kept at 4°C overnight. A LSM-410 Zeiss confocal microscope (Carl Zeiss) was then used to acquire twelve optical sections of the specimens. Each individual optical sections were 1 μm apart and the confocal apparatus was set to generate an image from which 50% of the light come from an optical slice of 1μm thick. The 488 nm and 647 nm lines of a Krypton/Argon laser were used to excite the Alexa488 and Alexa647 conjugates, respectively. The fluorescence emission of the Alexa488 and Alexa647 were alternatively collected from the same individual optical sections after been passed through a 515-540 nm and a 670-810 nm band pass filter, respectively, before being detected by the light detector.

2.13 Analysis of Results

Microsoft Excel 7.0 spreadsheet was used to analyze data and generate the graphs for the effect of PD98059, morin and SB203580 on Cx43 expression/localization. Western blot membranes were scanned using HP Precisionscan Pro. The densitometric analysis of the membrane was performed using Gel-Pro Analyzer 3.1 software.

3.0 RESULTS

3.1 Characterization of the Human Astrocytoma Cell Lines U-251 MG and U-87 MG

As previously mentioned, Cx43 expression differs in human astrocytoma depending on the malignancy of the tumor (Mesnil *et al.*, 2005): the more aggressive the tumor, the more limited the Cx expression and the intercellular communication which favors uncontrolled growth. Therefore one of the main purposes of this study is to compare signaling pathways involved in Cx43 expression and localization in two human astrocytoma cell lines of varying malignancy in the hope to find a new drug target to control the tumor cell's proliferation. The first cell line is U-87 MG, which derives from an anaplastic astrocytoma (Grade III) tumor, whereas the second cell line is U-251 MG, which derives from a glioblastoma multiforme (Grade IV) tumor. The difference in malignancy of the two cell models may help to shed some light on the similarities and differences in Cx43 related signaling in regards to levels of tumorogenicity.

3.1.1 Cellular Kinetics

It is widely accepted in the scientific community that cellular proliferation tends not only to increase significantly in tumors compared to their non-transformed tissue but also that tumors lose control of cell proliferation. To determine if the difference in malignancy between the two cell models was reflected in their growth pattern *in vitro*, the cellular proliferation rates were assessed. Cells were seeded at a density of $5x10^4$ cells per 10cm Petri dish and subsequently counted, using the trypan blue exclusion assay,

every day for 96 hours after seeding (Fig. 4, A). No fresh media or sera were added to the culture dishes for the duration of the experiment. For U-251 MG cells there was a lag period of 48 hours during which the number of cells increased only slightly. After 48 hours the number of cells approximately doubled (Fig. 4, A) and the cells reached confluence after 96 hours (Fig. 4, B). For the U-87 MG cell line, the lag period lasted only for 24h and the number of cells then increased between 48 hours and 72 hours, but to a lesser extent compared to the U-251 MG cell line. After 72 hours the U-87 cell number reached a plateau and stopped increasing likely due to cell-density arrest. Overall the cellular proliferation of the most malignant cell line, U-251 MG, is higher compared to the less malignant cell model and there is no cell density-arrest.

In addition to having varying growth rates the two cell lines show differences in their morphology. U-251 MG cells possess much less cellular processes or extensions compared to the U-87 MG cells (Fig. 4, B). In turn they present lamellipodia characteristic of high malignancy. This was expected since Grade III astocytoma share more similarities to non-transformed astrocytes, which are elongated cells and emit processes. Also U-87 MG cells will form clusters after 72 hours which coincide with the arrest of cellular proliferation and the formation of a plateau while U-251 MG cells maintain their proliferation.

3.1.2 Expression Profile and Sub-cellular Localization of Cx43 in U-251 MG and U-87 MG Cells

In order to identify and further determine the expression levels of Cx43, both RT-PCR and Western blotting were performed to obtain the mRNA transcripts and measure

Figure 4. Growth kinetics of U-251 MG and U-87 MG cells

A: Growth curve of U-251 MG and U-87 MG cells. Cells were seeded at a density of 5 x 10^5 cells per 10 cm diameter Petri dish (78 cm^2 total surface), and grown in the appropriate media as described in Material and Methods. Every 24 h for 4 days after seeding, cells were collected and counted using the trypan blue exclusion assay that permits the distinction of dead (dye permeable) versus live cells (dye impermeable). The numbers plotted indicate the total number of live cells and represent the mean value of 3 separate experiments.

B: Phase contrast microscopy of cultured cells. The phase contrast microscopy images depict the morphology of the cultured cells at 24 h, 48 h, 72 h and 96 h after seeding at a density of 5 x 10^5 cells per 10 cm diameter Petri dish. At 72h and 96h U-87 MG cells formed 3 dimensional clusters (out of focus). Original magnification: 10x.

A

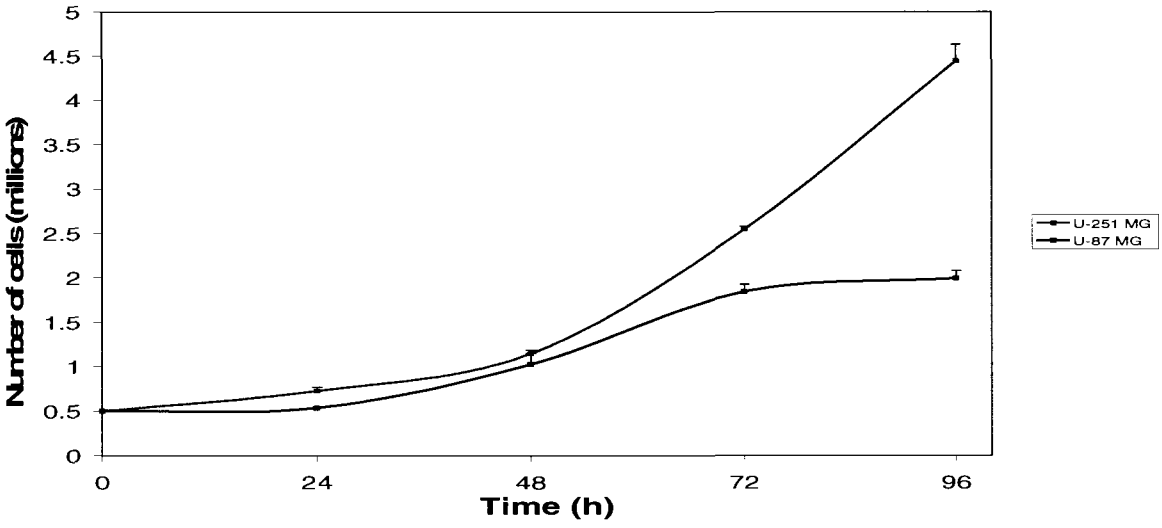
Number of cells (millions)
5
4.5
4
3.5
3
2.5
2
1.5
1
0.5
0
0
24
48
72
96
Time (h)
U-251 MG
U-87 MG

B

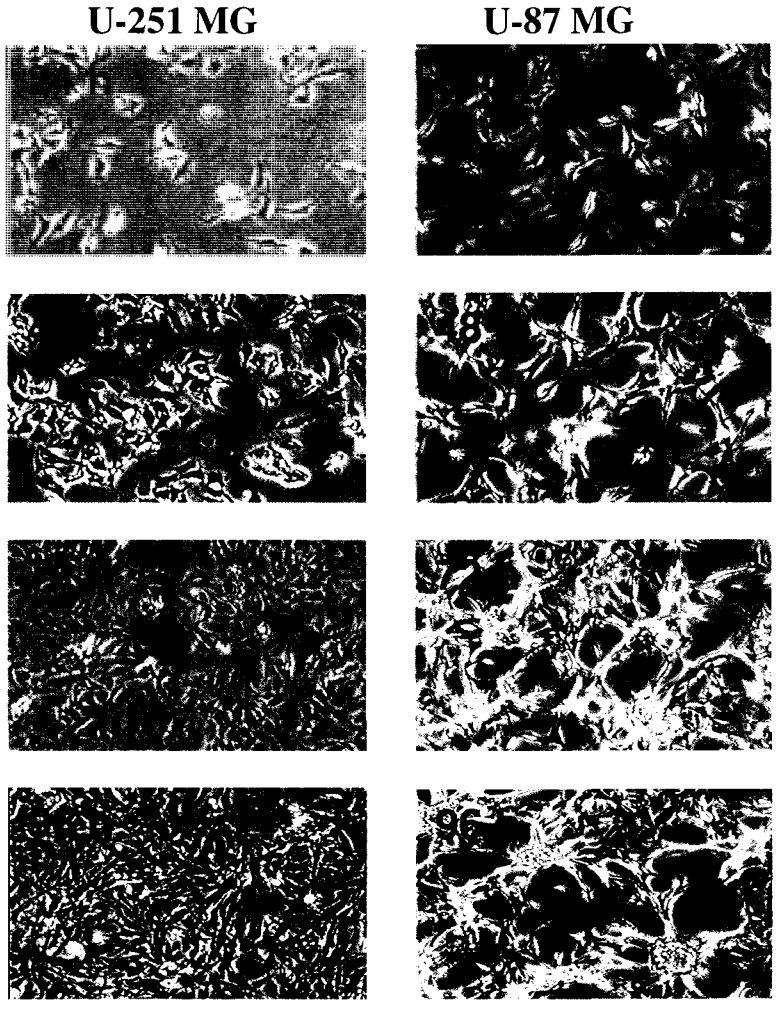
U-251 MG
U-87 MG

matching protein expression levels respectively. For RT-PCR, primers specific for human Cx43 were designed in our laboratory in collaboration with Dr. Jiahua Chen (sequences can be found in the Materials and Methods section). Human GAPDH was used as a house-keeping gene. The extracted mRNA from the two cell types was reverse transcribed; the resulting cDNA was submitted to 35 cycles of polymerase chain reaction and subsequently subjected to agarose gel electrophoresis. The results seem to indicate higher levels of Cx43 mRNA in U-87 MG cells compared to U-251 MGs (Fig. 5, A) although the method is not quantitative. As a positive control, Cx43 mRNA level was also determined in C6Cx43, a rat glioblastoma cell line transfected with a human Cx43 full-length gene. Cx43 mRNA levels in this particular cell line resulted in a much stronger transcript band at the expected position (275 base pairs) on the gel (Fig. 5, A), as is to be expected since the transfected cell line over-expresses Cx43. In order to compare mRNA transcripts between the neoplastic cell lines and normal tissue, mRNA from a normal human brain cortex biopsy was obtained. Results show a strong transcript band of Cx43 compared to the two cell lines but still not as strong as the one found in the transfected rat cell line (Fig. 5, A).

For the detection of Cx43 protein an antibody from SantaCruz H-150 was utilized. The antibody is known to recognize all forms of the Cx43, namely both the phosphorylated and non-phosphorylated forms. The most usual pattern observed in Western blotting is a tri-band: the lower band (~43kDa) representing the non-phosphorylated (NP) Cx43, the second band or P_1 (~45kDa) and the third band or P_2 (~47 kDa) both representing the phosphorylated forms (Crow *et al.*, 1990). Protein extracts

Figure 5. Expression profiles of mRNA and protein levels of Cx43 in U-251 MG and U-87 MG.

A: Qualitative cDNA expression levels of Cx43 in the two cell models, U-251 MG and U-87 MG; C6Cx43, a rat glioblastoma cell line transfected with the Cx43 gene (C6Cx43) (positive control) and in a human brain cortex biopsy (a second control). mRNA was extracted from the samples as described in the Materials and Methods section. mRNA was subsequently reverse transcribed to cDNA and submitted to 35 cycles of PCR. cDNA samples were then subjected to a 2% agarose gel electrophoresis supplemented with propidium iodide and the bands visualized with a light box equipped with a UV lamp . GAPDH primers were used to provide a loading control. Note that the most malignant cell line, U-251 MG, seems to express less cDNA compared to U-87 MG cells, although it should be confirmed via real time PCR.

B: Immunoblotting of Cx43 in human astrocytoma cell lines, U-251 MG, U-87 MG and the rat glioblastoma cell line C6Cx43 from whole cell extracts. Proteins were electrophoretically separated on 10% SDS-PAGE and transferred to a nitrocellulose membrane, as described in the Materials and Methods. The membrane was probed with antibodies anti-Cx43 (H-150) and β-tubulin as a loading control. The H-150 antibody detects the characteristic tri-band in U-251 and U-87 cells often seen for Cx43. In U-87 cells a higher level of the top two bands (P2 and P3) is observed compared to the U-251 cells.

C: Immunofluorescence staining of Cx43 in the human astrocytoma cell lines, U-251 MG and U-87 MG and the rat glioblastoma cell line C6Cx43. Cells were fixed with 4% paraformaldehyde and permeabilized with 0.1% Triton X-100 and probed with Cx43 (H-150) IgG and the appropriate secondary AlexaFluor 488 nm IgG as described in the Materials and Methods section. Reverse phase images are also included. Images were originally taken at 20x magnification. Cx43 is localized almost entirely in the nucleus in U-251 MG cells with some cytoplasmic staining, whereas a small amount can be seen on the cell membrane in U-87 (red arrow). The transfected cell line exhibits very strong membrane Cx43 (red arrow) localization.

A

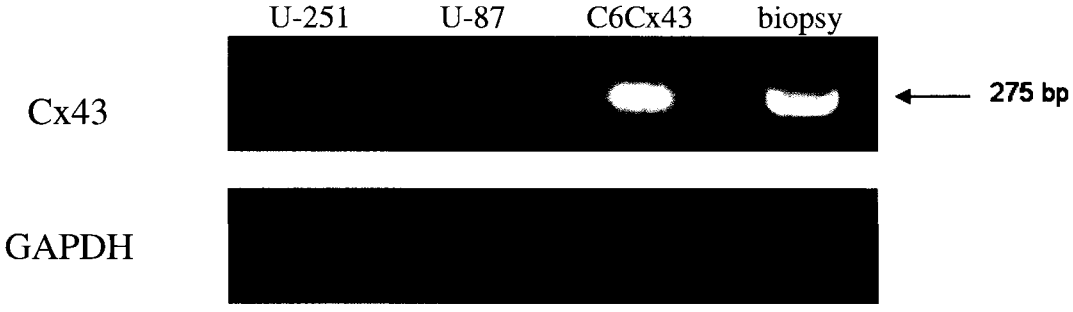
U-251
U-87
C6Cx43
biopsy
Cx43
275 bp
GAPDH

B

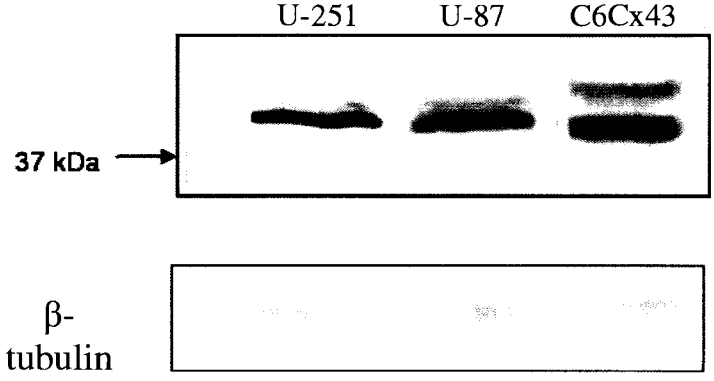
U-251
U-87
C6Cx43
37 kDa
β-
tubulin

C

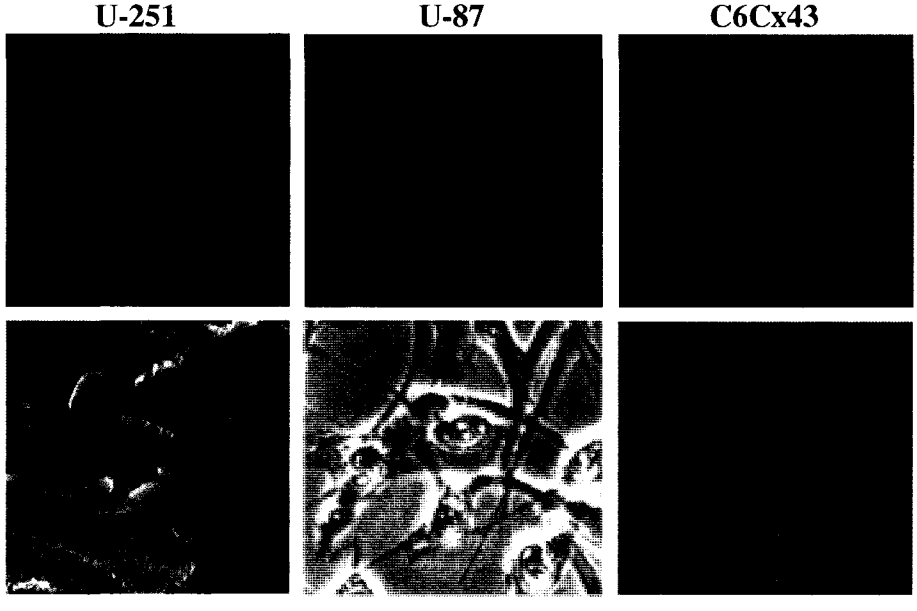
U-251
U-87
C6Cx43

from both cell lines as well as the ones from the transfected rat cell line were subjected to SDS-PAGE as described in the Materials and Methods and the blots were probed with the H-150 Cx43 antibody and the appropriate alkaline phosphatase conjugated secondary antibody. When comparing both astrocytoma cell lines the Cx43 protein phosphorylation levels (P2 and P3) seem to be higher in U-87 MG cells compared to U-251 MG (Fig. 5, B). These results seem to coincide with the RT-PCR results presented above which show a higher level of Cx43 mRNA in U-87 MG, the less malignant cell line. Cx43 protein levels in the rat transfected cell line also seem higher compared to the two neoplastic cell lines. The C6Cx43 cell line showed a Cx43 NP band that migrated more than the two astrocytoma Cx43, a trace of P1 and a wide P2 band that may contain the P3 Cx43. Overall the less malignant cell line, U-87 MG, seems to show higher levels of Cx43 as well as a higher level of Cx43 phosphorylation.

In order to confirm whether the observed bands are indeed phosphorylated in the astrocytoma cells, protein extracts from U-251 MG cells were treated with 1U/μg of calf intestinal alkaline phosphatase (Promega) for four hours at 37 degrees Celsius. Results show the almost complete disappearance of the upper phophorylated bands (P2 and P3) following alkaline phosphatase treatment (Fig. 6). This result indicates that these bands truly represent the phosphorylated isoforms of the Cx43 protein. The well represented lower band is also drastically reduced indicating that it is not the non-phosphorylated band found in the C6Cx43 cell line but is indeed, a phosphorylated band. The results strongly suggest that the connexins are all present as phosphorylated forms in the human astrocytoma cell lines.

Figure 6. Alkaline phosphatase dephosphorylates upper Connexin43 bands.

Immunoblotting of Cx43 in human astrocytoma cell line U-251 MG. Whole protein lysates were incubated for four hours at 37 degrees with or without calf intestinal alkaline phosphatase (1U/μg of protein, Promega). Proteins were then electrophoretically separated on 10% SDS-PAGE and transferred to a nitrocellulose membrane, as described in the Materials and Methods. The membrane was probed with anti-Cx43 (H-150) antibody. Results clearly show that the phosphorylated bands of Cx43 disappear following alkaline phosphatase (AP) treatment or are attenuated by the phosphatase treatment thus demonstrating the phosphorylated nature of the proteins. The lower, large band decreases in intensity without completely disappearing thus demonstrating that it is indeed the P1 band and not the non-phosphorylated isoform (NP).

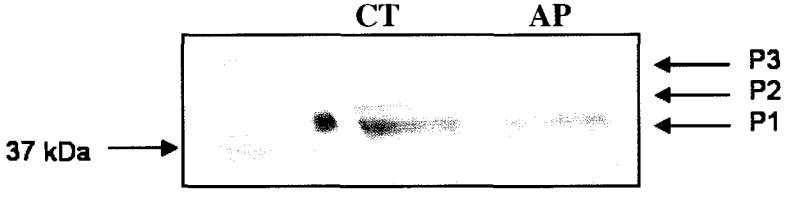
CT
AP
P3
P2
P1
37 kDa

Efficient intercellular communication is not only dependent on connexin expression but also on its membrane sub-cellular localization. In order to determine the sub-cellular localization of Cx43 in our cell models, imunocytochemistry was performed using the H-150 Cx43 antibody. In U-251 MG cells Cx43 is localized mainly in the nucleus and to a lesser extent in the cytoplasm (Fig. 5, C). This result is surprising since Cx43 is almost always found in the cytoplasm or the membrane and in a perinuclear localization in other malignant cell lines such as IMR-32 (Arnold *et al.*, 2005). Here a nuclear localization is shown for the first time in human astrocytoma. There is no evidence however, of Cx43 on the membrane of U-251 cells indicating a probable absence of functional gap junctions. In contrast, in U-87 MG cells, Cx43 is located in the nucleus and cytoplasm as well although at higher levels compared to the other cell line. In addition, the important characteristic of the Cx43 sub-localization in this cell line is its presence on the membrane, as evidenced by the small punctuated structures on the membrane characteristic of gap junctions (red arrow; Fig. 5, C). One speck represents a gap junction plaque which consists of hundreds of gap junction channels. In the transfected rat C6 glioma cell line, the membrane localization is very high thus demonstrating by comparison that membrane bound Cx43 is relatively minimal in U-87 MG.

In summary, the less malignant cell line, U-87 MG, seems to express higher levels of phosphorylated Cx43 than U-251 cells. Also, both cell lines exhibit nuclear and cytoplasmic localization of Cx43; however, only U-87 MG cells show a membrane localization of Cx43.

3.2 Connexin43 Phosphorylation Profiles of U-251 MG and U-87 MG Cells

As stated previously in the Introduction section, phosphorylation plays a crucial role in several steps in the Cx43 life cycle, such as connexon formation, proper translocation of Cx43 to the membrane (Lampe and Lau, 2004), gating of gap junction channels and turnover (Laird, 2005). In the previous section it was determined by Western Blotting that one cell line, U-87 MG, showed higher levels of phosphorylated Cx43 (P2 and P3) compared with the other cell line. In order to investigate in more detail whether the differences in connexin sub-localization were possibly related to the phosphorylation status, the phosphorylation profile of Cx43 in the cell models was assessed. There exist several phosphorylation sites on the human Cx43 protein but only the four main serine residues were examined: Four phospho-Cx43 antibodies were obtained: p-Cx43 (Ser-255), pCx43 (Ser-262), p-Cx43 (Ser-279/282) and p-Cx43 (Ser-368). Both qualitative Western Blotting and Immunocytochemistry were performed with each of the phospho-antibodies in order to determine the phosphorylation status of Cx43 in our cell models.

The first phosphorylation site examined was Ser-255, which is thought to be phosphorylated by MAPK (Lampe *et al.,* 2000). Western blot results show a similar level of phosphorylation on Ser-255 in both cell lines as a band of an apparent molecular weight of 47 kDa which is often referred as the hyperphosphorylated Cx43 (Fig. 7, A; left blot). When a blot probed with phospho-Cx43 (Ser-255) is put adjacent to a blot probed with the H-150 antibody it is clear that the observed tri-band at 43 kDa is absent when using the phospho antibody (Fig. 7, B). As a matter of fact only the upper P3 band is visible on the blot when probed with the Ser-255 antibody. This is interesting since the

Figure 7. Phosphorylation profile of phospho-Cx43 (Ser-255) in U-251 MG and U-87 MG.

A: Whole cell extracts of U-251 MG and U-87 MG cells were loaded on a 10% gel and proteins were resolved by SDS-PAGE. Western Blots were probed with an anti-phoshoCx43 antibody which recognizes phosphorylation on Serine 255. Protein was detected using colorimetry (left blot) and chemiluminescence (right blot) as described in the Materials and Methods section. Note that relatively weak bands are visible at the expected apparent molecular weight of the phosphorylated form of Cx43 (compare to B below) but more pronounced bands are observed in the blot area where degradation bands from connexin are commonly found. The molecular weights of the degradation bands are indicated on the right of the band in kDa.

B: Whole cell extracts of U-251 MG and U-87 MG cells were loaded on a 10% gel and proteins were resolved by SDS-PAGE. Western Blots were probed with an anti-Cx43 antibody (H-150). Note that the Cx43 tri-band observed on the blot probed with the H-150 Cx43 antibody is absent from the blot probed with the phosphorylated antibody. Only the highest band, P3, is detected with the Ser-255 antibody.

C: Immunofluorescence staining of Serine 255 phosphorylated Cx43 in the human astrocytoma cell lines, U-251 MG and U-87 MG. Cells were fixed, permeabilized and probed with pCx43 (Ser-255) IgG and the appropriate secondary AlexaFluor 488 nm IgG. Note the sublocalization of Ser-255 Cx43 in the nucleus in both cell lines as well as the lesser intensity staining in the cytoplasm and the processes in U87 cells. Fluorescent images were merged with the reverse phase to emphasize nuclear localization. Images were originally taken at 10x magnification.

A

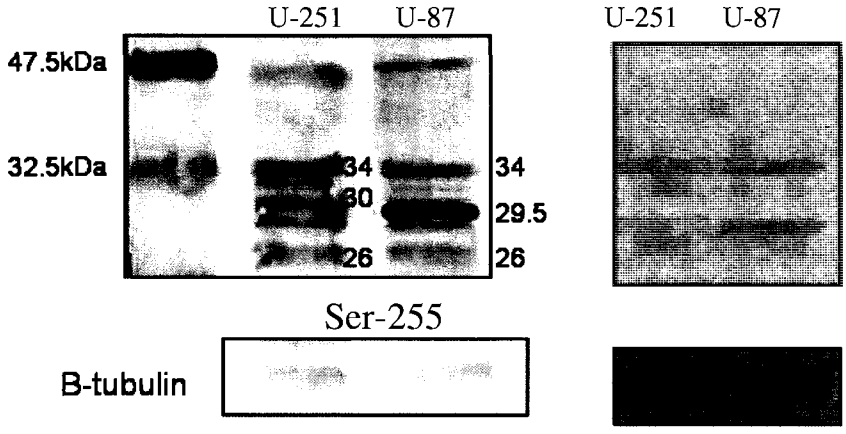
U-251
U-87
U-251
U-87
47.5kDa
32.5kDa
34
30
26
34
29.5
26
Ser-255
B-tubulin

B

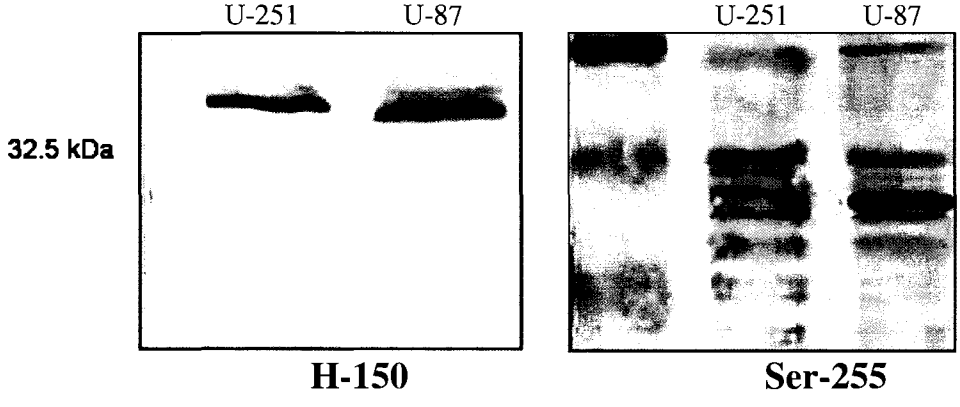
U-251
U-87
U-251
U-87
32.5 kDa
H-150
Ser-255

C

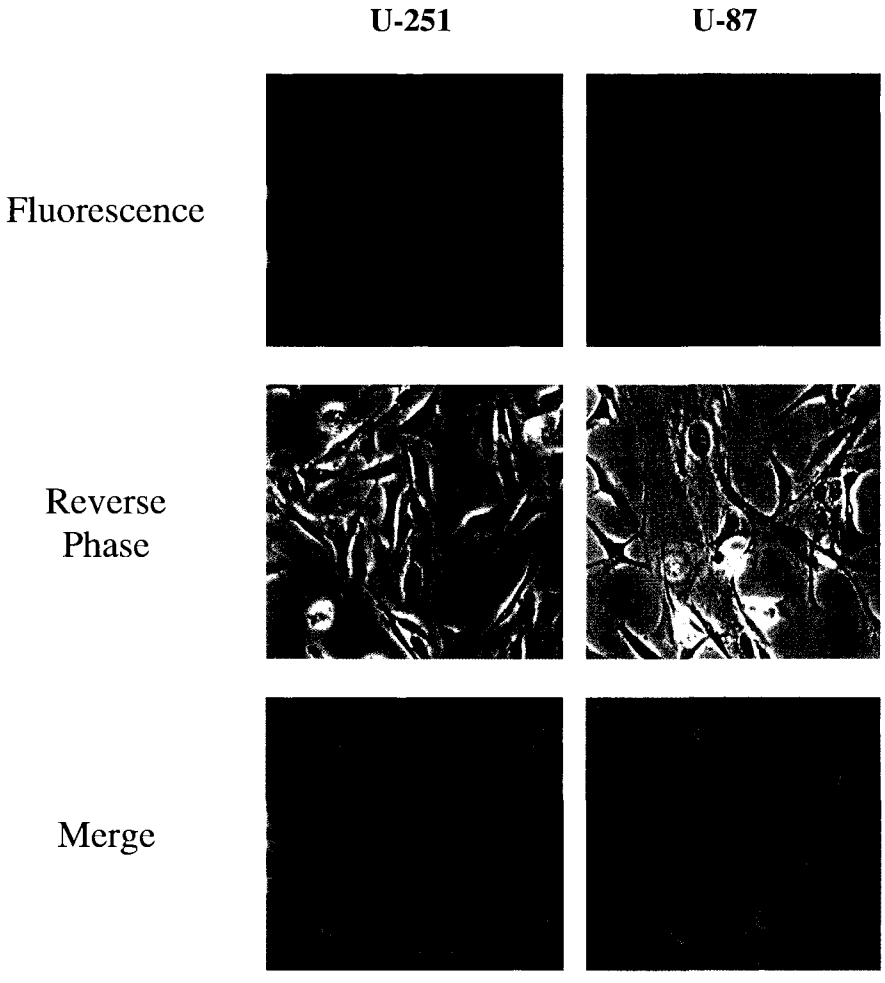

Ser-255 antibody seems to recognize only a hyperphosphorylated, higher molecular weight, form of Cx43 offering an explanation as to why more degradation bands can be observed with this specific antibody. Faint degradation bands are thus visible on the blot reacted with the H-150 antibody. Blots were also subjected to chemiluminescence detection as a mean of comparison (Fig 7, A; right blot). However, only the strongest fragmented bands can be observed with the latter procedure. All other bands were not detected. For this reason colorimetric detection was chosen for all future experiments.

Three important remarks have to be made at this point. Firstly, the basic fragmentation profile detected with the H-150 antibody is always the same in terms of bands migration and apparent molecular weight as measured by scanning. The fragmentation profile differs in the two cell lines. Secondly this profile is also seen when the blots are probed with the phosphorylated specific antibodies and identical in terms of apparent molecular weight. Only the band density is altered depending on the targeted site. Thirdly, the intensity of the bands as a whole may vary from one experiment set to another, however, variations in band density within the sets was always determined in comparison with their matching controls. The fragmentation profile is depicted in the figure 7, A.

There are five bands that appear below 47 kDa in U-251 MG cells (34 kDa, 33 kDa, 30 kDa and 29 kDa as a doublet and 27-26 kDa) that constitute the basic fragmentation profile. In U-87 MG cells, there are less degradation fragments. The main bands are as follows: 34 kDa, 29.5kDa (that appears as a very intense band upon pSer-255 antibody exposure) with a faint band underneath (not measured) and the doublet 27-26 kDa. When comparing the blot probed with the Ser-255 antibody with the one probed

with the H-150 antibody from the same extract (Fig. 7, B) it becomes clear that the phospho-antibody detects the fragmented bands to a much higher degree. This is very interesting as it indicates that the Cx43 fragments are phosphorylated and therefore that they may be part of connexin degradation/turnover. Since all precautions were taken during the cell extraction and Western blotting to avoid artefactual proteolysis, I found it of interest to analyze these bands more thoroughly. It is one of the first reports where degradation bands are taken into consideration. In U-251, the bands at 34 kDa and the 30-29 doublet are pSer-255 positive while heavy phosphorylation of this site is recognized on the 29.5 band in U-87 cells.

Experiments show strong nuclear staining of Ser-255 phosphorylated Cx43 in both cell lines (Fig. 7, C). In addition, both cell lines exhibit cytoplasmic localization of the Cx which seems more extensive in the U-87 MG cells, but this is probably only due to the morphologically more elongated cells.

The next phosphorylation site studied was Ser-262, which has been shown to be phosphorylated by PKC (Lampe *et al.,* 2000). The phosphorylated 47 kDa band was detected in the U-251 MG cell extracts; in contrast this band was absent in the U-87 MG cells (Fig. 8, A). As with the previous phosphorylation site detection, there are several fragments. However, they appear to be of the same molecular weight as was seen for Ser-255. In U-251, bands at 34 kDa, 33 kDa and 30 kDa are pSer-262 positive and thus differ from the ones detected with the Ser-255 antibody. As opposed, in U-87 MG cells all fragmented bands are fainter except for the 29.5 kDa band that was also recognized by the pSer-255 antibody is much stronger (Fig. 8, A; left blot). Again, the chemiluminescence blot only shows the strong 29.5 kDa band in the U-87 cells. As was

Figure 8. Phosphorylation profile of phospho-Cx43 (Ser-262) in U-251 MG and U-87 MG.

A: Whole cell extracts of U-251 MG and U-87 MG cells were loaded on a 10% gel and proteins were resolved by SDS-PAGE. Western Blots were probed with an anti-phoshoCx43 antibody which recognizes phosphorylation on Serine 262. Protein was detected using colorimetry (left blot) and chemiluminescence (right blot) as described in the Materials and Methods section.

B: Whole cell extracts of U-251 MG and U-87 MG cells were loaded on a 10% gel and proteins were resolved by SDS-PAGE. Western Blots were probed with an anti-Cx43 antibody (H-150).

C: Immunofluorescence staining of Serine 262 phosphorylated Cx43 in the human astrocytoma cell lines, U-251 MG and U-87 MG. Cells were fixed, permeabilized and probed with pCx43 (Ser-262) IgG and the appropriate secondary AlexaFluor 488 nm IgG. Note that the Ser-262 Cx43 form is again present in the nuclei, an unusual location in normal cells. Cytoplasmic staining is still present in U-87 MG cells but to a much lesser degree compared to Ser-255 phosphorylated Cx43 (Fig. 7,C). Fluorescent images were merged with the reverse phase to emphasize nuclear localization. Images were originally taken at 10x magnification.

A

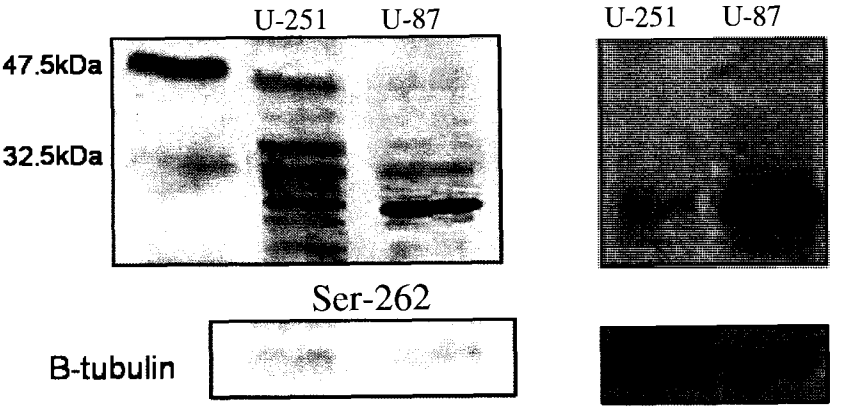
U-251
U-87
47.5kDa
32.5kDa
Ser-262
B-tubulin
U-251
U-87

B

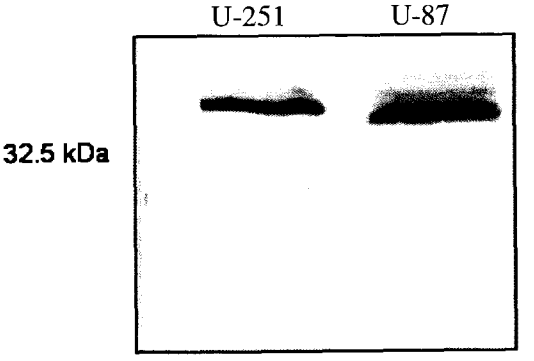
U-251
U-87
32.5 kDa

C

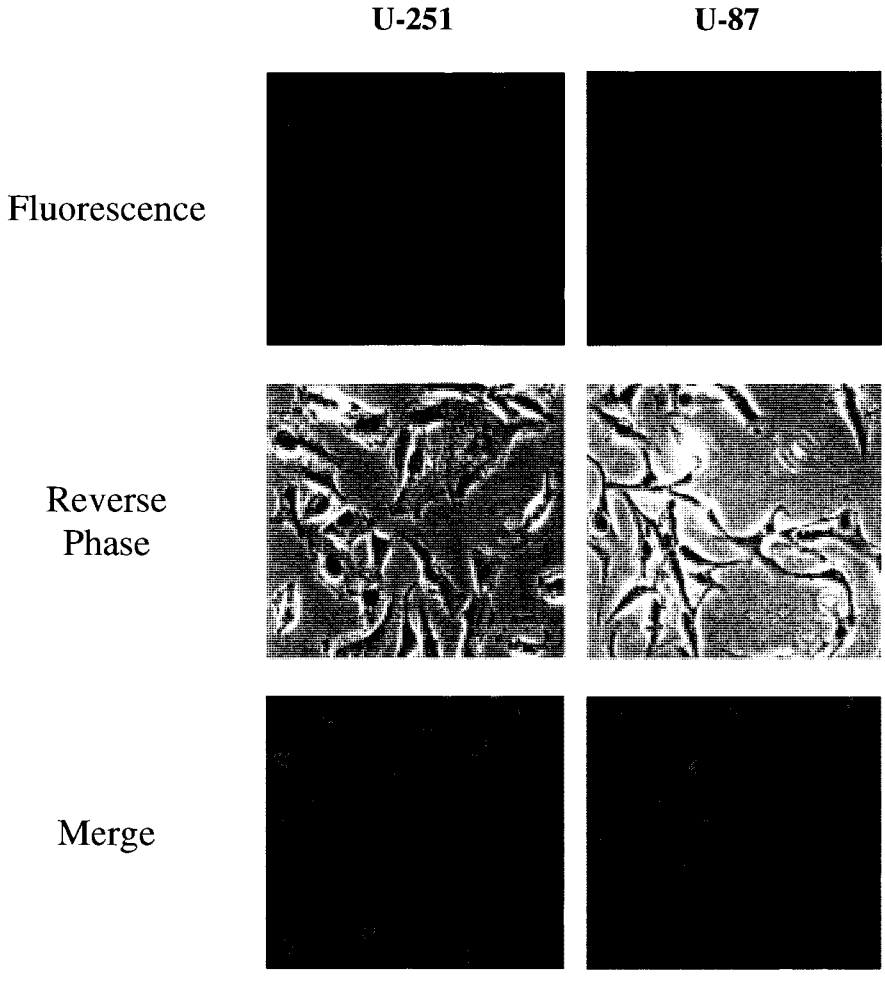

the case with Ser-255, the fragmented bands are much more present compared to the blot probed with the H-150 antibody (Fig. 8, B). This again illustrates that phosphorylation may be associated with most of the fragmented Cx43 bands observed.

Immunocytochemistry experiments showed again a nuclear localization in both cell lines with an absence of staining in the nucleoli (Fig. 8, C). In the U-251 MG cell line there is an almost complete absence of staining elsewhere in the cell, whereas in U-87 MGs there is a slight staining in the cytoplasm (Fig. 8, C).

The third phosphorylation site that was examined in this project was Ser-279/282 which was also been shown to be phosphorylated by MAPK (Lampe *et al.,* 2000). Western blotting experiments showed a higher phosphorylation level on Ser-279-282 in U-251 MG at the non degraded Cx43 molecular weight of 47 kDa (Fig. 9, A; left blot). This site did not react with a matching band in the U-87 cell line. Therefore Ser-262 and 279-282 are not phosphorylated in the Cx43 of U-87 cells. Fragmented bands for this phosphorylation site are less numerous when compared to Ser-255 and Ser-262. U-251 cells show a positive response to the pSer-279/282 antibody on the 29-30 kDa doublet as previously observed for the other two sites investigated. Labeling occurs on the 26-27 kDa doublet. Once again in the U-87 MG cell line the band at 29.5 kDa is recognized. In addition, the 27-26 kDa band is labeled. The blot with H-150 is shown for comparison purposes (Fig. 9, B).

Sub-cellular localization of phosphorylated Cx43 on Ser-279-282 in U-251 MG cells seems to be cytoplasmic with a perinuclear concentration (Fig. 9, C). In U-87 cells however the staining is essentially cytoplasmic and fainter.

Figure 9. Phosphorylation profile of phospho-Cx43 (Ser-279/282) in U-251 MG and U-87 MG.

A: Whole cell extracts of U-251 MG and U-87 MG cells were loaded on a 10% gel and proteins were resolved by SDS-PAGE. Western Blots were probed with an anti-phoshoCx43 antibody which recognizes phosphorylation on Serine 279/282. Protein was detected using colorimetry (left blot) and chemiluminescence (right blot) as described in the Materials and Methods section.

B: Whole cell extracts of U-251 MG and U-87 MG cells were loaded on a 10% gel and proteins were resolved by SDS-PAGE. Western Blots were probed with an anti-Cx43 antibody (H-150).

C: Immunofluorescence staining of Serine 279/282 phosphorylated Cx43 in the human astrocytoma cell lines, U-251 MG and U-87 MG. Cells were fixed, permeabilized and probed with pCx43 (Ser-279/282) IgG and the appropriate secondary AlexaFluor 488 nm IgG. A striking difference is seen in the two models: the Ser-279/282 Cx43 is located at definite sites in or around the nucleus in U251 MG whereas it is diffuse throughout the U87 MG cells. Images were originally taken at 10x magnification.

A

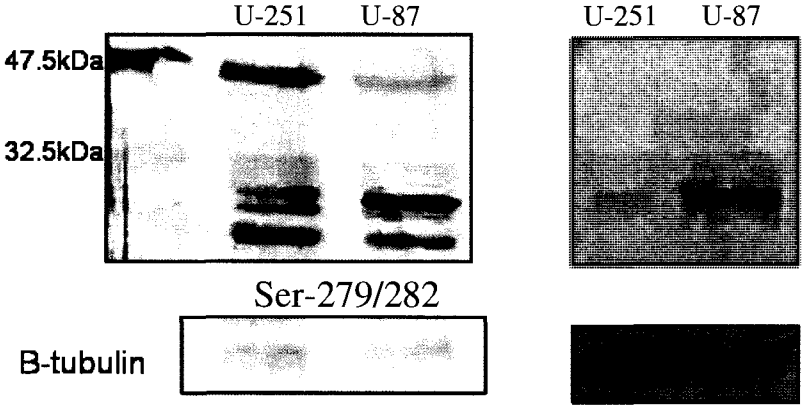
U-251
U-87
47.5kDa
32.5kDa
Ser-279/282
B-tubulin
U-251
U-87

B

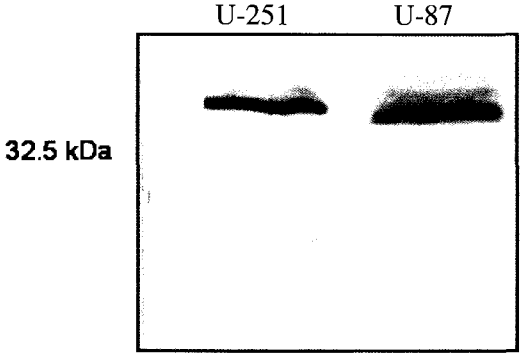
U-251
U-87
32.5 kDa

C

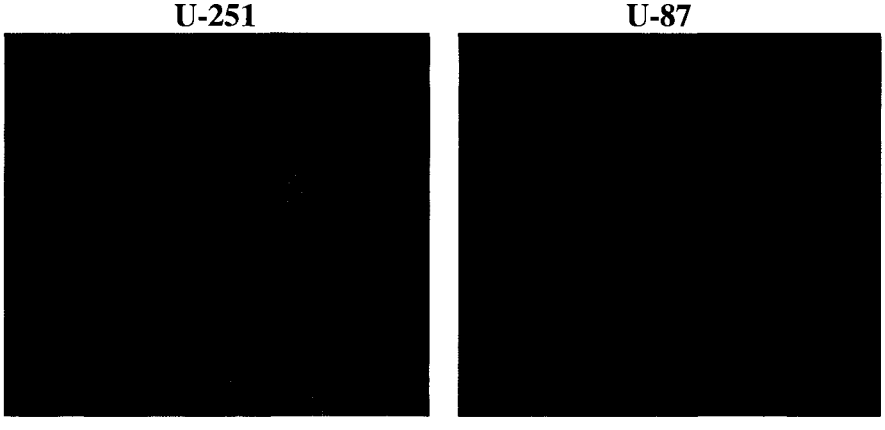
U-251
U-87

Lastly, the level of phosphorylation on Ser-368, the main PKC phosphorylation site, was determined by Western blotting. Western Blots show faint levels of Ser-368 phosphorylytion in U-251 MG cells at the molecular weight of 47 kDa and no band for U-87 MG cells (Fig. 10, A; left blot). Blots probed with this antibody show the typical fragmented bands weakly labeled except for the 34 kDa band that did not react. Unlike the other three phosphorylation sites, the 30 kDa band is very intense in the U-251 MG and the 29.5 kDa band of U-87 is again highly labeled (Fig. 10, A; left blot). In addition, the 32 kDa band is more intense in U-87 MG cells compared to the other cell line. The blot with H-150 is shown for comparison purposes (Fig. 10, B).

Immunocytochemistry experiments show that Cx43 phosphorylated on Ser-368 is found both in the nucleus and the cytoplasm in U-251 MG and U-87 MG cells, (Fig. 10, C). The difference in staining intensity however is hard to distinguish by immunocytochemistry, suggesting very similar levels of phosphorylation on Ser-368.

When performing immunocytochemistry experiments and nuclear staining is shown, it is very hard to determine if the protein is inside the nucleus or bound to the nuclear membrane. In order to confirm whether phosphorylated Cx43 on Ser-255 and Ser-262 was indeed nuclear (Fig. 7, C and Fig. 8, C respectively) confocal microscopy was utilized. Cross-section images of 1 μm were taken to observe whether or not nuclear staining remained present throughout the different sections. In a case where the staining is perinuclear, the phosphorylated Cx43 in the middle cross-sections would appear as a ring around the nucleus. Phosphorylation on Ser-255 in U-251 MG (Fig. 11, A) and U-87 MG cells (Fig. 11, B) show mainly nuclear staining; however a few cells also show perinuclear staining. The same results can be observed with the Ser-262 antibody in both

Figure 10. Phosphorylation profile of phospho-Cx43 (Ser-368) in U-251 MG and U-87 MG.

A: Whole cell extracts of U-251 MG and U-87 MG cells were loaded in a 10% gel and proteins were resolved by SDS-PAGE. Western Blots were probed with an anti-phoshoCx43 antibody which recognizes phosphorylation on Serine 368. Protein was detected using colorimetry (left blot) and chemiluminescence (right blot) as described in the Materials and Methods section.

B: Whole cell extracts of U-251 MG and U-87 MG cells were loaded in a 10% gel and proteins were resolved by SDS-PAGE. Western Blots were probed with an anti-Cx43 antibody (H-150).

C: Immunofluorescence staining of Serine 368 phosphorylated Cx43 in the human astrocytoma cell lines, U-251 MG and U-87 MG. Cells were fixed, permeabilized and probed with pCx43 (368) IgG and the appropriate secondary AlexaFluor 488 nm IgG. Images were originally taken at 10x magnification.

A

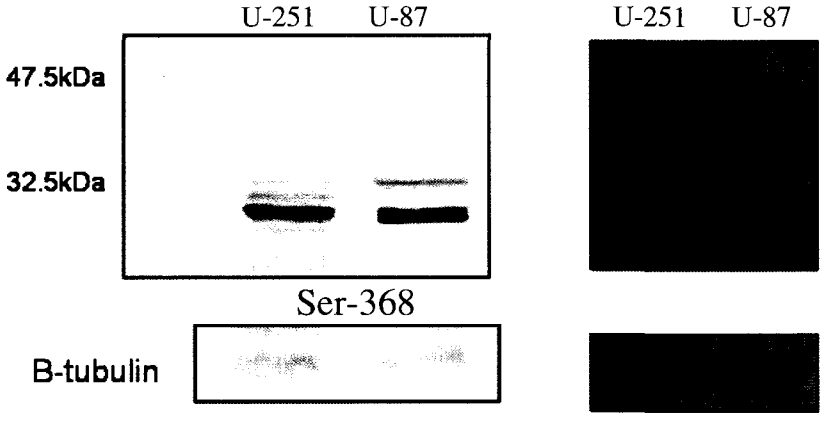
U-251
U-87
47.5kDa
32.5kDa
Ser-368
B-tubulin
U-251
U-87

B

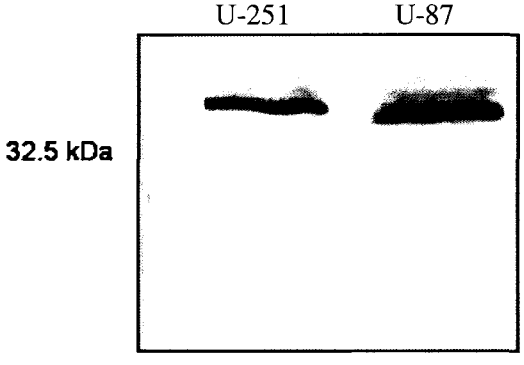
U-251
U-87
32.5 kDa

C

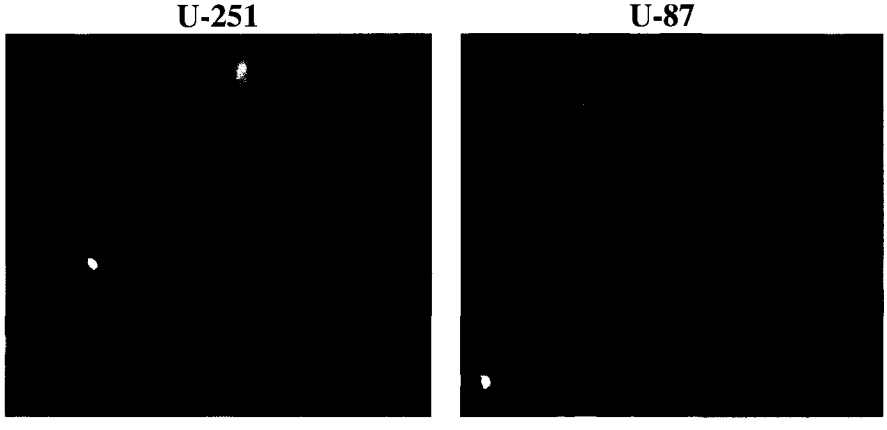
U-251
U-87

Figure 11. Cross-sections of U-251 MG and U-87 MG cells probed with phosphoCx43 (Ser-255) using confocal miscoscopy.

Cross-sections of both **A)** U-251 MG and **B)** U-87 MG cells using confocal miscroscopy. Cells were fixed, permeablized and probed with a Ser-255 phosphoCx43 antibody and the appropriate Alexa 488 secondary antibody. Using confocal microscopy 10 cross-sections of 1 μm each were taken. Sections 3-8 are represented in this figure. The labelling is in the nucleus and the nucleoli are not labeled. Images were originally taken at 66.6x magnification.

A

3

4

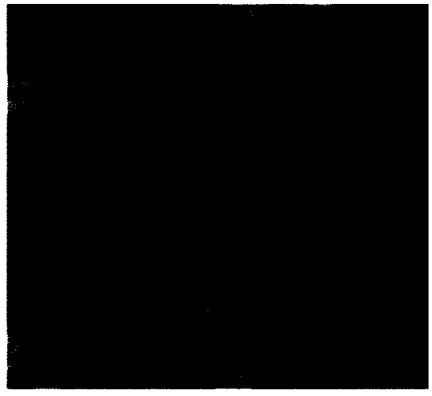

5

6

7

8

B

3

4

5

6

7

8

U-251 MG (Fig. 12, A) and U-87 MG cells (Fig. 12, B) except that perinuclear staining was not observed. Taken together the confocal results confirm that the immuno-stained phosphorylated Cx43 on Ser-255 and Ser-262 are indeed nuclear.

In addition, as a second method to confirm the nuclear presence of Cx43, U-251 MG cells were extracted using a nuclear enrichment method resulting in a nuclear-enriched and a cytoplasmic fraction. Both fractions were subjected to SDS-PAGE, transferred to a nitrocellulose membrane and probed with anti-Cx43 (H-150). Results show a definite band in the nuclear fraction as well as in the cytoplasmic fraction (Fig. 13). These results thus confirm that Cx43 as well as its degradation fragments is indeed mostly nuclear in our cell models. Degradation fragments were barely detectable in the enrichment experiment. This was typical of our experimental results: it was observed that in the majority of the cases (about 60 to 80 extractions and Western blots) fragmentation of the full length protein was observed. The band patterning did not vary but the intensity of the bands did, which we attributed to the physiological state of the culture at the very time of the extraction. Minor proteolysis during extraction however, cannot be ruled out.

In summary the phosphorylation profiles are different in both cell lines. The data indicate that the phosphorylation sites investigated in our experiments, with the exception of pSer-279/282, are not responsible for the phosphorylation of the P1 and P2 but contribute to the P3 bands of the full length Cx43 in U-251 cells. Phosphorylation of the full length Cx43 in U-87 is not (or very weakly) phosphorylated at these sites. There is instead a clear presence of Cx43 fragments that differ in molecular weight and levels depending on their phosphorylation site and are more evidenced in the blots probed with the phospho-specific antibodies than in those probed with H-150 antibody. This seems to

Figure 12. Cross-sections of U-251 MG and U-87 MG cells probed with phosphoCx43 (Ser-262) using confocal miscoscopy.

Cross-sections of both **A)** U-251 MG and **B)** U-87 MG cells using confocal miscroscopy. Cells were fixed, permeablized and probed with a Ser-262 phosphoCx43 antibody and the appropriate Alexa 488 secondary antibody. Using confocal microscopy 10 cross-sections of 1 μm each were taken. Sections 3-8 are represented in this figure. The nucleoli again do not show any staining in the two cell lines. Images were originally taken at 66.6x magnification.

A

3

4

5

6

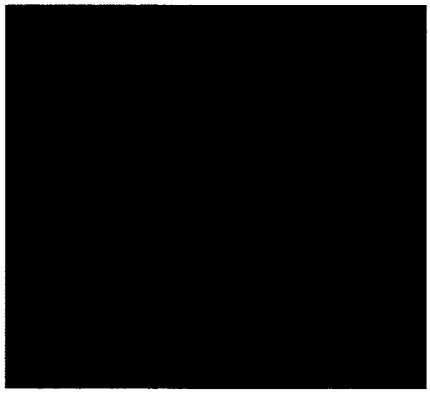

7

8

B

3

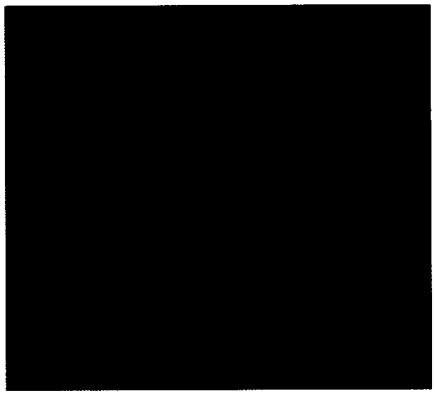

4

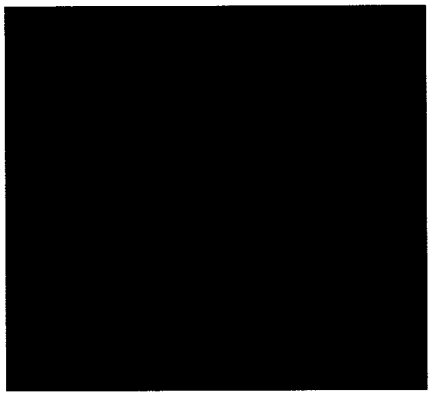

5

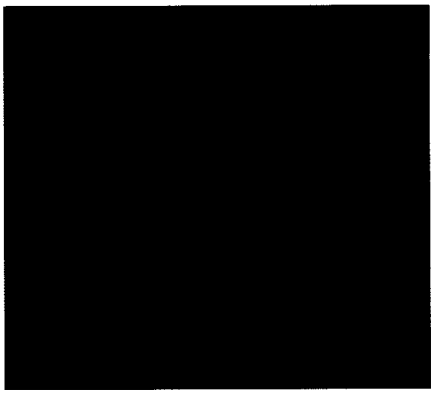

6

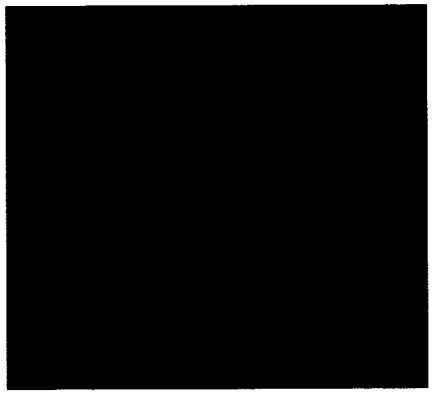

7

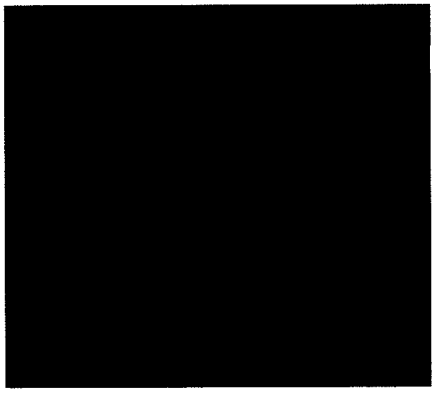

8

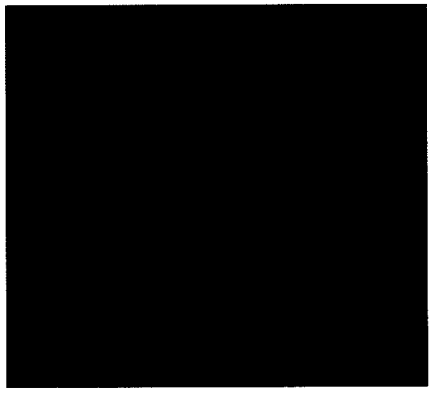

Figure 13. Cx43 Expression and Sub-localization in Nuclear and Cytoplasmic-enriched Fractions in U-251 MG Cells

Immunoblotting of Cx43 (H-150) in U-251 MG cells. Cells were extracted in order to separate the cytoplasmic and the nuclear fractions as described in the Materials and Methods section. Both fractions were electrophoretically separated on 10% SDS-PAGE and transferred to a nitrocellulose membrane. The membrane was probed with the anti-Cx43 (H-150) antibody. Results show the presence of Cx43 in the nuclear-enriched fraction and in the cytoplasmic fraction.

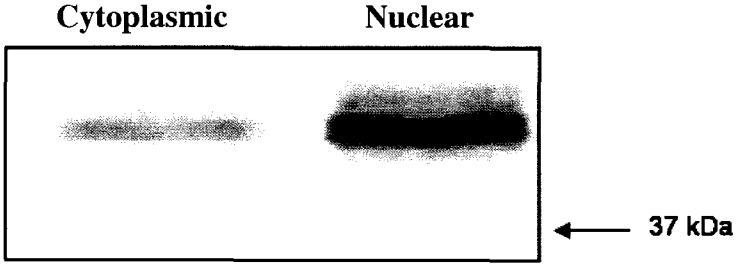
Cytoplasmic
Nuclear
37 kDa

indicate that the phosphorylation sites investigated play a role in the fragmentation of the Cx43 in astrocytoma cells. The fact that some fragments reacts to several specific phospho-antibodies such as the 30 kDa band in U-251 and the 29.5 kDa band in U-87 means that the fragment encompasses these sites from Ser-255 to Ser-279/282. The positive fragment to pSer-368 may generate a band of similar molecular weight that may or may not contain other sites. The band at 27-26 kDa which is characteristic of the pSer-279/282 consensus site in both cell lines may result of further degradation of the previous bands. The fact that there are differences in the specific labeling on given bands supports the hypothesis that the degradation occurs inside the cells and is not artefactual. Most importantly, these fragments are abnormally located inside the nuclei.

3.3 Connexin43 Aberrant Function in Astrocytoma

Connexin43 expression and sub-cellular localization is important in a cell since an absence or an aberrant localization of Cx43 results in a lack or decrease in intercellular communication and a subsequent altered function in terms of proliferation, differentiation and probably apoptosis (Andrade-Rozental *et al.*, 2000). It was previously shown however, in Dr. Jenny Phipps' laboratory that in spite of having restored normal membrane localization in neuroblastoma cells by an increase in intracellular cAMP, the newly formed Cx43 channels are not necessarily functional. In view of our results, it is thus important to assess gap-junctional function especially in U-87 where some of the Cx43 protein was in a normal membrane sub-localization.

3.3.1 Gap Junction Function in U-251 MG and U-87 MG Astrocytoma

The most common method utilized to detect gap junction intercellular communication is Scrape Loading. It consists in applying a small volume of Lucifer Yellow on a confluent monolayer of cells, and then a fine scratch is performed using a 26½ gauge needle. Lucifer Yellow (457.24 Da) cannot penetrate the cell membrane, but it is small enough to pass through gap junction channels. Once the cells have been scraped, the Lucifer Yellow penetrates the cells that are on the edge of the scratch since their membrane integrity has been physically compromised. If gap junctions are present and open, the Lucifer Yellow will diffuse from the damaged cell to neighboring undamaged cells.

Scrape Loading experiments were thus performed on both cell lines in order to determine if they possessed functional gap junctions. Results show that in U-251 MGs only the cells on the edge of the scratch showed Lucifer Yellow fluorescence (Fig. 14), indicating a complete lack of intercellular communication. This result was to be expected since this cell line does not exhibit any Cx43 on its plasma membranes. In U-87 MGs all the cells showed Lucifer Yellow fluorescence, indicating the presence of gap junctional intercellular communication (Fig. 14). The reverse phase (RP) of the scratch in U-251 MG cell's monolayer is shown to illustrate the procedure. As a control, scrape loading was performed on C6Cx43 rat glioblastoma cells transfected with Cx43. Results show strong Lucifer Yellow transfer demonstrating the presence of intercellular communication. Dextran Blue was also added at the same time as Lucifer Yellow. Since Dextran Blue molecules are too big to diffuse through gap junctions (10 000 Daltons) the dye remains in the cells on the edge of the scratch. This confirms the presence of

Figure 14. Gap junction-mediated dye coupling of U-251 MG and U-87 MG cells.

Cultured U251 MG and U-87 MG **(A)** as well as C6Cx43 **(B)** cells as a positive control were scrape-loaded with Lucifer yellow to assess the function of the GJ. Briefly, 70 μL of Lucifer yellow dye was added on top of a confluent monolayer of cells and a small scratch was performed with a 26½ Gauge needle. Cells were then subsequently washed with PBS after 3 minutes of incubation. The reverse phase (RP) of the scratch in U251 MG cell's monolayer below is shown to illustrate the procedure (right side picture). As a control, Scrape loading was performed on C6Cx43 which are known to exhibit strong intercellular communication. Dextran blue (high molecular weight dye) was added as a control to the cells at the same time as Lucifer Yellow. In **(A)** images illustrate the contrast between the two cell lines, one showing extensive dye diffusion (U-87 MG) via GJ, the other showing that the U-251 cell's gap junctions are not functional. In **(B)** images show extensive Lucifer Yellow diffusion whereas the dextran blue dye did not diffuse at all. Images were originally taken at 20x magnification.

A

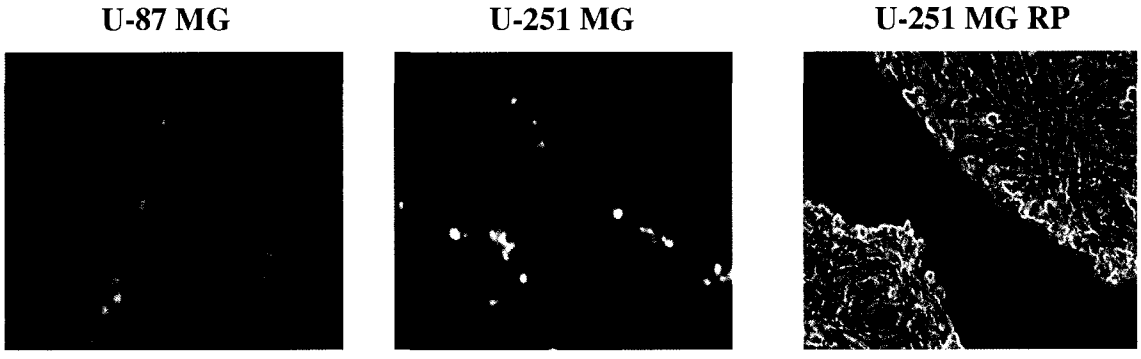

B

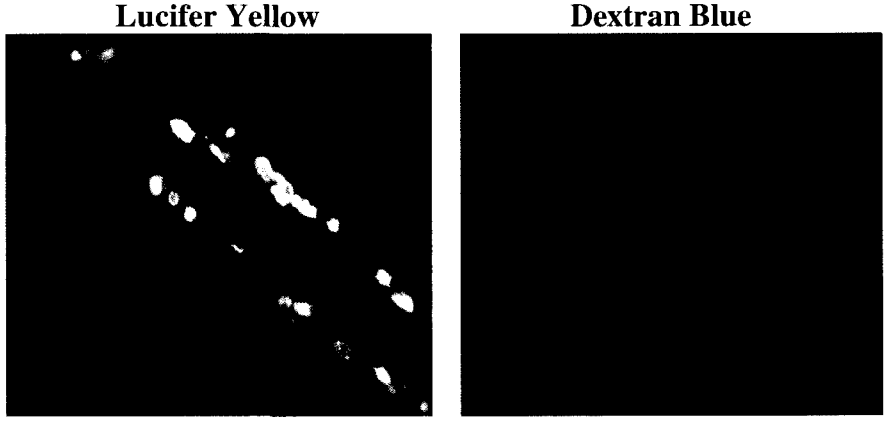

functional gap junctions in C6Cx43 and U-87 MG cells.

3.3.2 Presence of Hemichannels in U-87 MG Astrocytoma

As previously mentioned, recent literature has suggested a non-junctional role for Cx43; such roles could involve functional hemichannels (Plotkin *et al.*, 2002; Evans *et al.*, 2006). The presence or absence of hemichannels was thus determined in both astrocytoma cell lines. Briefly, a small volume of Lucifer Yellow was applied on a monolayer of cells and washed after 3 minutes. Since Lucifer Yellow is cell impermeable, it can only penetrate a cell if open hemichannels are present on the membrane. The hemichannel test was performed on U-251 MG cells and it showed a lack of hemichannels (Fig. 15). In U-87 MG cells however, results show that all the cells in the field possess Lucifer Yellow fluorescence suggesting the presence of functional hemichannels.

In order to confirm the presence of hemichannels U-87 MG cells were treated with a specific hemichannel blocker, flufenamic acid (Knight *et al.*, 2009). Results show a decrease in Lucifer Yellow penetration following treatment with 3 μM of flufenamic acid (Fig. 16). Treatment with flufenamic acid is not expected to completely block the entry of Lucifer Yellow since it does not block all hemichannels. The decrease of penetration observed suggests the presence of open hemichannels in U-87 MG cells. In light of these results we can no longer say that the presence of Lucifer Yellow in U-87 MG cells other than those next to the scratch is the result of functional gap junctions (Fig.14), since some dye would have been incorporated in all cells before the scratch was made. The hemichannels on the contrary are likely responsible for the incorporation of

Figure 15. Detection of hemichannels in U-251 MG and U-87 MG cells.

Cultured U251 MG and U-87 MG cells were seeded as a monolayer and loaded with Lucifer yellow (fluorescent images on the left; corresponding reverse phase images on the right). Briefly, 70 μL of Lucifer yellow dye was added on top of a monolayer of cells and incubated for 3 minutes. Cells were then subsequently washed and observed under an epifluorescence microscope. Although there is no cell loading through membrane injury in the U87 cells, the Lucifer yellow dye penetrates the cells. U251 cells do not show any dye incorporation. Images were originally taken at 20x magnification.

U-251

U-87

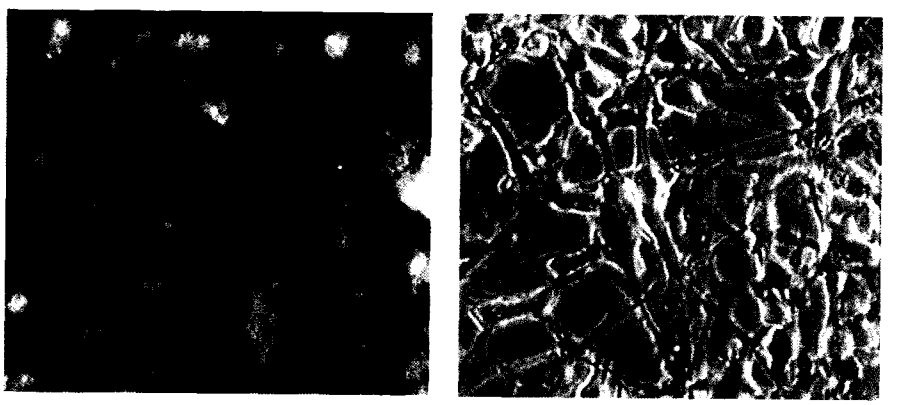

Figure 16. Inhibition of hemichannels with flufenamic acid in U-87 MG cells.

Cultured U-87 MG cells were seeded as a monolayer upon treatment with 3 μM of a hemichannel inhibitor, flufenamic acid, and loaded with Lucifer yellow (fluorescent images on the left; corresponding reverse phase images on the right). Briefly, 70 μL of Lucifer yellow dye was added on top of a monolayer of cells and incubated for 3 minutes. Cells were then subsequently washed and observed under an epifluorescence microscope. The inhibition of dye incorporation in U87 cells treated with the specific hemichannel inhibitor flufenamic acid confirms the presence of functional hemichannels. Images were originally taken at 20x magnification.

Control

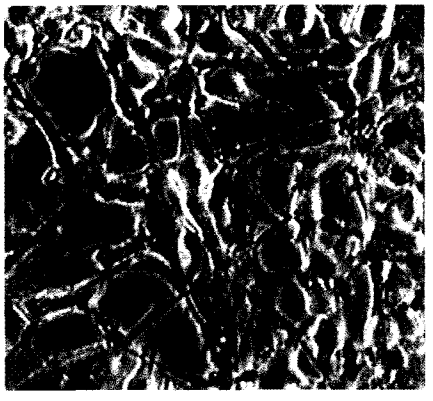

Flufenamic acid treated

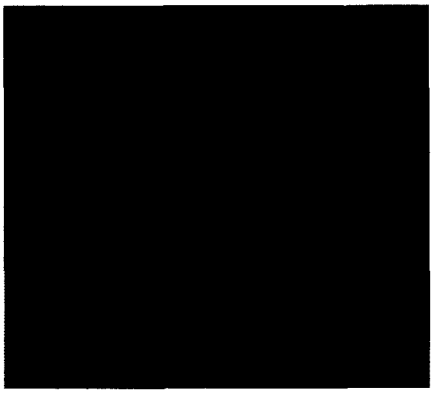

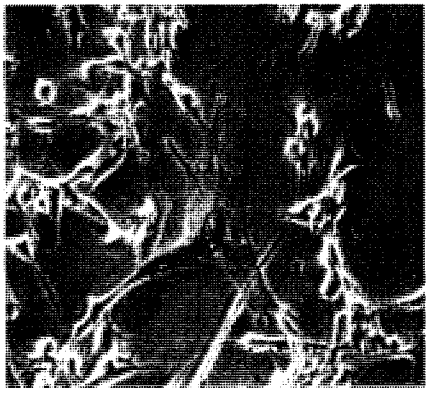

the dye during the scrape loading experiment.

In summary the most malignant cell line, U-251 MG, shows a complete lack of gap junctional intercellular communication (GJIC). On the other hand, U-87 MG cells show the presence of functional connexons in the form of open hemichannels.

3.4 Main Signaling Pathways Involved in Cx43 Expression and Localization in U251 and U87 Astrocytoma

It has been specified in the introduction that phosphorylation plays an essential role in the life cycle of Cx43. These phosphorylation events are modulated by various protein kinases either directly or indirectly, the protein kinases themselves being activated by growth factors or hormones. We observed differences in the phosphorylation patterns of Cx43 in both the specific serine sites that were investigated and in the general phopho-sites studied with the H-150 antibody. It became of interest to investigate the related phosphorylation pathways in order to shed some light on the ones associated with the degradation fragments of Cx43. Three main protein kinases have been shown to modulate Cx43 phoshorylation in various cell types: PKC, PKA and ERK-MAPK (Lampe and Sloan, 2005). In order to determine the effect of the inhibition of these protein kinases on Cx43 expression and/or sub-cellular localization in human astrocytoma, a pharmacological approach was taken. Specific conventional inhibitors were used for each investigated kinase. U-251 MG and U-87 MG cells were treated with 5 μM of BisI (PKC inhibitor), 2 μM of PKAI (PKA inhibitor) or 50 μM of PD98059 (ERK-MAPK inhibitor) for 24 hours. The effects of the inhibition on Cx43 expression and sub-cellular localization were assessed by Western blotting and

immunocytochemistry respectively using the H-150 Cx43 antibody as well as all four phospho-Cx43 antibodies. Since the H-150 antibody does not seem to react strongly to the degradation fragments as discussed earlier, special attention was given to the detection of the phosphorylation sites on the degradation fragments by using the specific phospho-antibodies.

U-251 MG cells treated with 5 μM of BisI for 24 hours did not alter Cx43 expression when probed with the H-150 Cx43 antibody (Fig. 17, A). Cx43 sub-cellular localization was not affected either; Cx43 remained mainly nuclear with slight cytoplasmic localization (Fig. 17, B). U-251 MG cells that were probed with the same H-150 Cx43 antibody following treatment with 2 μM of PKAI still did not show any alteration of Cx43 expression (Fig. 17, A) or sub-cellular localization (Fig. 17, B). When U-251 MG cells were treated with 50 μM of PD98059 however, using the same antibody, all the fragmented isoforms of Cx43 seem to increase. This result suggests that the ERK-MAPK pathway plays a role in Cx43 fragmentation. Moreover, the same PD98059 inhibitor altered Cx43 sub-cellular localization. Cx43 can now be seen on the membrane as small punctuated structures (Fig. 17, B, red arrows). This result is very important since ERK-MAPK inhibition seemed to partially restore a normal Cx43 localization on the cell membrane.

U-87 MG cells were subjected to the same treatments as the other cell line and still probed with the H-150 Cx43 antibody. In this cell line BisI and PKAI did not have any effects on Cx43 expression (Fig. 18, A). When cells were treated with PD98059 however all three bands (P1, P2 and P3) increased in intensity (Fig. 18, A). The P1

Figure 17. Effect of the inhibition of PKC, PKA and ERK-MAPK on Cx43 expression and sub-cellular localization in U-251 MG cells using the H-150 Cx43 antibody.

A: U-251 MG cells were exposed to various protein kinase inhibitors, 5 μM BisI (PKC), 2 μM PKAI (PKA) and 50 μM PD98059 (ERK-MAPK) for 24 hours. Whole protein lysates were separated on 10% SDS-PAGE and transferred to nitrocellulose membranes. Cx43 protein levels were assessed by immunoblot analysis by probing with Cx43 (H150) IgG. No differences in Cx43 levels are observed at the expected molecular weight of 43 kDa following the treatments. However, following PD98059 treatment all the fragmented isoforms of Cx43 seem to increase.

B: Immunofluorescence staining of Cx43 in the human astrocytoma cell line U-251 MG upon treatment with 5 μM BisI, 2 μM PKAI and 50 μM PD98059 for 24 hours. Cells were fixed, permeabilized and probed with Cx43 (H-150) IgG and the appropriate secondary AlexaFluor 488 nm IgG. Images were originally taken at 20x magnification. Upon treatment with PD98059 in U-251 MG cells, Cx43 localization changed from the nucleus to the cell membrane (red arrow).

A

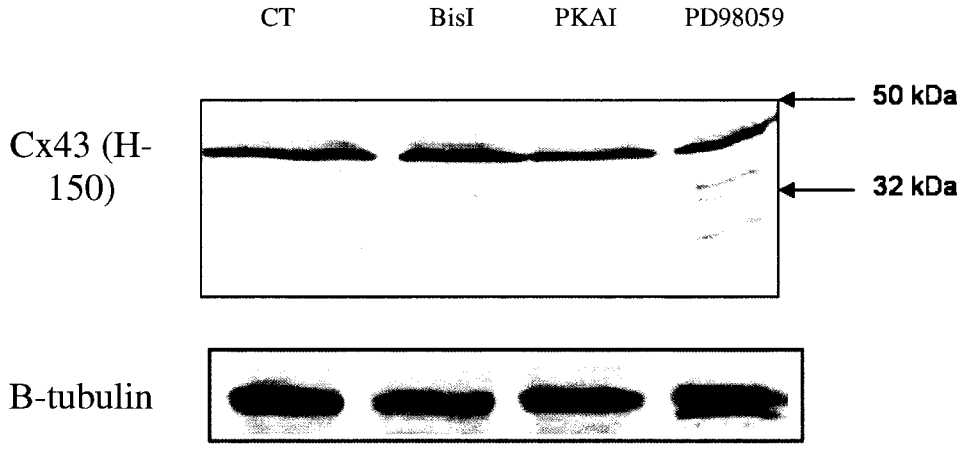
CT
BisI
PKAI
PD98059
Cx43 (H-150)
50 kDa
32 kDa
B-tubulin

B

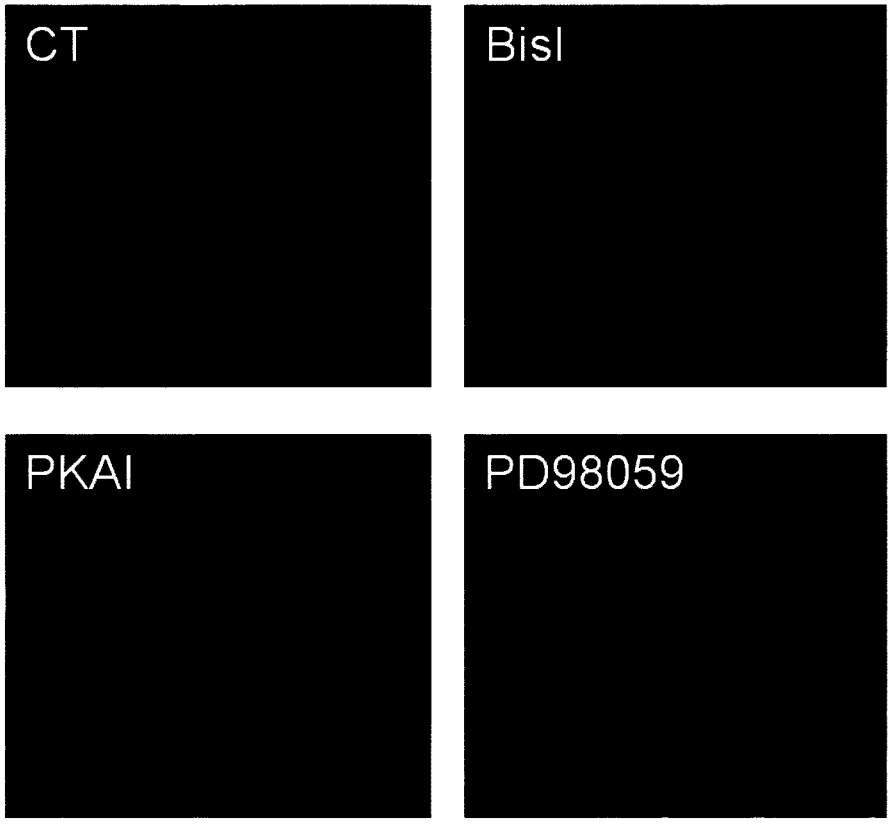
CT
BisI
PKAI
PD98059

Figure 18. Effect of the inhibition of PKC, PKA and ERK-MAPK on Cx43 expression and sub-cellular localization in U-87 MG cells using the H-150 Cx43 antibody.

A: U-87 MG cells were exposed to various protein kinase inhibitors, 5 μM BisI, 2 μM PKAI and 50 μM PD98059 for 24 hours. Whole protein lysates were separated on 10% SDS-PAGE and transferred to nitrocellulose membranes. Cx43 protein levels were assessed by immunoblot analysis by probing with Cx43 (H150) IgG. Following PD98059 treatment, Cx43 expression and phosphorylation (P1 and P2) increase.

B: Immunofluorescence staining of Cx43 in the human astrocytoma cell line U-87 MG upon treatment with 5 μM BisI, 2 μM PKAI and 50 μM PD98059 for 24 hours. Cells were fixed, permeabilized and probed with Cx43 (H-150) IgG and the appropriate secondary AlexaFluor 488 nm IgG. Images were originally taken at 20x magnification. Upon treatment with PD98059 in U-87 MG cells, Cx43 expression appears increased.

C: Densitometric analysis of Cx43 expression following treatment with 5 μM BisI, 2 μM PKAI and 50 μM PD98059 for 24 hours in U-87 MG cells. Data are expressed as the percentage intensity of the control band and are the mean ± SD of three separate experiments. Level of significance: $P<0.05$ (*) compared with control cells according to the Student's t-test. Results show a significant increase in the P1 and P2 isoforms of Cx43 following PD98059 treatment.

A

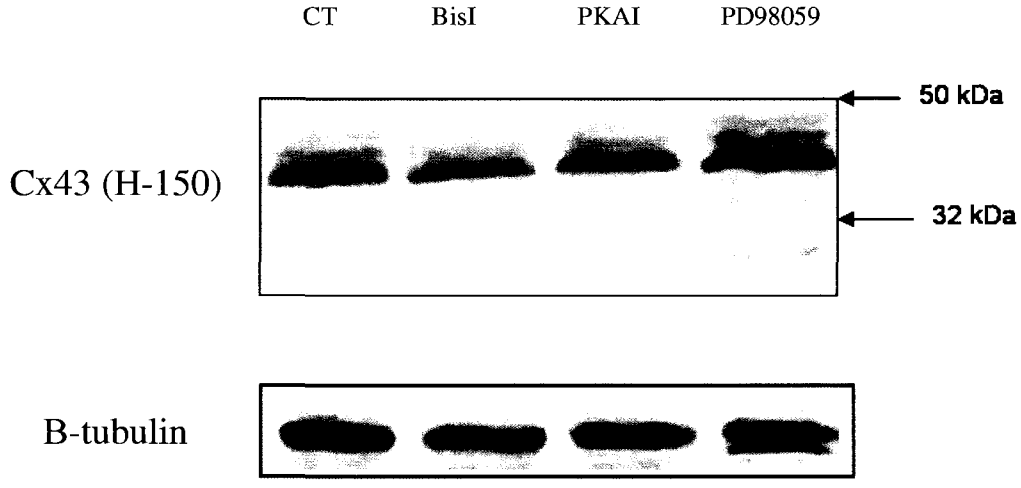
CT
BisI
PKAI
PD98059
50 kDa
32 kDa
Cx43 (H-150)
B-tubulin

B

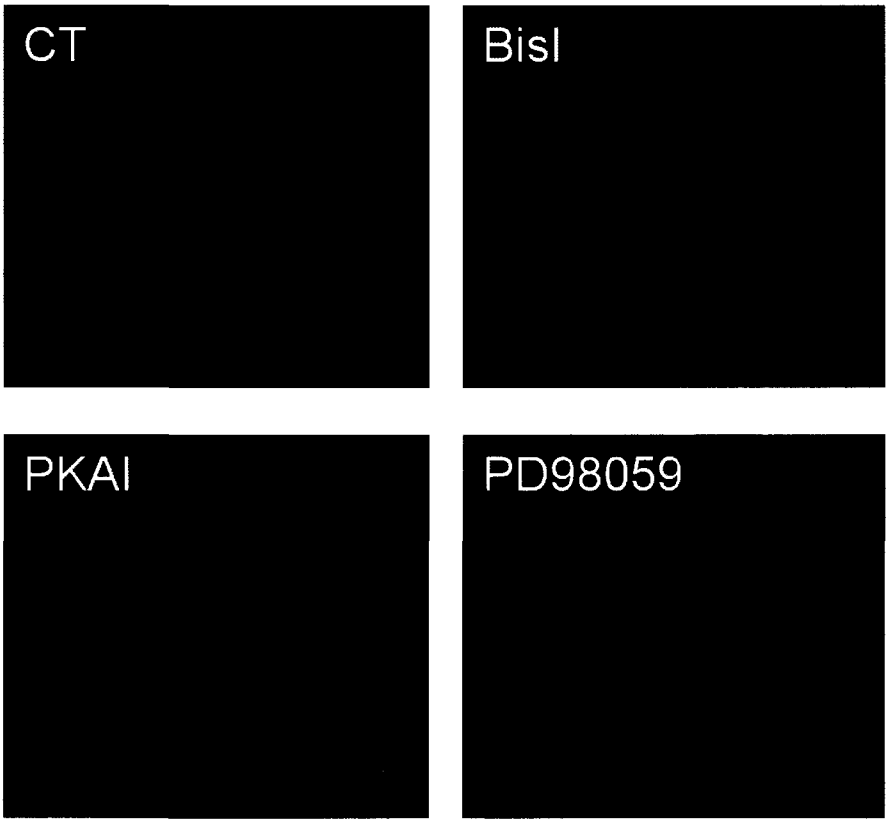
CT
BisI
PKAI
PD98059

C

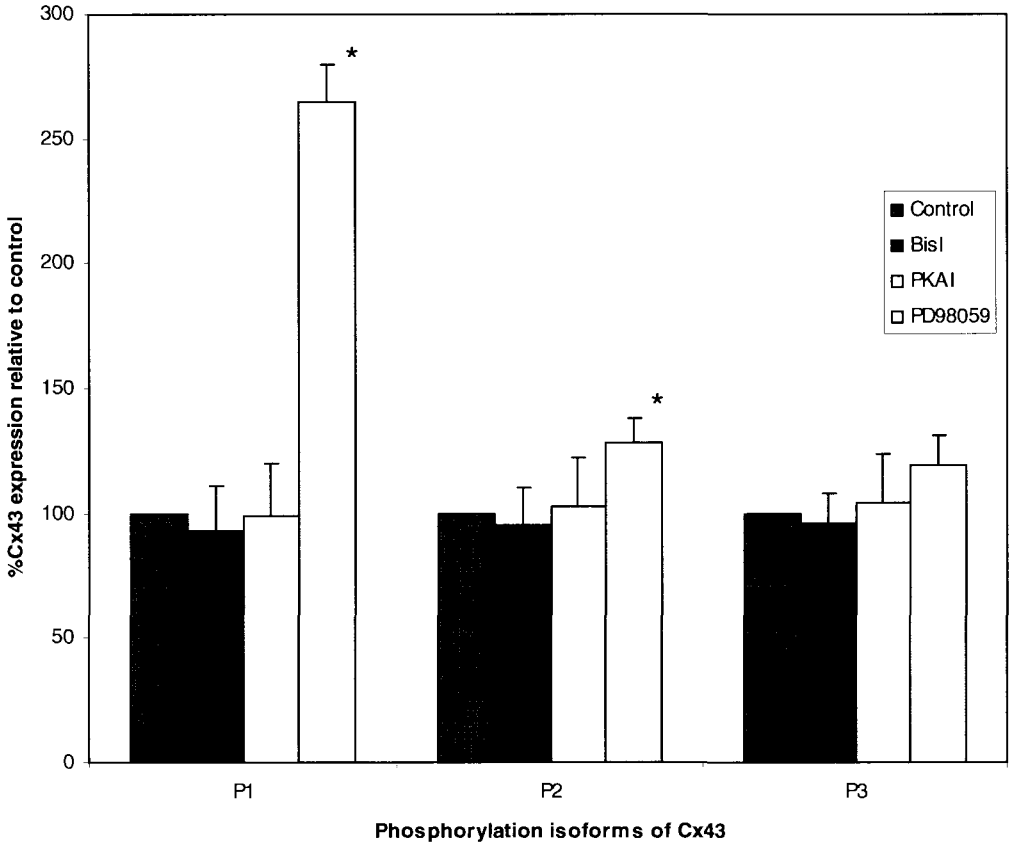
300
250
200
150
100
50
0
%Cx43 expression relative to control
*
*
Control
BisI
PKAI
PD98059
P1
P2
P3
Phosphorylation isoforms of Cx43

isoform of Cx43 increased 2.7 fold, the P2 isoform by a factor of 1.3 and the P3 isoform by 1.15, although the last isoform result is not statistically significant (Fig. 18, C). Immunocytochemistry images show no differences in Cx43 location after treatment with BisI and PKAI (Fig. 18, B). However, when treated with PD98059 Cx43 levels increased (Fig. 18, B) thus supporting Western Blot results.

When probed by the Ser-255 antibody the full-length Cx43 protein is recognized, but none of the inhibitors exerted any effects (Fig. 19, A). Blots of U-251 MG cells probed with the Ser-255 phospho-antibody show a decrease in the 29-30 kDa bands following PKAI and PD98059 treatment (Fig. 19, A). No differences can be observed following BisI treatment. In this experiment set, the band at 34kDa was not labeled. In U-87 the Ser-255 phosphorylated Cx43 at the expected molecular weight of 43 kDa was not affected at all by the three inhibitors which is common to both cell lines (Fig. 19&20, A). In blots of U-87 MG cells however, the pattern differs from that observed in figure 7A since the band at 34 kDa is labeled at the same intensity (also in the controls). The band at 29.5 kDa is labeled as expected but is not sensitive to the inhibitors. As opposed, the doublet band at 27-26 kDa increased following cells treated by all three inhibitors (Fig. 20, A). Immunocytochemistry experiments does not show any changes in sub-cellular localization of Ser-255 phosphorylated Cx43 following treatment with the three inhibitors in U-251 (Fig. 19, B) and U-87 MG (Fig. 20, B) cells.

Blots of U-251 MG cells probed with the Ser-262 phospho-Cx43 antibody do not show any changes in full-length Cx43 phosphorylation following treatment (Fig. 21, A). The band at 34-33 kDa was well labeled in treatments and control. When the cells were

Figure 19. Effect of the inhibition of PKC, PKA and ERK-MAPK on Cx43 expression and sub-cellular localization in U-251 MG cells using the Ser-255 phospho-Cx43 antibody.

A: U-251 MG cells were exposed to various protein kinase inhibitors, 5 μM BisI, 2 μM PKAI and 50 μM PD98059 for 24 hours. Whole protein lysates were separated on 10% SDS-PAGE and transferred to nitrocellulose membranes. Cx43 protein levels phosphorylated on Ser-255 were assessed by immunoblot analysis by probing with pCx43 (Ser-255) IgG. Treatment with the PKA inhibitor (PKAI) and ERK-MAPK inhibitor (PD98059) seems to decrease fragmented Cx43 mainly the 29-30 kDa bands.

B: Immunofluorescence staining of Cx43 in the human astrocytoma cell line U-251 MG upon treatment with 5 μM BisI, 2 μM PKAI and 50 μM PD98059 for 24 hours. Cells were fixed, permeabilized and probed with pCx43 (Ser-255) IgG and the appropriate secondary AlexaFluor 488 nm IgG. Images were originally taken at 20x magnification. Cx43 sub-localization remains unchanged following treatment.

A

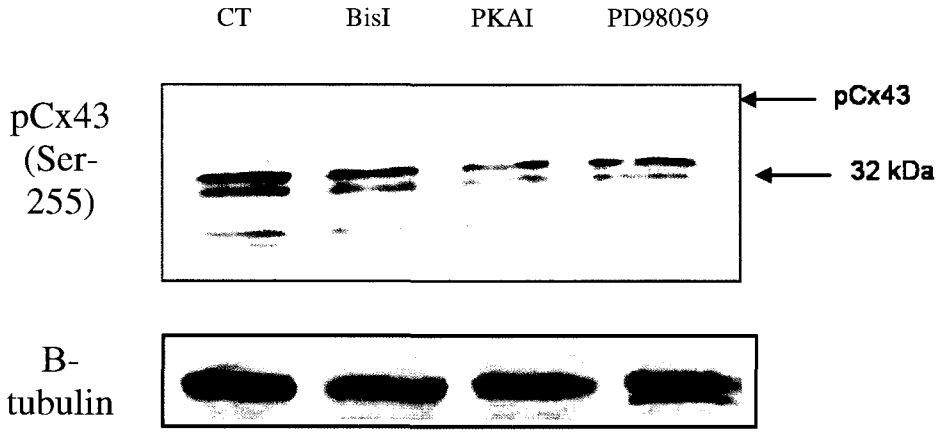
CT
BisI
PKAI
PD98059
pCx43 (Ser-255)
pCx43
32 kDa
B-tubulin

B

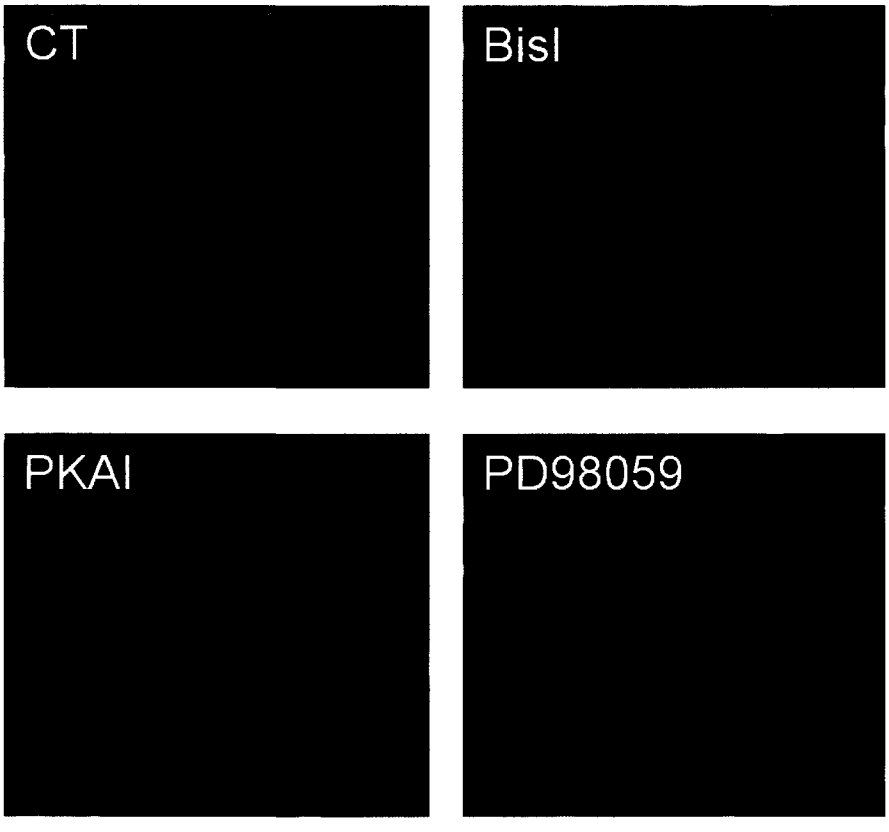
CT
BisI
PKAI
PD98059

Figure 20. Effect of the inhibition of PKC, PKA and ERK-MAPK on Cx43 expression and sub-cellular localization in U-87 MG cells using the Ser-255 phospho-Cx43 antibody.

A: U-87 MG cells were exposed to various protein kinase inhibitors, 5 μM BisI, 2 μM PKAI and 50 μM PD98059 for 24 hours. Whole protein lysates were separated on 10% SDS-PAGE and transferred to nitrocellulose membranes. Cx43 protein levels phosphorylated on Ser-255 were assessed by immunoblot analysis by probing with pCx43 (Ser-255) IgG. Intact phosphorylated Cx43 found at 43 kDa is not altered by any of the treatments. However, the doublet band at 27-26 kDa is increased with all three treatments.

B: Immunofluorescence staining of Cx43 in the human astrocytoma cell line U-87 MG upon treatment with 5 μM BisI, 2 μM PKAI and 50 μM PD98059 for 24 hours. Cells were fixed, permeabilized and probed with pCx43 (Ser-255) IgG and the appropriate secondary AlexaFluor 488 nm IgG. Images were originally taken at 20x magnification. Cx43 sub-localization remains unchanged following treatments.

A

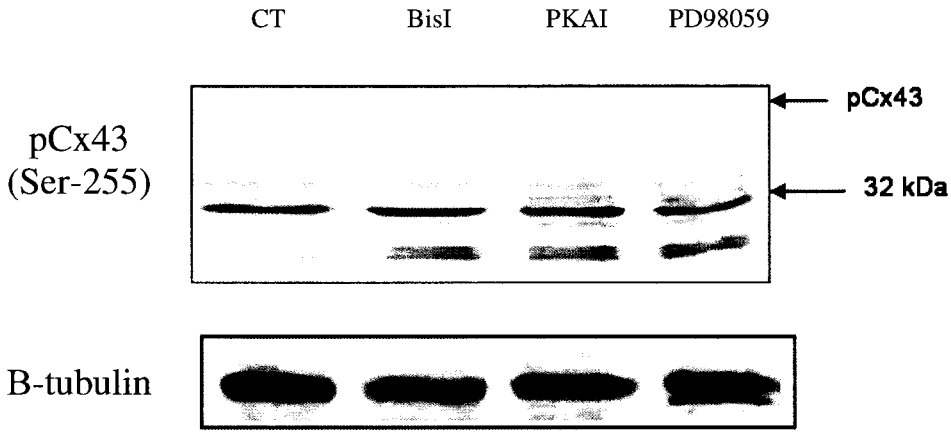
CT
BisI
PKAI
PD98059
pCx43
(Ser-255)
pCx43
32 kDa
B-tubulin

B

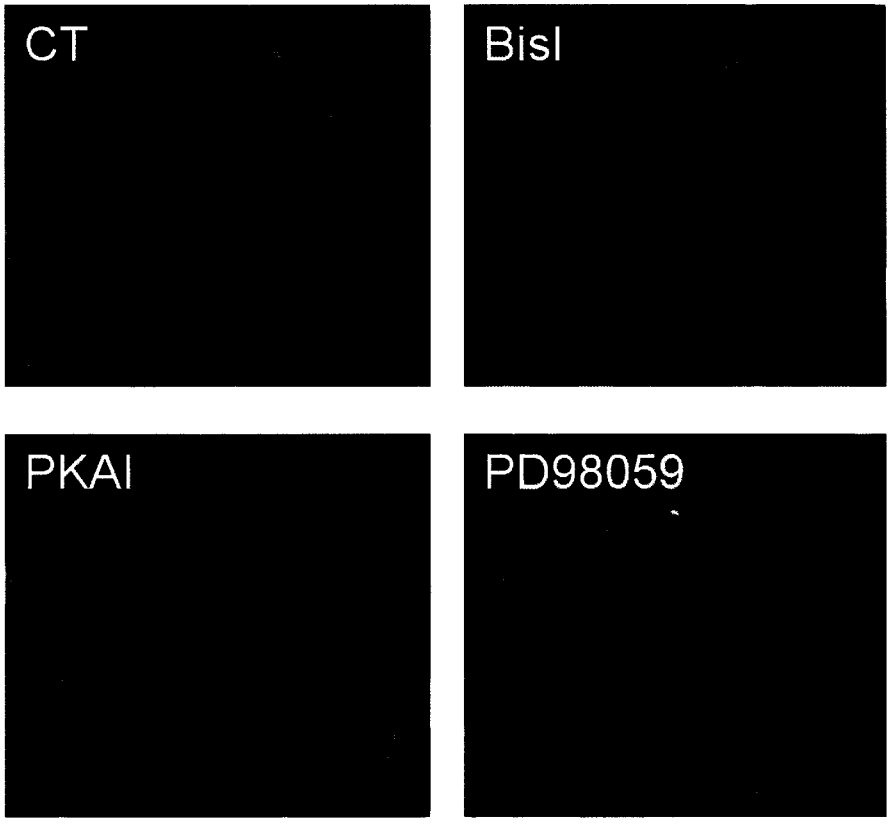
CT
BisI
PKAI
PD98059

Figure 21. Effect of the inhibition of PKC, PKA and ERK-MAPK on Cx43 expression and sub-cellular localization in U-251 MG cells using the Ser-262 phospho-Cx43 antibody.

A: U-251 MG cells were exposed to various protein kinase inhibitors, 5 μM BisI, 2 μM PKAI and 50 μM PD98059 for 24 hours. Whole protein lysates were separated on 10% SDS-PAGE and transferred to nitrocellulose membranes. Cx43 protein levels phosphorylated on Ser-262 were assessed by immunoblot analysis by probing with pCx43 (Ser-262) IgG. The upper band of the 34-33 kDa doublet is increased following BisI treatment.

B: Immunofluorescence staining of Cx43 in the human astrocytoma cell line U-251 MG upon treatment with 5 μM BisI, 2 μM PKAI and 50 μM PD98059 for 24 hours. Cells were fixed, permeabilized and probed with pCx43 (Ser-262) IgG and the appropriate secondary AlexaFluor 488 nm IgG. Images were originally taken at 20x magnification. Cx43 sub-localization remains unchanged following treatments.

A

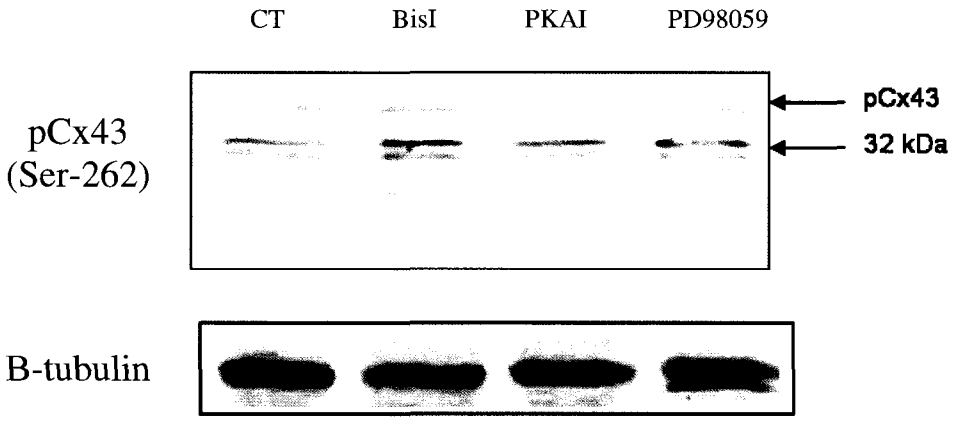
CT
BisI
PKAI
PD98059
pCx43
(Ser-262)
pCx43
32 kDa
B-tubulin

B

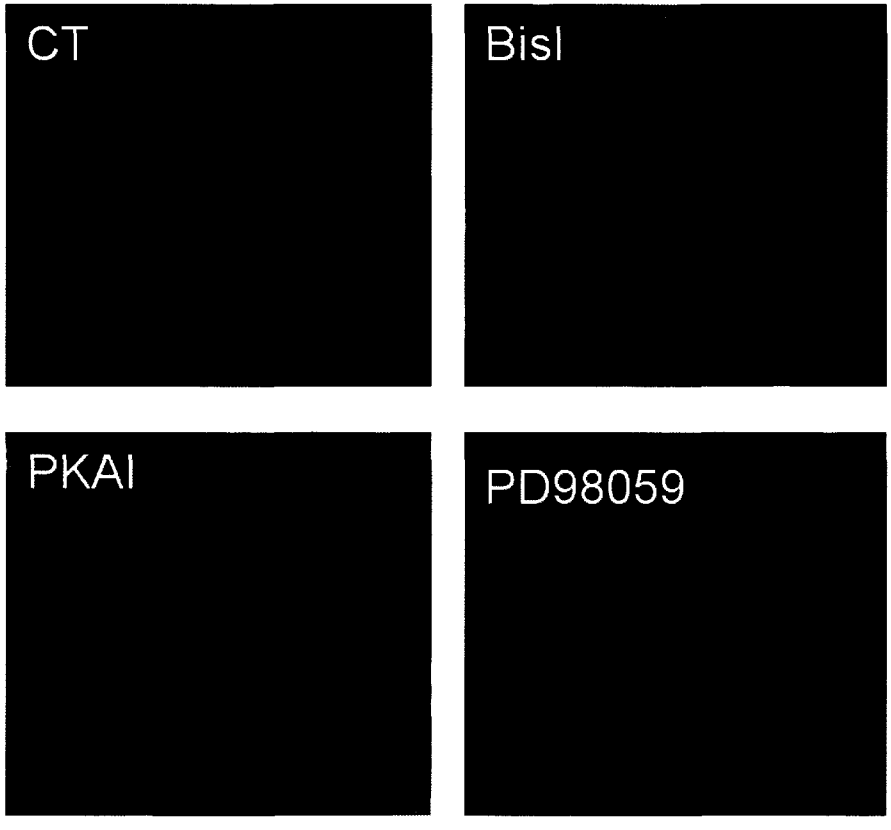
CT
BisI
PKAI
PD98059

treated with BisI the upper band of this doublet was enhanced. There was no change in the faster migrating next doublet (30-29 kDa). For U-87 MG cells no changes in Ser-262 phosphorylation of full-length Cx43 were observed although the protein was labeled. Although the quality of the blots does not allow for solid interpretation it is likely that among the fragments the 29.5 kDa band that can be very intense (Fig. 8, A) still appears to be intense (Fig. 22, A) albeit less than in the blot of Figure 8. There is no clear effect of the inhibitors in comparison with the control. Immunocytochemistry experiments do not show any changes in sub-cellular localization of Ser-262 phosphorylated Cx43 following treatment with the three inhibitors in U-251 (Fig. 21, B) and U-87 MG (Fig. 22, B) cells.

Blots probed with the Ser-279/282 phospho-Cx43 antibody do not show any changes in Cx43 phosphorylation following treatments in U-251 MG (Fig. 23, A). In this set of experiments the labeling of the 30-29 kDa bands is less apparent than in the figure 9 while the faint 34-33 kDa bands in the figure 9 blot are weakly recognized in this set. There is no change exerted by the inhibtors. The fragments at 27-26 kDa are labeled as expected but are not sensitive to the inhibitors either. Immunocytochemistry experiments does not show any changes in sub-cellular localization of Ser-279/282 phosphorylated Cx43 following treatment with the three inhibitors in U-251 (Fig. 23, B). As in the U-251 cells, in U-87 MG cells, there was no effect shown by the inhibitors in comparison to controls in Cx43 full length protein or its degradation fragments (Fig. 24, A); there were also no changes in sub-cellular localization (Fig. 24, B). Therefore, the ERK-MAPK, PKC or PKA kinases do not seem to have any impact on the Ser-279/282 phosphorylation site.

Figure 22. Effect of the inhibition of PKC, PKA and ERK-MAPK on Cx43 expression and sub-cellular localization in U-87 MG cells using the Ser-262 phospho-Cx43 antibody.

A: U-87 MG cells were exposed to various protein kinase inhibitors, 5 μM BisI, 2 μM PKAI and 50 μM PD98059 for 24 hours. Whole protein lysates were separated on 10% SDS-PAGE and transferred to nitrocellulose membranes. Cx43 protein levels phosphorylated on Ser-262 were assessed by immunoblot analysis by probing with pCx43 (Ser-262) IgG. No changes in phosphorylated Cx43 (both fragmented or not) is observed following the three treatments.

B: Immunofluorescence staining of Cx43 in the human astrocytoma cell line U-87 MG upon treatment with 5 μM BisI, 2 μM PKI and 50 μM PD98059 for 24 hours. Cells were fixed, permeabilized and probed with pCx43 (Ser-262) IgG and the appropriate secondary AlexaFluor 488 nm IgG. Images were originally taken at 20x magnification. Cx43 sub-localization remains unchanged following treatments.

A

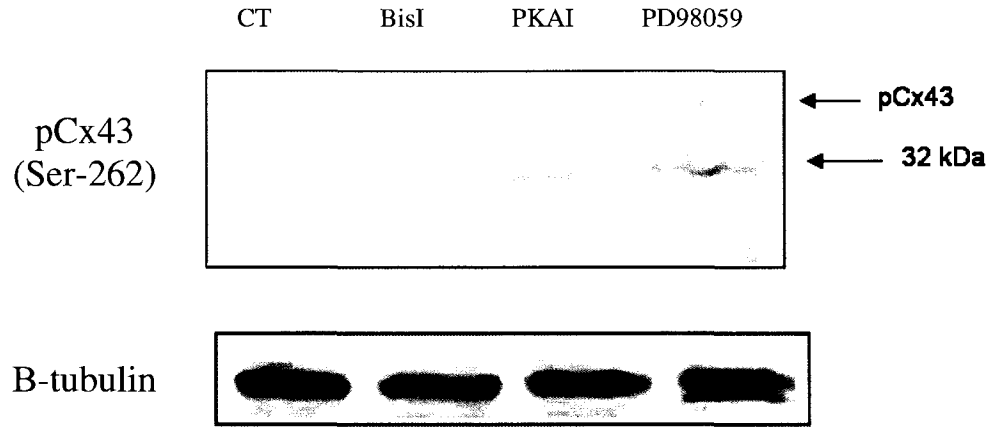
CT
BisI
PKAI
PD98059
pCx43
(Ser-262)
pCx43
32 kDa
B-tubulin

B

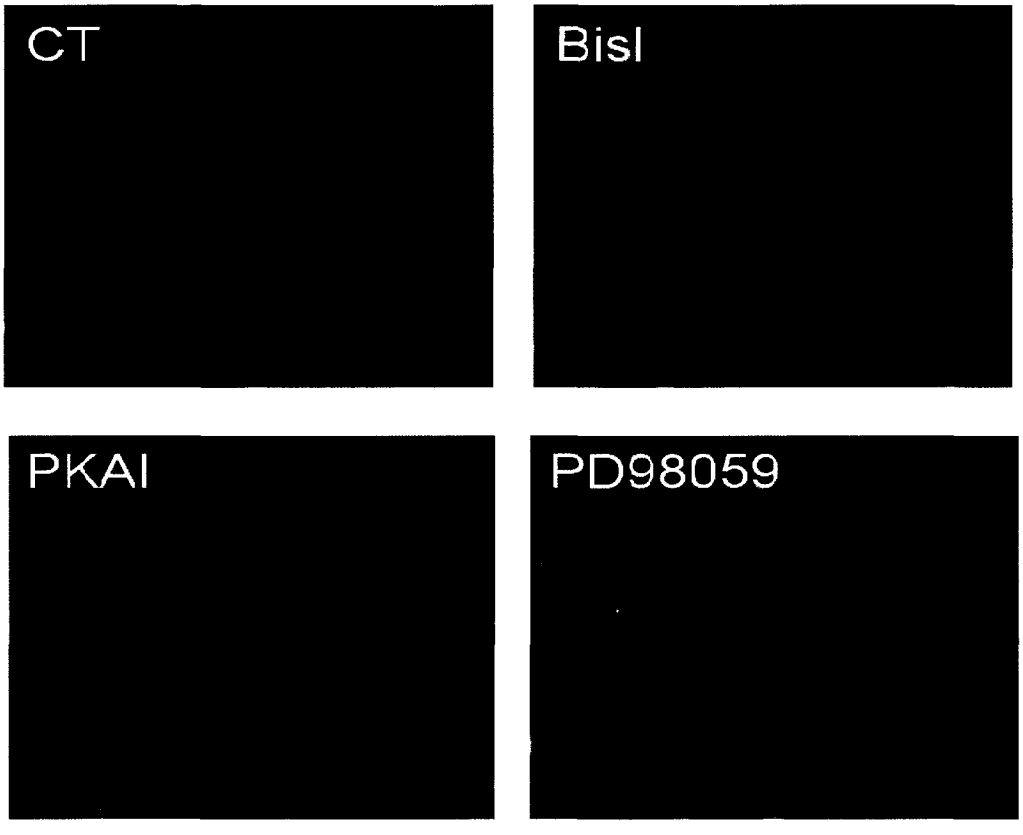
CT
BisI
PKAI
PD98059

Figure 23. Effect of the inhibition of PKC, PKA and ERK-MAPK on Cx43 expression and sub-cellular localization in U-251 MG cells using the Ser-279/282 phospho-Cx43 antibody.

A: U-251 MG cells were exposed to various protein kinase inhibitors, 5 μM BisI, 2 μM PKAI and 50 μM PD98059 for 24 hours. Whole protein lysates were separated on 10% SDS-PAGE and transferred to nitrocellulose membranes. Cx43 protein levels phosphorylated on Ser-279/282 were assessed by immunoblot analysis by probing with pCx43 (Ser-279/282) IgG. No changes in phosphorylated Cx43, including the fragments, can be observed.

B: Immunofluorescence staining of Cx43 in the human astrocytoma cell line U-251 MG upon treatment with 5 μM BisI, 2 μM PKAI and 50 μM PD98059 for 24 hours. Cells were fixed, permeabilized and probed with pCx43 (Ser-279/282) IgG and the appropriate secondary AlexaFluor 488 nm IgG. Images were originally taken at 20x magnification. Cx43 sub-localization remains unchanged following treatments.

A

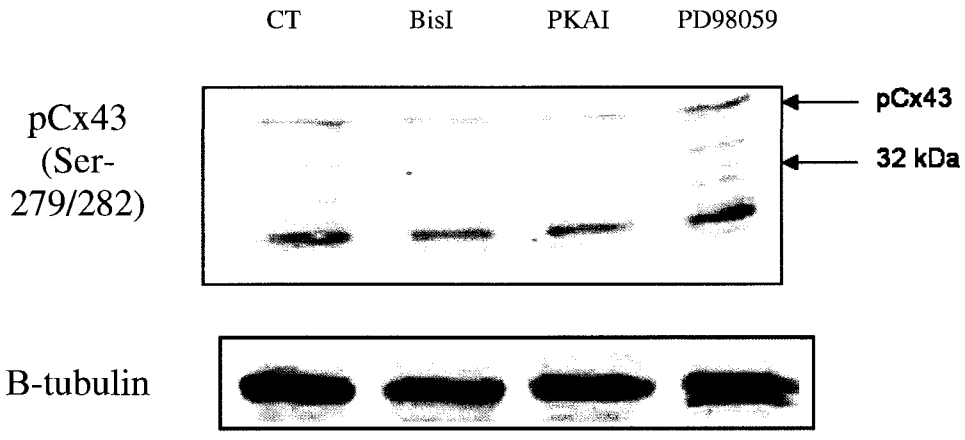
CT
BisI
PKAI
PD98059
pCx43
(Ser-
279/282)
pCx43
32 kDa
B-tubulin

B

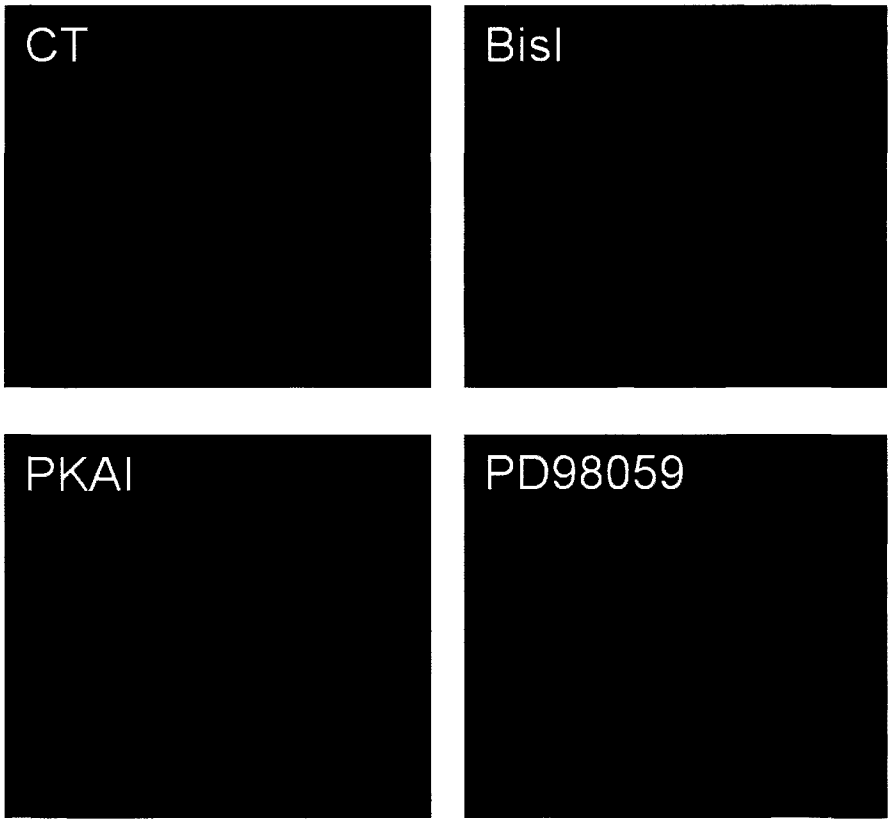
CT
BisI
PKAI
PD98059

Figure 24. Effect of the inhibition of PKC, PKA and ERK-MAPK on Cx43 expression and sub-cellular localization in U-87 MG cells using the Ser-279/282 phospho-Cx43 antibody.

A: U-87 MG cells were exposed to various protein kinase inhibitors, 5 μM BisI, 2 μM PKAI and 50 μM PD98059 for 24 hours. Whole protein lysates were separated on 10% SDS-PAGE and transferred to nitrocellulose membranes. Cx43 protein levels phosphorylated on Ser-279/282 were assessed by immunoblot analysis by probing with pCx43 (Ser-279/282) IgG. No changes can be observed in phosphorylated Cx43.

B: Immunofluorescence staining of Cx43 in the human astrocytoma cell line U-87 MG upon treatment with 5 μM BisI, 2 μM PKAI and 50 μM PD98059 for 24 hours. Cells were fixed, permeabilized and probed with pCx43 (Ser-279/282) IgG and the appropriate secondary AlexaFluor 488 nm IgG. Images were originally taken at 20x magnification. Cx43 sub-localization remains unchanged following treatments.

A

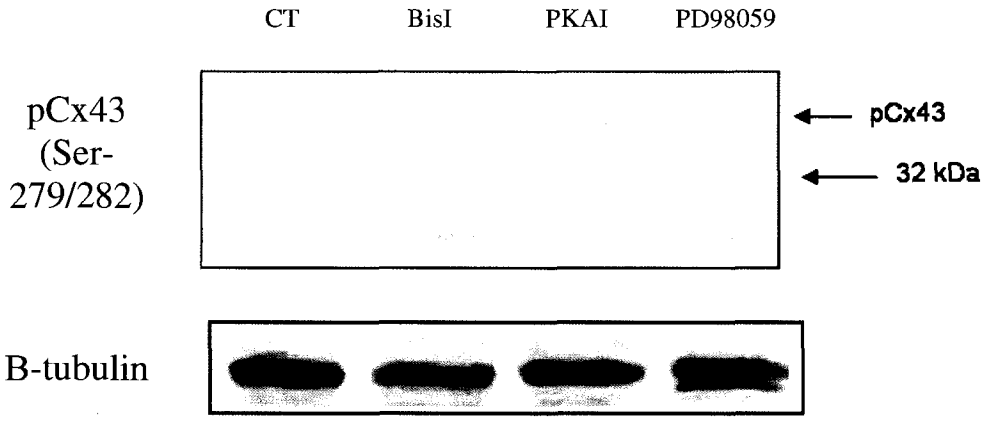
CT
BisI
PKAI
PD98059
pCx43 (Ser-279/282)
pCx43
32 kDa
B-tubulin

B

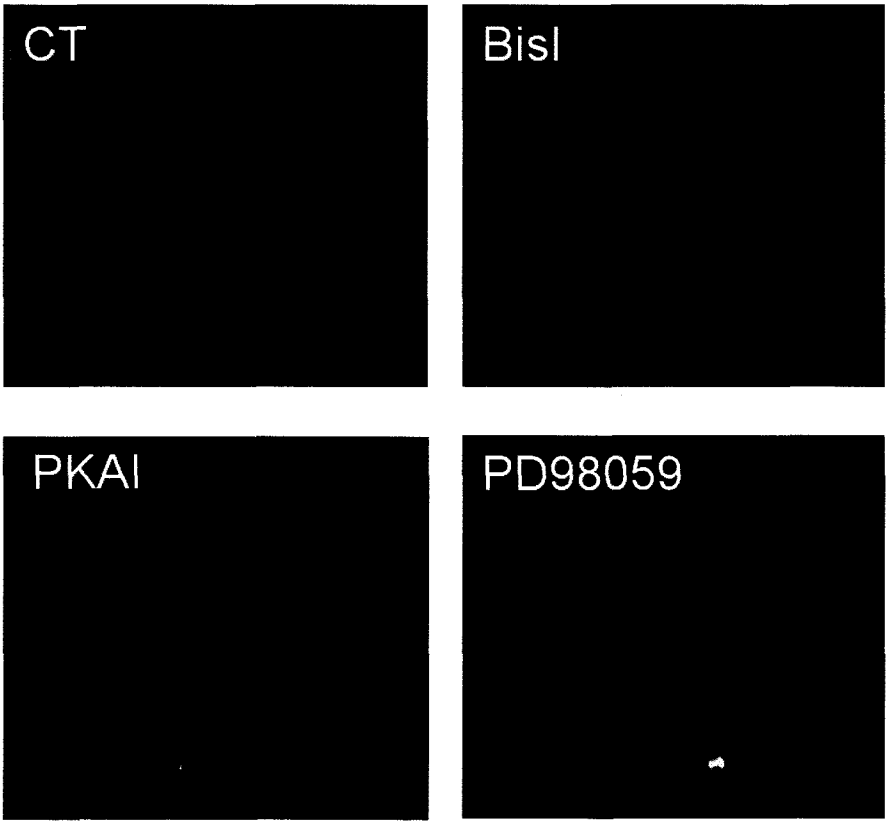
CT
BisI
PKAI
PD98059

Blots of the U-251 cell line probed with the Ser-368 phospho-Cx43 antibody do no show any changes in Cx43 phosphorylation at the 43 kDa band in U-251 MG cells (Fig. 25, A). When the cells were treated with PD98059, the 30-29 kDa fragmentation band increase (Fig. 25, A). In U-87 MG cells, no changes are observed in the intact forms of Cx43 following treatment with the three inhibitors (Fig. 26, A). Albeit less intensively labeled than the similar band at 29.5 kDa (Fig. 10, A), the band is recognized by the phospho-antibody. An increase in intensity can be observed upon exposure to the cells to BisI and PD98059 inhibitors (Fig. 26, A). Immunocytochemistry experiments does not show any changes in sub-cellular localization of Ser-368 phosphorylated Cx43 following treatment with the three inhibitors in U-251 (Fig. 25, B) and U-87 MG (Fig. 26, B) cells.

In summary, when both cell lines were treated with three protein kinase inhibitors only PD98059 had an effect observed on the 43 kDa bands in the cell lines. Importantly, in U-251 MG cells, it was associated with the restoration of Cx43 sub-cellular localization on the plasma membrane that was visualized as punctuate H-150 decoration on the plasma membrane (Fig. 17, B). The same effect did not occur in U-87 MG cells suggesting a difference in the cellular signaling pathways controlling the transit of Cx43 (not previously reported in the literature). The MAPK ERK ½ pathway or an enzyme upstream of MAPK ERK ½ enzyme seems to be responsible for altering the transfer of Cx43 from its cytoplasmic and nuclear localization to the membrane in the U-251 strain. Furthermore, PD98059 treatment increased Cx43 expression in U-87 MG cells. The different effects of PD98059 in U-251 MG and U-87 MG cells suggest different mechanisms that control Cx43 trafficking and expression between those cell lines. In

Figure 25. Effect of the inhibition of PKC, PKA and ERK-MAPK on Cx43 expression and sub-cellular localization in U-251 MG cells using the Ser-368 phospho-Cx43 antibody.

A: U-251 MG cells were exposed to various protein kinase inhibitors, 5 μM BisI, 2 μM PKAI and 50 μM PD98059 for 24 hours. Whole protein lysates were separated on 10% SDS-PAGE and transferred to nitrocellulose membranes. Cx43 protein levels phosphorylated on Ser-368 were assessed by immunoblot analysis by probing with pCx43 (Ser-368) IgG. Following PD98059 treatment the phosphorylated Cx43 fragment of 30-29 kDa is increased.

B: Immunofluorescence staining of Cx43 in the human astrocytoma cell line U-251 MG upon treatment with 5 μM BisI, 2 μM PKAI and 50 μM PD98059 for 24 hours. Cells were fixed, permeabilized and probed with pCx43 (Ser-368) IgG and the appropriate secondary AlexaFluor 488 nm IgG. Images were originally taken at 20x magnification. Cx43 sub-localization remains unchanged following treatments.

A

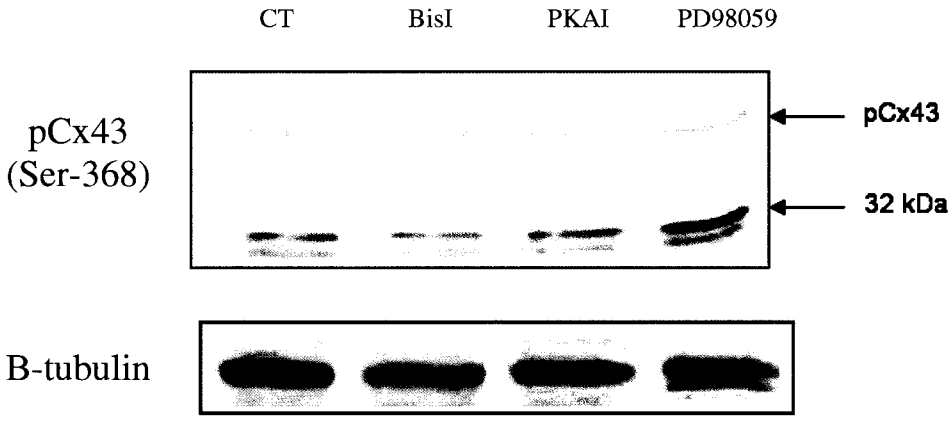
CT
BisI
PKAI
PD98059
pCx43
(Ser-368)
pCx43
32 kDa
B-tubulin

B

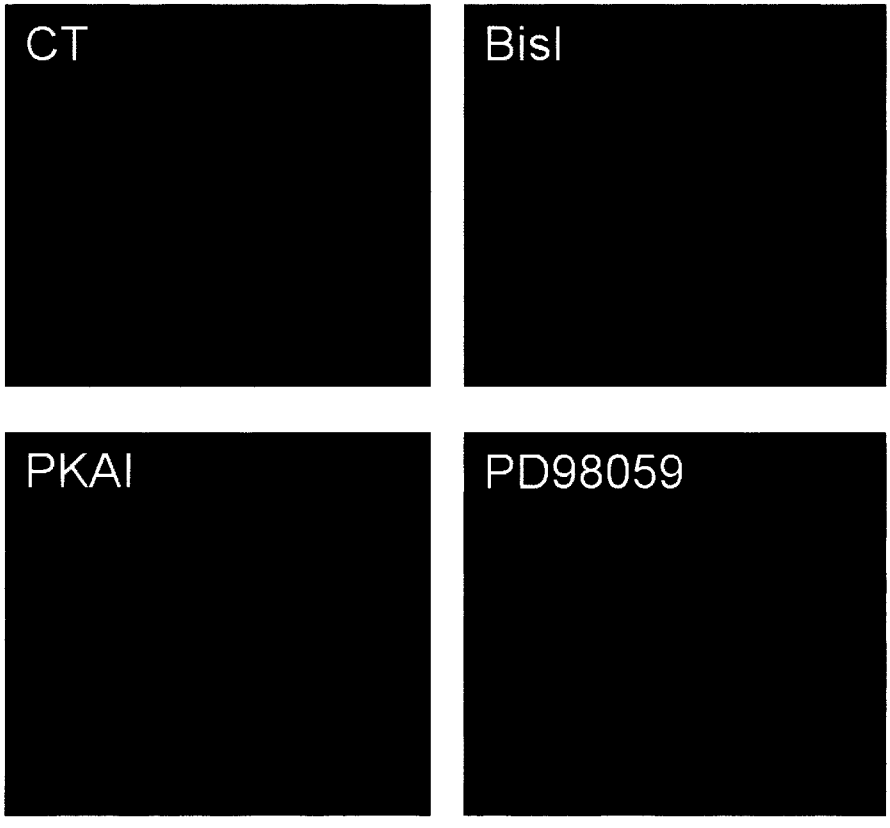
CT
BisI
PKAI
PD98059

Figure 26. Effect of the inhibition of PKC, PKA and ERK-MAPK on Cx43 expression and sub-cellular localization in U-87 MG cells using the Ser-368 phospho-Cx43 antibody.

A: U-87 MG cells were exposed to various protein kinase inhibitors, 5 μM BisI, 2 μM PKAI and 50 μM PD98059 for 24 hours. Whole protein lysates were separated on 10% SDS-PAGE and transferred to nitrocellulose membranes. Cx43 protein levels phosphorylated on Ser-368 were assessed by immunoblot analysis by probing with pCx43 (Ser-368) IgG. No changes can be observed in phosphorylated full length Cx43. The 29.5 kDa band increases following BisI and PD98059 treatment.

B: Immunofluorescence staining of Cx43 in the human astrocytoma cell line U-87 MG upon treatment with 5 μM BisI, 2 μM PKAI and 50 μM PD98059 for 24 hours. Cells were fixed, permeabilized and probed with pCx43 (Ser-368) IgG and the appropriate secondary AlexaFluor 488 nm IgG. Images were originally taken at 20x magnification. Cx43 sub-localization remains unchanged following treatments.

A

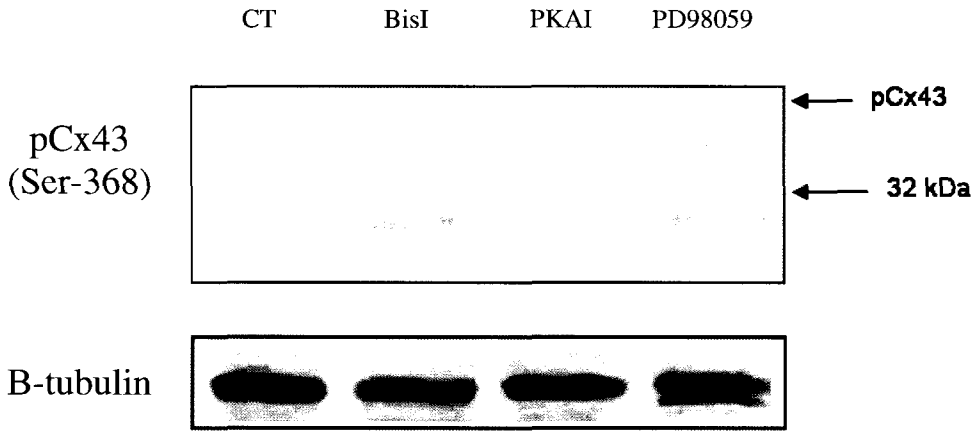
CT
BisI
PKAI
PD98059
pCx43
(Ser-368)
pCx43
32 kDa
B-tubulin

B

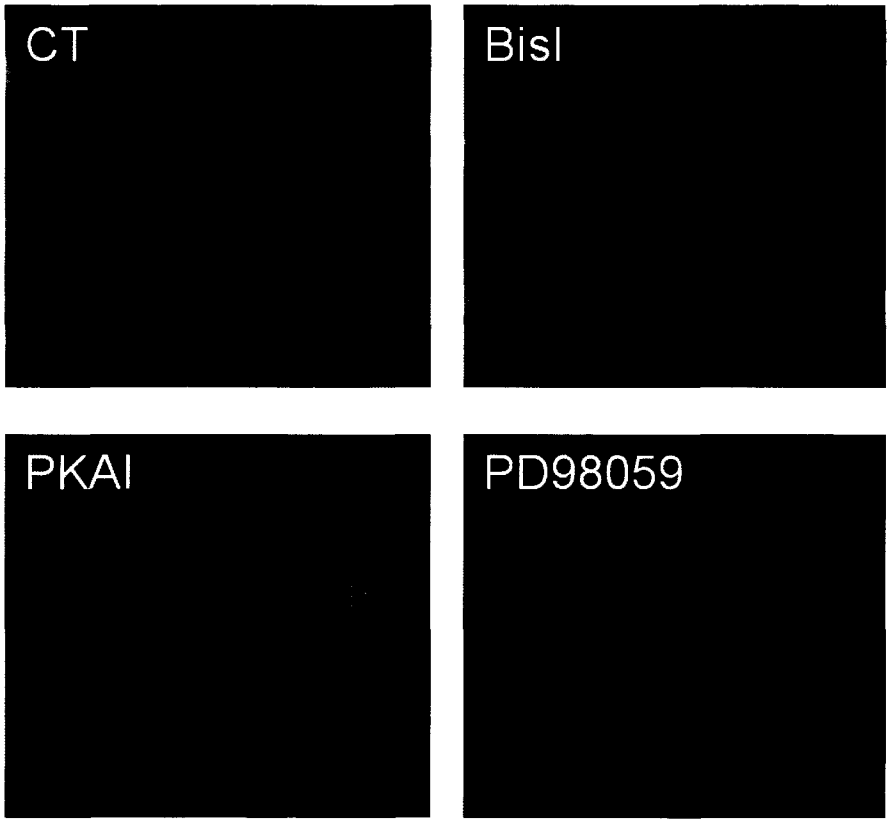
CT
BisI
PKAI
PD98059

addition, the various Cx43 fragments in both cell lines were affected (either positively of negatively) following the treatment with different inhibitors. This would seem to suggest that the fragmentation of Cx43 is regulated by different signaling pathways in both cell lines. Furthermore, the Cx43 fragments were not affected the same way depending on which sites were phosphorylated on the protein. This is very interesting since Cx43 degradation/turn-over is a very important aspect of the protein's life cycle.

3.5 Effect of the Flavanoid Morin on Cx43 Expression and/or Sub-Cellular Localization in Human Astrocytoma

Several natural compounds have been shown in our laboratory and others to possess anti-inflammatory, anti-proliferative and anti-tumorogenic effects by inhibiting one or several signaling pathways. Since a lack of gap junction function and abnormal Cx43 expression and/or sub-cellular localization has been linked to various degrees of tumor development it was deemed important to try to investigate the effects of polyvalent natural compounds on human astrocytoma cell lines. One such group of compounds is the flavanoid family. Flavanoids are part of a large group of natural products and they can be found mainly in fruits, vegetables as well as tea and wine (Hsiang *et al.*, 2005).

One such flavanoid is called morin, a 3, 5, 7, 2', 4'-pentahydroxyflavone (Fig. 27). Morin has been shown to act as an anti-cancer agent against some types of oral cancers (Brown *et al.*, 2003). Even if morin was shown to exhibit anti-tumor effects its signaling mechanism still remains unclear. It was thus our interest to complement this study by observing the effects of morin on U-251 MG and U-87 MG cells in regards to Cx43 expression and sub-cellular localization.

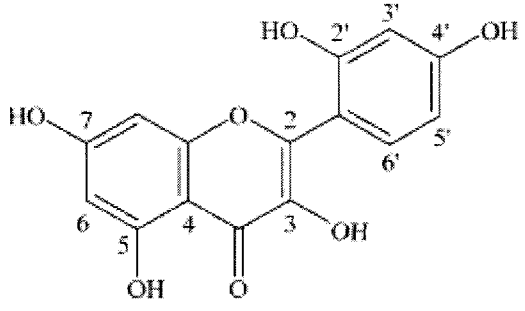

Morin

Figure 27. Chemical structure of the flavanoid Morin (3, 5, 7, 2', 4'-pentahydroxyflavone).

Adapted from Hsiang *et al.*, 2005.

3.5.1 The Flavanoid Morin Increases Cx43 Phosphorylation in U-251 MG Human Astrocytoma Cells

U-251 MG and U-87 MG cells were seeded and treated with 40 μM of morin for 24 hours. Cx43 expression and sub-cellular localization was assessed using Western blotting and immunocytochemistry respectively. We essentially focused on the full length protein Cx43. Western blots show an increase in the P2 and P3 bands of Cx43 in U-251 MG cells after treatment when the blot was probed with the H-150 Cx43 antibody (Fig. 28, A). Densitometric analysis of the band shows a 1.4 fold increase in P2 phosphorylation and a 1.9 fold increase in P3 phosphorylation following treatment with morin (Fig. 28, B). Blots were also probed with all four phospho-Cx43 antibodies to potentially determine the origin of the increase in phosphorylation. Results show an increase in Ser-262 phosphorylation following treatment with morin (Fig. 28, A). Densitometric analysis shows a 3.4 fold increase in Ser-262 phosphorylation (Fig. 28, C). Treatment with morin did not however, exert any effect on Ser-255, Ser-279/282 and Ser-368 phosphorylation levels of Cx43 in U-251 MG cells (Fig. 28, C). In addition, treatment with morin did not seem to alter the fragmented Cx43 in U-251 MG cells, suggesting it affects only the connexin at the full length molecular weight of 43 kDa.

Fluorescence microscopy images confirmed Western Blot data. Following treatment with morin, H-150 probed Cx43 staining increases both in the nucleus and the cytoplasm (Fig. 28, D). Furthermore, cytoplasmic staining of Ser-262 phosphorylated Cx43 increases after treatment with morin for 24 hours (Fig. 28, D). Just as demonstrated by Western blots analyses no changes were observed after treatment when cells were probed with Ser-255, Ser-279/282 and Ser-368 Cx43 antibodies (Fig. 28, D).

Figure 28. Effect of the flavanoid morin on Cx43 expression and sub-cellular localization in U-251 MG cells.

A: U-251 MG cells were exposed to 40 μM of morin for 24 hours. Whole protein lysates were separated on 10% SDS-PAGE and transferred to nitrocellulose membranes. Cx43 protein levels and phosphorylation levels were assessed by immunoblot analysis by probing with Cx43 antibodies, anti-Cx43 (H-150), anti-pCx43 (Ser-255), anti-pCx43 (Ser-262), anti-pCx43 (Ser-279/282) and anti-pCx43 (Ser-368). Upon treatment with morin in U-251 MG cells Cx43 phosphorylation was increased, more specifically on Ser-262. It is important to note that none of the Cx43 fragments below 43 kDa changed following morin treatment.

B: Densitometric analysis of Cx43 expression using the anti-Cx43 (H-150) antibody following treatment with 40 μM of morin for 24 hours in U-251 MG cells. Data are expressed as the percentage intensity of the control band and are the mean ± SD of three separate experiments. Level of significance: $P<0.05$ (*) compared with control cells according to the Student's t-test. Cx43 phosphorylation increased (both P2 and P3 isoforms but not P1) following the treatment with morin.

C: Densitometric analysis of Cx43 phosphorylation following treatment with 40 μM of morin for 24 hours in U-251 MG cells. Data are expressed as the percentage intensity of the control band and are the mean ± SD of three separate experiments. Level of significance: $P<0.05$ (*) compared with control cells according to the Student's t-test. Results show an increase in Ser-262 phosphorylation after treatment with morin.

D: Immunofluorescence staining of Cx43 in the human astrocytoma cell line U-251 MG upon treatment with 40 μM of morin for 24 hours. Cells were fixed, permeabilized and probed with Cx43 (H-150), pCx43 (Ser-255), pCx43 (Ser-262), pCx43 (Ser-279/282) and pCx43 (Ser-368) IgGs and the appropriate secondary AlexaFluor 488 nm IgG. Images were originally taken at 20x magnification. Using the H-150 antibody it is observed that Cx43 increases in the cytoplasm and nucleus following morin treatment. Furthermore, Ser-262 phosphorylation increases in the cytoplasm of U-251 cells following the treatment.

A

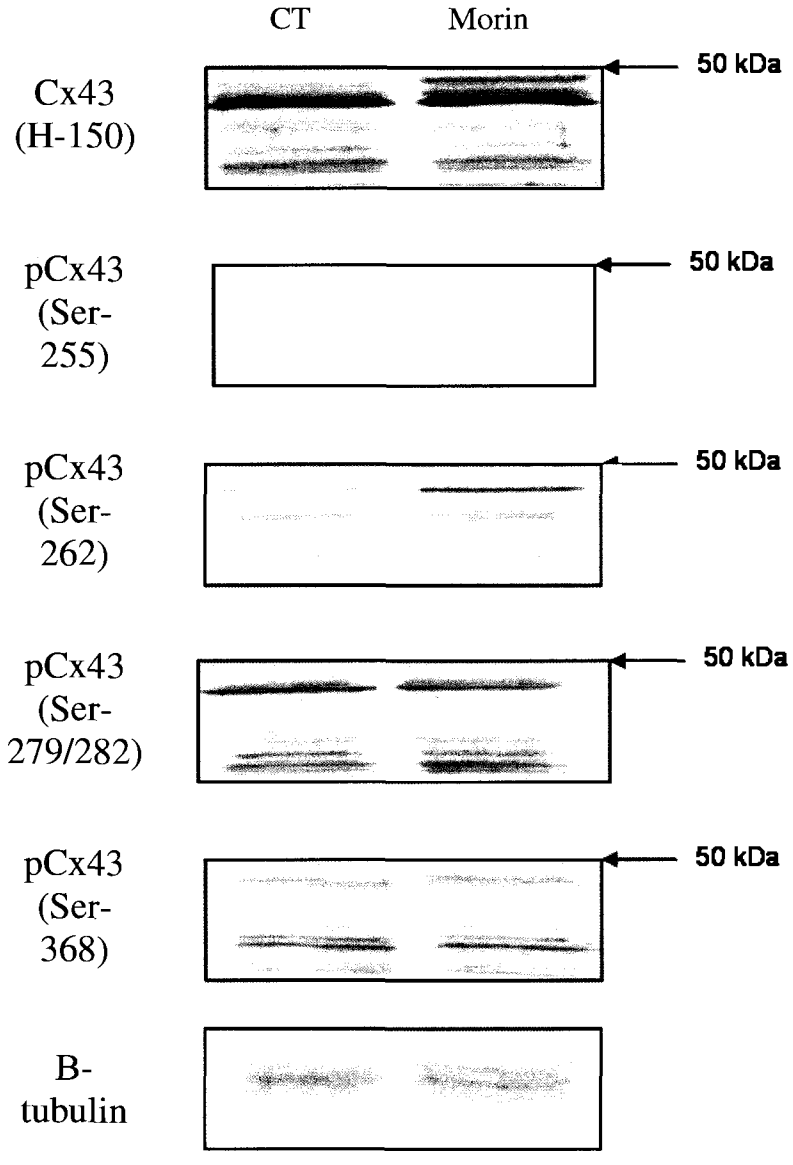
CT
Morin
Cx43 (H-150)
50 kDa
pCx43 (Ser-255)
50 kDa
pCx43 (Ser-262)
50 kDa
pCx43 (Ser-279/282)
50 kDa
pCx43 (Ser-368)
50 kDa
B-tubulin

B

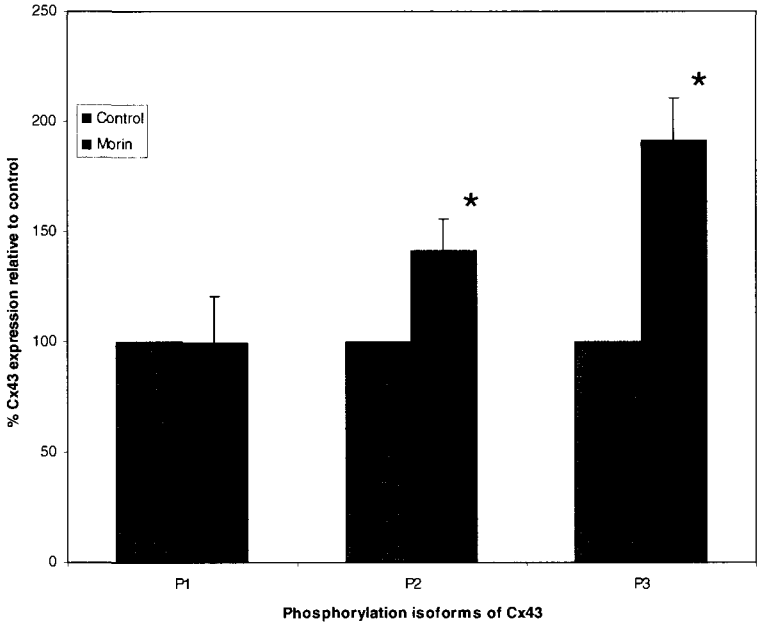
250
200
150
100
50
0
% Cx43 expression relative to control
Control
Morin
*
*
P1
P2
P3
Phosphorylation isoforms of Cx43

C

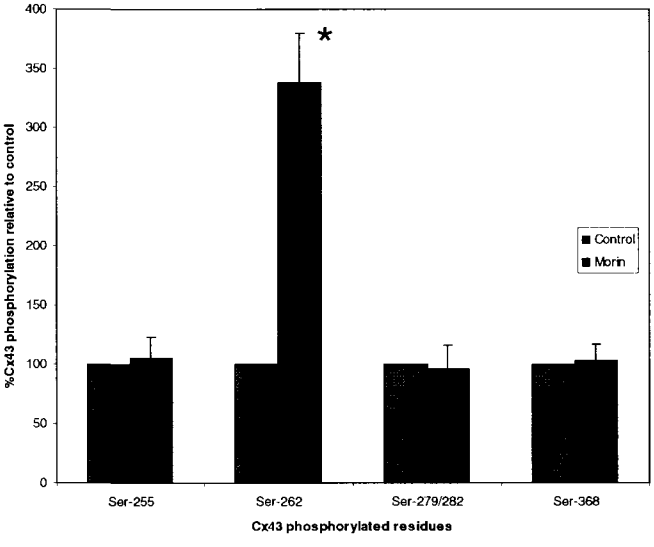
400
350
300
250
200
150
100
50
0
%Cx43 phosphorylation relative to control
Control
Morin
*
Ser-255
Ser-262
Ser-279/282
Ser-368
Cx43 phosphorylated residues

D

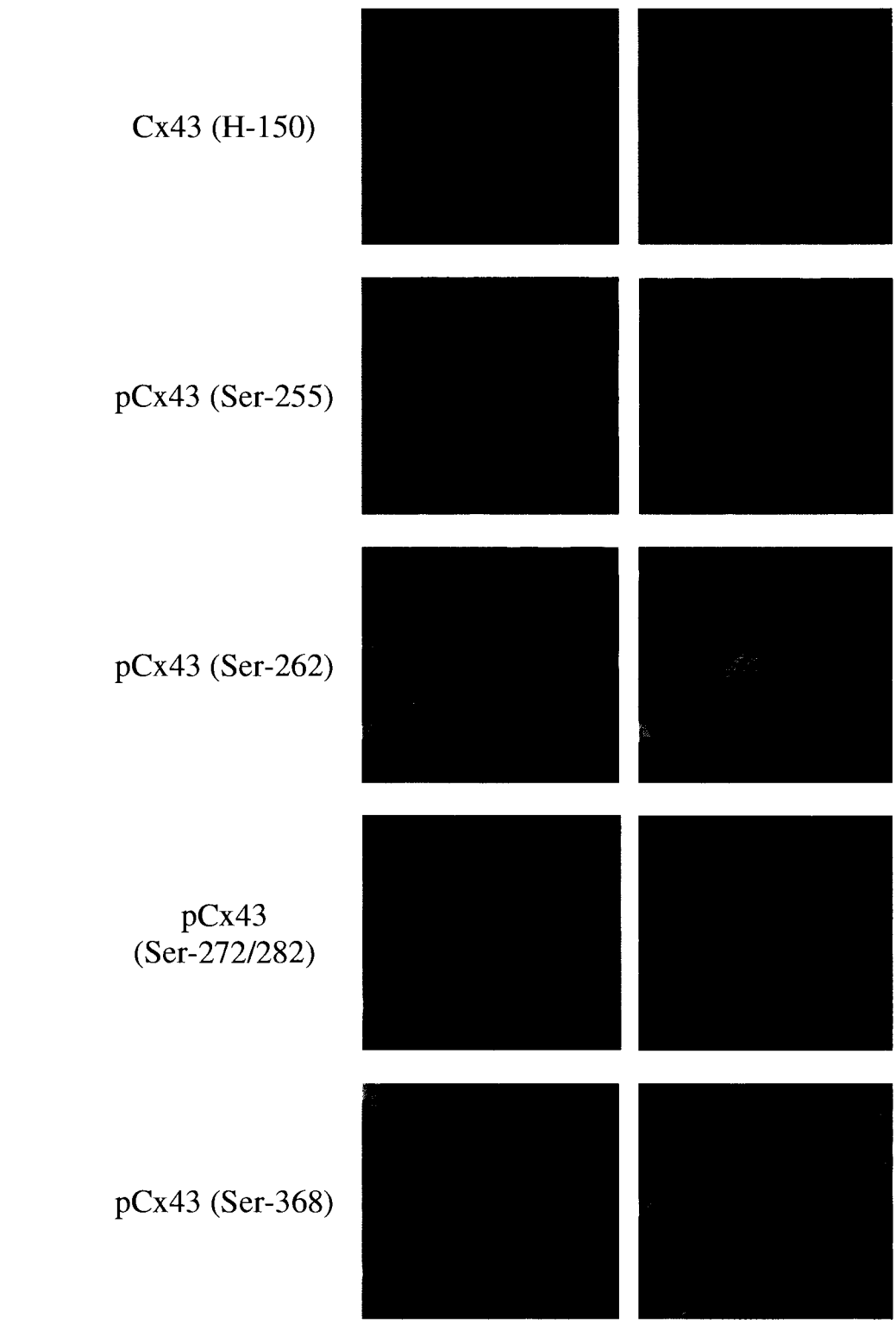
Control
Morin
Cx43 (H-150)
pCx43 (Ser-255)
pCx43 (Ser-262)
pCx43
(Ser-272/282)
pCx43 (Ser-368)

As a comparison the same experiments were performed on U-87 MG cells. Contrary to the other cell line, morin did not have any effects on Cx43 expression and phosphorylation (Fig. 29, A) as well as sub-cellular localization (Fig. 29, B) in U-87 MG cells. In addition, treatment with morin did not alter the fragmented Cx43 with the exception of the Ser-368 site in U-87 MG cells, suggesting it affects mainly the connexin at the correct molecular weight of 43 KDa. The former requires further analyses. These results again suggest that the two cell models possess different signaling pathway mechanisms. These encouraging results seem to indicate that the inhibition of an unknown pathway associated with morin treatment may restore part of the normal function of Cx43 in U-251 MG cells. In order to reduce the proliferation of these aggressive astrocytoma the function of GJ should also be restored.

3.5.2 Effect of PD98059 and Morin on Gap Junction Function in U-251 MG Cells

As mentioned previously, treatment of U-251 MG cells with PD98059 shifted Cx43 localization to the membrane (Fig. 17, B). In addition, treatment of these same cells with morin was shown to increase Cx43 in the nucleus and cytoplasm. Scrape-loading experiments were thus performed to observe whether the effects of those treatments resulted in an increase of gap junctional communication as well. U-251 MG cells were treated with 50 μM of PD98059 alone, 40 μM of morin alone and both of these compounds together for 24 hours. Scrape-loading was then performed to observe the effect on gap junctional communication. Results show that treatment with either PD98059 or morin does not increase gap junctional communication in any way (Fig. 30). Even though normal Cx43 localization is partly restored by PD98059 treatment, there is

Figure 29. Effect of the flavanoid morin on Cx43 expression and sub-cellular localization in U-87 MG cells.

A: U-87 MG cells were exposed to 40 μM of morin for 24 hours. Whole protein lysates were separated on 10% SDS-PAGE and transferred to nitrocellulose membranes. Cx43 protein levels and phosphorylation levels were assessed by immunoblot analysis by probing with Cx43 antibodies, anti-Cx43 (H-150), anti-pCx43 (Ser-255), anti-pCx43 (Ser-262), anti-pCx43 (Ser-279/282) and anti-pCx43 (Ser-368). No changes in Cx43 expression/phosphorylation as well as Cx43 fragments were observed following treatment with morin in U-87 MG cells.

B: Immunofluorescence staining of Cx43 in the human astrocytoma cell line U-87 MG upon treatment with 40 μM of morin for 24 hours. Cells were fixed, permeabilized and probed with Cx43 (H-150), pCx43 (Ser-255), pCx43 (Ser-262), pCx43 (Ser-279/282) and pCx43 (Ser-368) IgGs and the appropriate secondary AlexaFluor 488 nm IgG. Images were originally taken at 20x magnification. No changes in Cx43 sub-localization were observed following treatment with morin in U-87 MG cells.

A

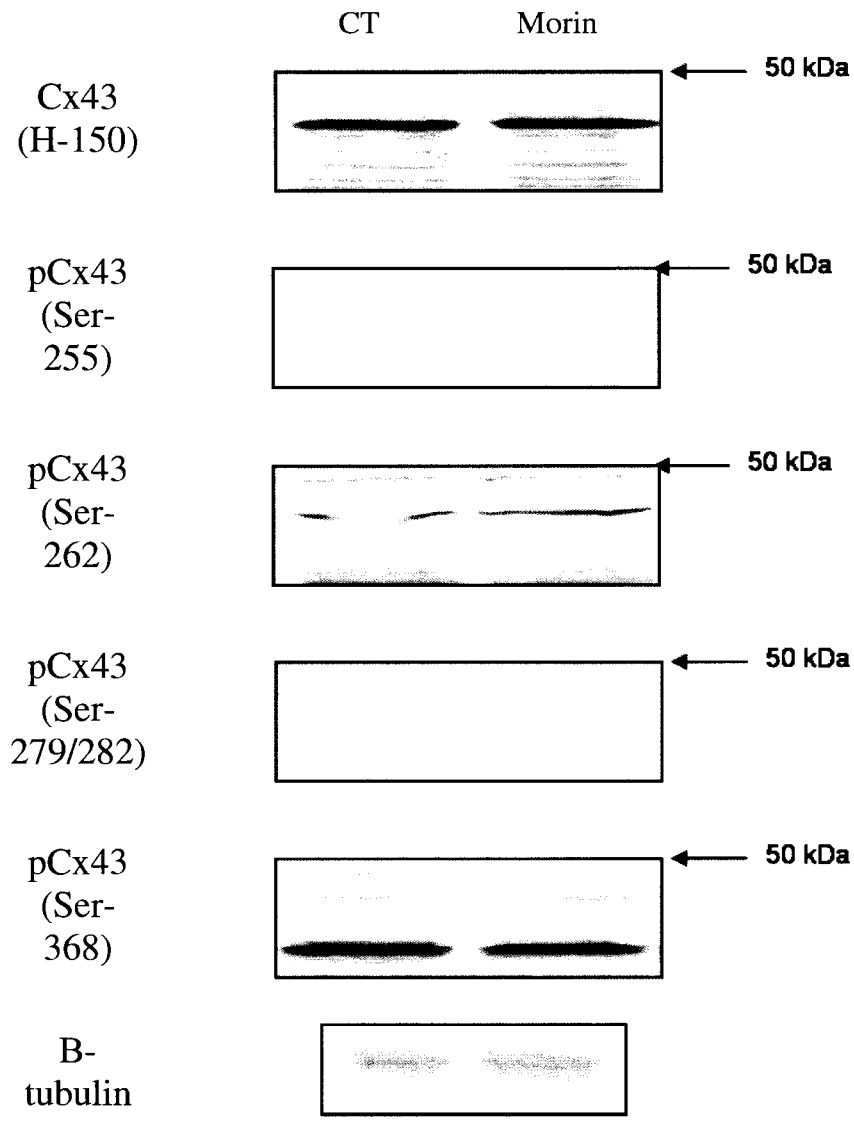
CT
Morin
Cx43 (H-150)
50 kDa
pCx43 (Ser-255)
50 kDa
pCx43 (Ser-262)
50 kDa
pCx43 (Ser-279/282)
50 kDa
pCx43 (Ser-368)
50 kDa
B-tubulin

B

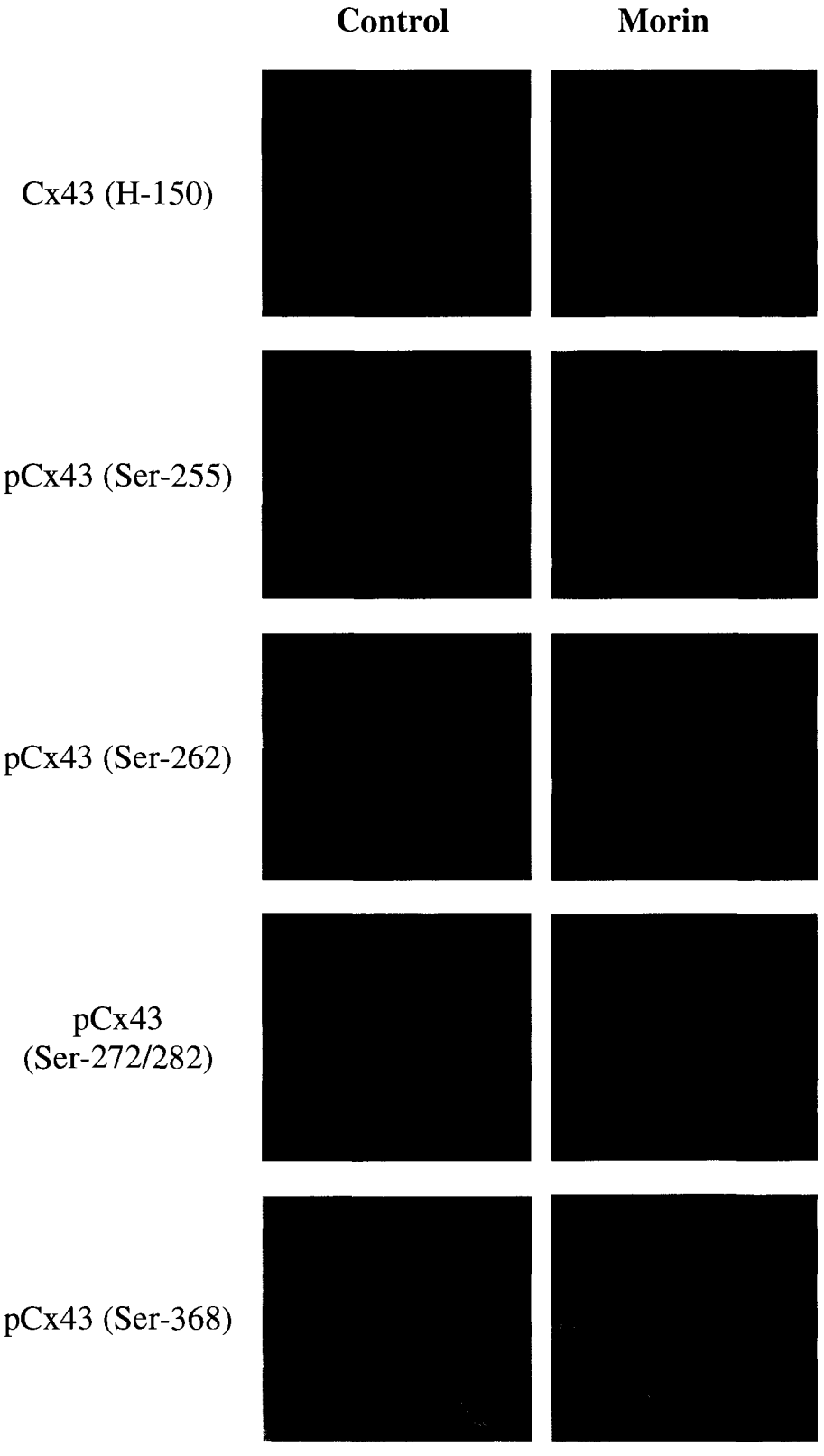
Control
Morin
Cx43 (H-150)
pCx43 (Ser-255)
pCx43 (Ser-262)
pCx43
(Ser-272/282)
pCx43 (Ser-368)

Figure 30. Effect of PD98059 and Morin on gap junction-mediated dye coupling of U-251 MG cells.

Cultured U251 MG cells were treated with 50 μM of PD98059 and 40 μM of morin, alone or in combination and scrape-loaded with Lucifer yellow (fluorescent images on the left; corresponding reverse phase images on the right). Briefly, 70 μL of Lucifer yellow dye was added on top of a monolayer of cells and a small scratch was performed with a small needle. Cells were then subsequently washed with PBS 3 minutes. Images were originally taken at 20x magnification. Neither treatment, alone or in combination, restored intercellular communication as shown by a lack of dye transfer.

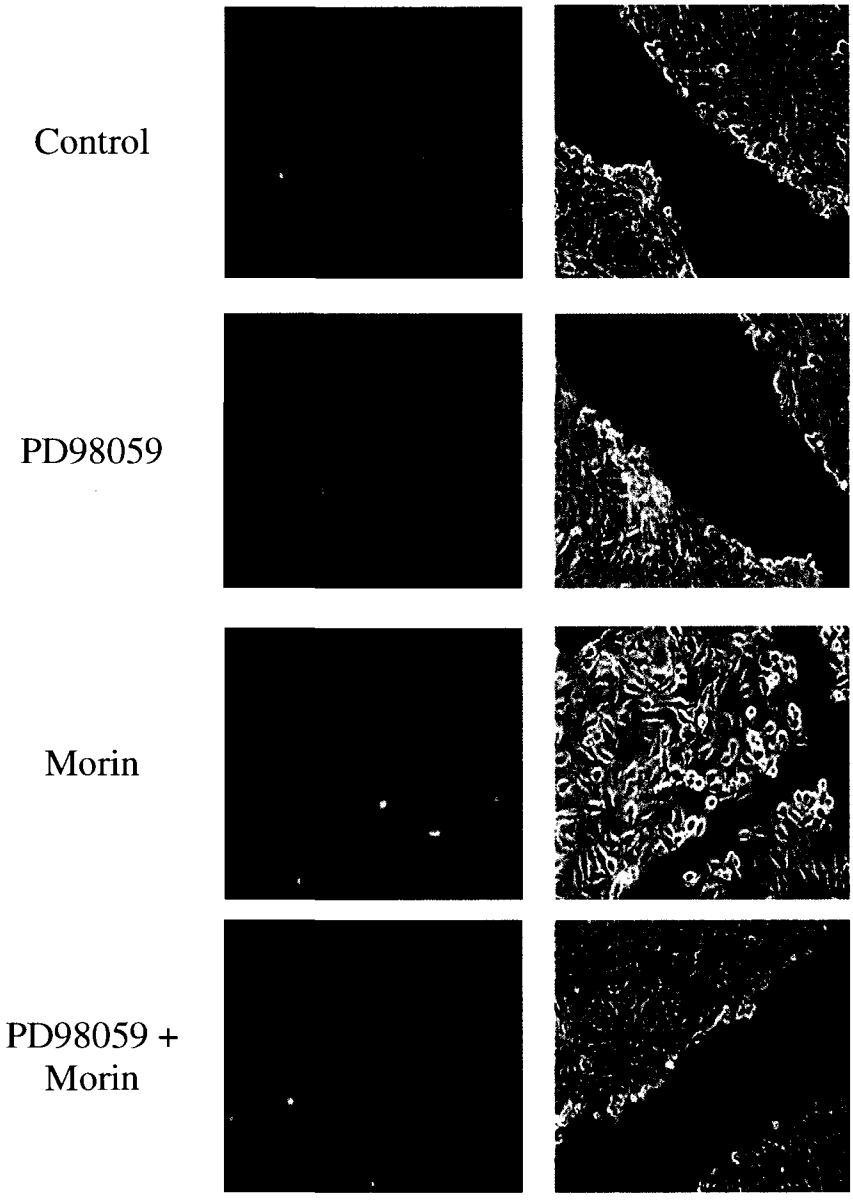
Control
PD98059
Morin
PD98059 +
Morin

no increase in gap junction function. Other signaling pathways may need to be induced or inhibited in order to modulate the gating and restore the function.

3.6 Inhibition of the p38 MAPK Pathway Increases Cx43 Expression and Phosphorylation

As seen in Figure 28 morin increases Cx43 phosphorylation on Ser-262. The mechanism or signaling pathway having this effect has not been identified. It has been previously reported however, that morin is an inhibitor of the p38 MAPK pathway in Chang liver cells (Hsiang *et al.*, 2005). In order to determine if morin also inhibited the p38 MAPK pathway in U-251 MG, cells were treated with SB203580, a specific p38 MAPK inhibitor. If the inhibition through SB203580 could mimic the effects seen with morin it could then be suggested that the increase in Cx43 phosphorylation derives from changes in p38 MAPK activity.

U-251 MG cells were treated with 10 μM SB203580 for 24 hours and Cx43 expression and sub-localization were determined by Western blotting and immunocytochemistry respectively. Since the effects following treatment with morin were only seen with the Cx43 (H-150) and pCx43 (Ser-262) antibodies, only those two were used in the experiment. Western Blots show a significant increase in the P2 band of Cx43 following SB203580 treatment whereas no changes are seen in regards to the P1 band (Fig. 31, A). In addition, Ser-262 phosphorylation increased following treatment as well. Densitometric analyses show an increase of 1.6 fold of the P2 band when probed with the Cx43 (H-150) antibody (Fig. 31, B) and a 3 fold increase in Ser-262

Figure 31. Effect of the p38 MAPK inhibitor SB203580 on Cx43 expression and sub-cellular localization in U-251 MG cells.

A: U-251 MG cells were exposed to 10 μM of SB203580 for 24 hours. Whole protein lysates were separated on 10% SDS-PAGE and transferred to nitrocellulose membranes. Cx43 protein levels and phosphorylation levels were assessed by immunoblot analysis by probing with Cx43 antibodies, anti-Cx43 (H-150) and anti-pCx43 (Ser-262). SB203580 treatment increased phosphorylation of Cx43 on Ser-262 just as morin did but to a lesser extent, suggesting that morin is an effector of p38MAPK signalling. Note that the P3 phosphorylated band is absent.

B: Densitometric analysis of Cx43 expression using the anti-Cx43 (H-150) antibody following treatment with 10 μM of SB203580 for 24 hours in U-251 MG cells. Data are expressed as the percentage intensity of the control band and are the mean ± SD of three separate experiments. Level of significance: $P<0.05$ (*) compared with control cells according to the Student's t-test.

C: Densitometric analysis of Cx43 phosphorylation on Ser-262 following treatment with 10 μM of SB203580 for 24 hours in U-251 MG cells. Data are expressed as the percentage intensity of the control band and are the mean ± SD of three separate experiments. Level of significance: $P<0.05$ (*) compared with control cells according to the Student's t-test.

D: Immunofluorescence staining of Cx43 in the human astrocytoma cell line U-251 MG upon treatment with 10 μM of SB203580 for 24 hours. Cells were fixed, permeabilized and probed with Cx43 (H-150) and pCx43 (Ser-262) IgGs and the appropriate secondary AlexaFluor 488 nm IgG. Images were originally taken at 20x magnification. Increase in cytoplasmic Ser-262 phopshorylation can be observed following SB203580 treatment, as was the case with morin.

A

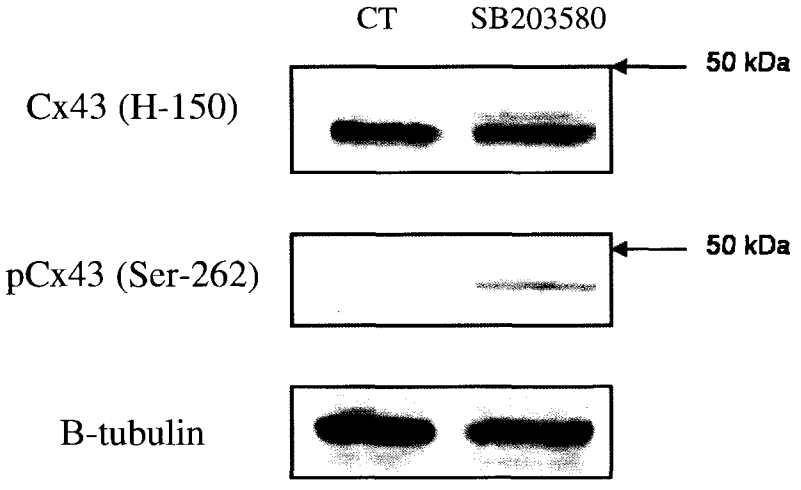

B

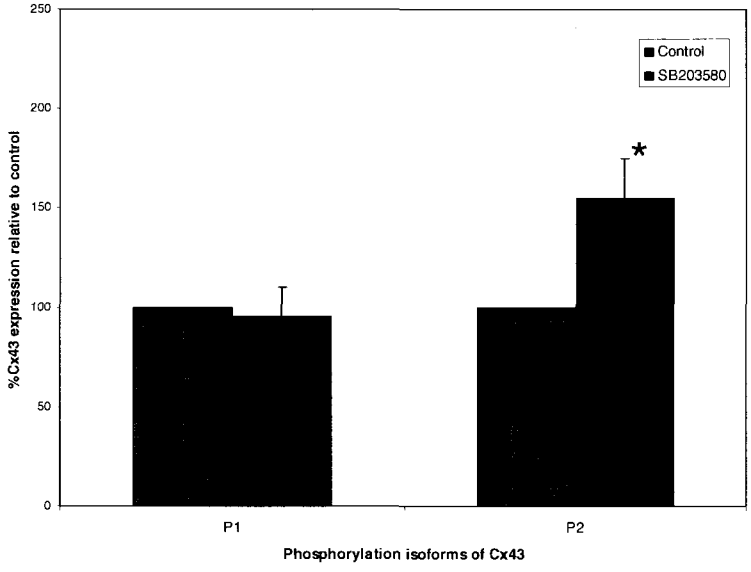
250
200
150
100
50
0
%Cx43 expression relative to control
Control
SB203580
*
P1
P2
Phosphorylation isoforms of Cx43

C

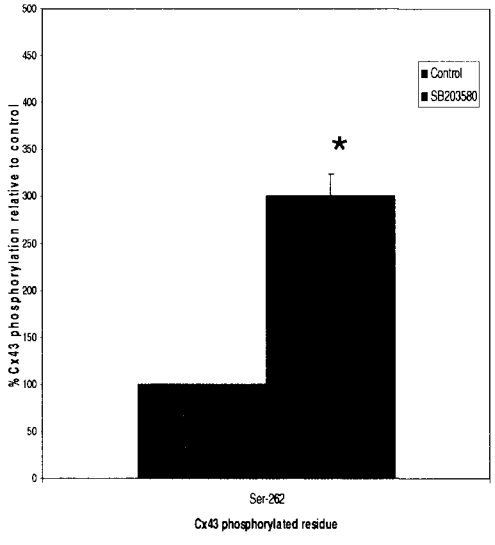
500
450
400
350
300
250
200
150
100
50
0
% Cx43 phosphorylation relative to control
Control
SB203580
*
Ser-262
Cx43 phosphorylated residue

D

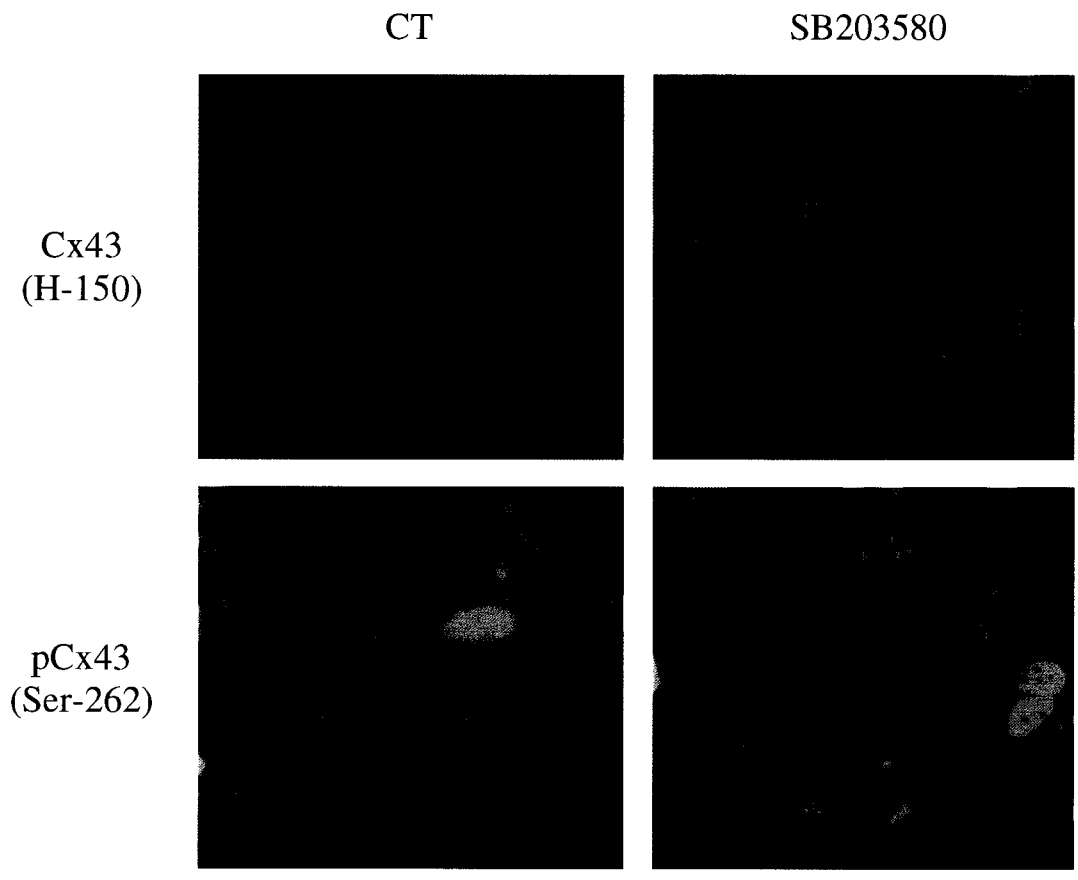

phosphorylation (Fig. 31, C). Immunocytochemistry experiments show an increase in nuclear and cytoplasmic Cx43 when probed with the H-150 antibody following treatment with 10 μM of SB203580 (Fig. 31, D). Ser-262 phosphorylation went from strictly nuclear in the controls to nuclear and partially cytoplasmic after treatment, suggesting an effect of the increase in Ser-262 phosphorylation on expression or protection of the Cx43 against degradation (Fig. 31, D).

Taking into account the results obtained after treatment with SB203580 these seem to mimic the effects following morin exposure. This would tend to suggest that an increase in Cx43 phosphorylation, more specifically on Ser-262, is a result of p38 MAPK inhibition. It also suggests that the inhibition of p38 MAPK indirectly allows for the activation of a different unidentified kinase.

3.7 Interaction of Cx43 and the caveolae marker, caveolin-1

Our results demonstrated that Cx43 is redirected to the plasma membrane upon inhibition of the phosphorylation site targeted by ERK-MAPK but that the gap junction channels were not functional. In order for Cx43 to interact with various protein kinases following translocation to the membrane, they all have to be guided to specific regions in the membranes containing a variety of protein kinases. One of these structures is called caveolae. They are small invaginations of the plasma membrane and contain complexes of several protein kinases, scaffolding and anchoring proteins. Their main role is to compartmentalize protein kinases with their targets to ensure efficiency.

The main protein, or marker, for caveolae is caveolin-1. Altered caveolin-1 expression has been shown to be associated with cancer; in fact several high-grade

tumors possess decreased levels of the protein (Zhang *et al.*, 2006; Burgermeister *et al.*, 2007). Caveolin 1 has also been shown to directly interact with Cx43 (Schubert *et al.*, 2002; Lin *et al.*, 2003). Since altered Cx43 expression and/or cellular sub-localization is also associated with cancer in at least 90% of the cases, it is hypothesized that in human astrocytoma cells the connexin protein may not associate with caveolin-1 in the caveolae as it should.

3.7.1 Cx43 do not localize to membrane caveolae

In order to determine if Cx43 localizes to caveolae in U-251 MG and U-87 MG cells, a fractionation and sucrose gradient separation was performed in Dr. Z. Yao's laboratory. Briefly, cells were scraped, added to MES buffer and mixed with Triton X-100 (on ice). The Triton X-100 mixture was then added to 80% sucrose and overlaid with gradients of 30% sucrose and 5% sucrose respectively. The suspension was then ultracentrifuged at 189 000 g for 18 hours. Thirteen fractions of 900 µL were collected, submitted to 10% SDS-PAGE and transferred to a nitrocellulose membrane. Blots were then probed with anti-Cx43 (H-150) and anti-caveolin-1 (7C8).

In those blots, fractions 5 and 6 represent proteins found in caveolae whereas fractions 9 through 13 are composed of non-caveolae membrane proteins as well as soluble proteins found in the cell (Zhang *et al.*, 2004). Results show that caveolin-1 is expressed in fractions 5 and 6 (caveolae fractions) in both cell lines (Fig. 32). However, caveolin-1 is expressed at higher levels in U-87 MG cells compared to U-251 MG. These results support data that suggests a correlation between caveolin-1 expression and tumor malignancy. It is important to note that caveolin-1 is also expressed in fractions 9

Figure 32. Caveolae isolation and sub-cellular localization of Cx43 and caveolin-1.

20×10^6 cells were scraped, centrifuged and mixed with Triton X-100. The cell suspension was added to 80% sucrose and overlaid with two layers of 30% and 5% sucrose respectively. Samples were then ultracentrifuged at high speed for 18 hours and 13 fractions of equal volume were collected, and submitted to SDS-PAGE. Following transfer to a nitrocellulose membrane Cx43 and caveolin-1 proteins were assessed in both **A)** U-251 MG and **B)** U-87 MG cells by immunoblot analysis by probing with anti-Cx43 (H-150) and anti-caveolin-1 (7C8). U-87 MG cells show higher levels of caveolin-1 compared to U-251 MG cells. Cx43 however does not seem to localize with caveolin-1 in caveolae structures (fractions 4-6).

A

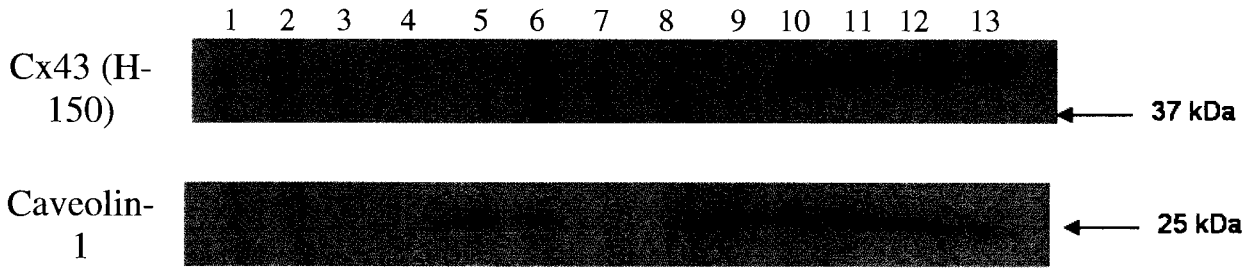
1 2 3 4 5 6 7 8 9 10 11 12 13
Cx43 (H-150)
37 kDa
Caveolin-1
25 kDa

B

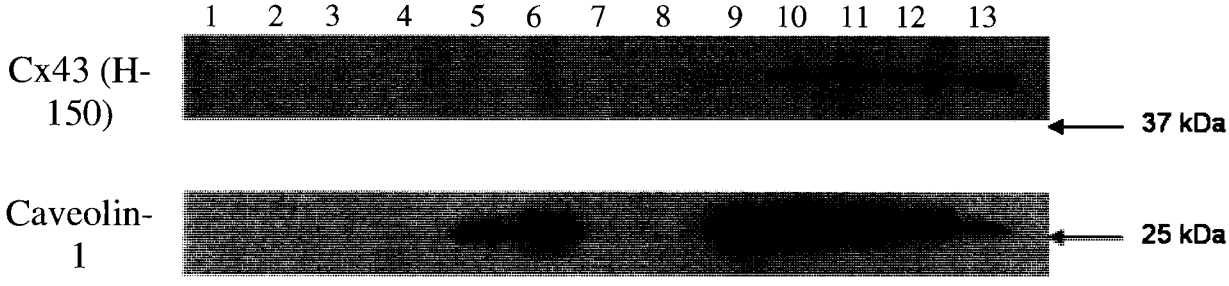
1 2 3 4 5 6 7 8 9 10 11 12 13
Cx43 (H-150)
37 kDa
Caveolin-1
25 kDa

through 13. It most probably represents caveolin-1 proteins that have not reached caveolae yet or that cancer cells exhibit abnormal caveolin-1 sub-localization. Cx43 on the other hand seems to be localized exclusively in fractions 9 through 13 (Fig. 32). As a matter of fact Cx43 is completely absent from the caveolae fractions. In U-251 MG cells it is understandable since no Cx43 are localized to the membranes. In U-87 MG cells however, this may suggest that the Cx43 observed on the membrane are localized outside caveolae domains or that caveolae domain do not shelter Cx43 in these cells.

3.7.2 Cx43 and caveolin-1 does not co-localize in U-251 MG cells

In order to verify if Cx43 and caveolin-1 do not co-localize, confocal microscopy was performed in U-251 MG cells. Cells were fixed, permeabilized and probed with anti-Cx43 (H-150) or anti-caveolin-1 (7C8). As a membrane marker, wheat-germ agglutinin linked with an Alexa 647 was used.

Images show that Cx43 is mainly nuclear and cytoplasmic, with a complete absence from the membrane (Fig. 33, yellow arrow). On the other hand images show that caveolin-1 is indeed localized to the plasma membrane, as well as the cytoplasm of the cells (Fig. 33, red arrow) consistent with the fractionation results. These results thus fully confirm the previous fractionation experiment suggesting an absence of interaction between Cx43 and caveolin-1.

Figure 33. Co-localization of Cx43 and caveolin-1 by confocal microscopy in U-251 MG cells.

Immunofluorescence of Cx43 and caveolin-1 using confocal microscopy. U-251 MG cells were fixed, permeabilized and probed with anti-Cx43 (H-150) and caveolin-1 (7C8) and the Alexa 488 secondary antibody (green fluorescence). Cells were also stained with an Alexa 647 wheat germ agglutinin to stain the membranes (red fluorescence). Images were originally taken at 66.6x magnification. Cx43 localization is clearly nuclear (yellow arrow) and absent from the membrane, where as caveolin-1 is mainly on the cell membrane (red arrow) and mostly absent from the nucleus. This seems to indicate a lack of co-localization between these two proteins.

Cx43 Caveolin-1

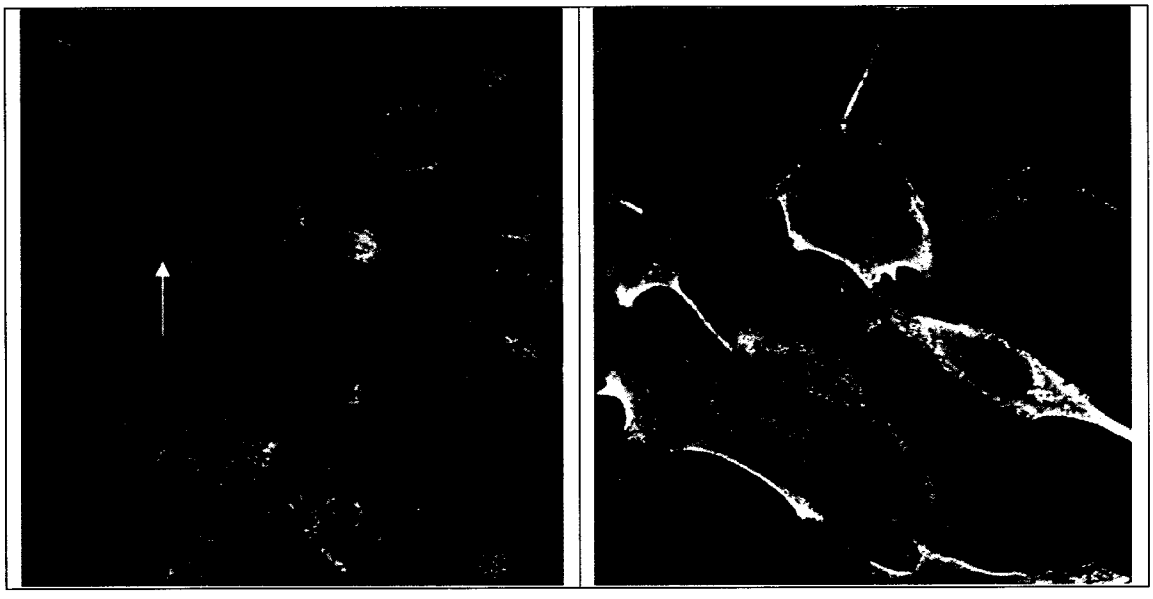

4.0 DISCUSSION

Gap junctions have been the topic of much discussion upon their initial discovery in the 1960s. These intercellular channels have been shown to play a crucial role in cellular homeostasis; namely proliferation, differentiation and apoptosis. The absence of intercellular communication through gap junctions leads to uncontrolled proliferation—a defining feature of cancer. In the vast majority of cancers, gap junctions are not functional, thus making the restoration of these channels an important aspect of cancer research.

The absence of functional gap junctions in cancer cells are mainly attributed to an abnormal connexin cellular sub-localization, where the connexin protein retains a perinuclear or cytoplasmic localization rather than translocating to the plasma membrane. A general decrease in connexin expression can also explain the loss of gap junctional intercellular communication (GJIC) in cancer cells. In astrocytoma, a tumor derived from normal astrocyte cells, this absence is indeed dramatic since astrocytes are of the most intercellularly coupled cells in the body thus forming a syncytium. Notably Cx43, the main connexin normally found in astrocytes, is very poorly expressed in malignant forms of astrocytoma. In normal cells, phosphorylation plays a crucial role in the trafficking of Cx43 to the plasma membrane. It was shown that the increase of phosphorylation on a specific site, Ser-364, caused by the activation of PKA leads to higher levels of Cx43 on the plasma membrane (Solan and Lampe, 2009). It is thus possible that other signaling pathways are responsible for the aberrant expression and/or sub-localization of Cx43 in astrocytoma cells especially in view of the numerous

phosphorylation consensus sites found in the carboxyl end of the connexins (except for Cx26).

The purpose of this study was to examine the role of various signaling pathways in the cellular sub-localization and expression of Cx43 in human astrocytoma cell lines.

4.1 Characterization of Human Astrocytoma Cell Lines, U-251 MG and U-87 MG

Since astrocytoma can exist as four different types of varying malignancies it was decided that a Grade III (U-87 MG) and a Grade IV (U-251 MG) cell line would be chosen to compare connexin behaviour associated or not with tumor malignancy. In order to determine if the difference in tumorogenicity of our two cell models reflected a change in cell growth, the cellular proliferation rates were determined over a 96 hour period. Figure 4 shows a higher cell population increase in U-251 MG cells compared to U-87 MG cells. These results are in accordance with the literature that demonstrates a direct relationship between cellular proliferation and tumor malignancy (Tagliaferri *et al.*, 1999). Moreover, the cellular morphology of the least malignant cell line, U-87 MG, shows more processes indicating a state closer to normal astrocytes (Fig. 4, B). Interestingly, following 72 hours of incubation U-87 MG cells form clusters that are absent from the other cell line. These structures could be pseudoganglia that are indicative of more differentiated cells (Santos *et al.*, 2004) which would be in line with the more limited aggressivity of the U-87 MG cells.

It is known that in cancer cells tumor malignancy is inversely proportional to connexin expression (Pu *et al.*, 2004). To determine if this was the case in our cell models RT-PCR was performed using specific primers designed for human Cx43 in our

laboratory. Results showed possibly higher Cx43 mRNA levels in U-87 MG cells compared to the U-251 MG cells (Fig. 5, A). As a positive control, a rat glioblastoma cell line transfected with Cx43 showed levels of Cx43 mRNA that seemed higher compared to the two neoplastic cell lines. In addition, a normal human brain cortex biopsy was used which also showed higher Cx43 mRNA than the cell lines but to a lesser extent compared to the transfected cell line (Fig. 5, A). These results fully support the literature which states that more malignant tumor cells exhibit lower Cx43 expression (Soroceanu *et al.*, 2001) but clearly need the confirmation with real time PCR.

A specific antibody was used to detect Western Blots in order to observe Cx43 expression in our two cell models. The antibody used, H-150 is classically used by most authors. It recognizes all forms of Cx43, namely the phosphorylated and non phosphorylated forms of Cx43 (Shen *et al.*, 2007). Results show that both cell lines exhibit the usual tri-band normally observed using this antibody (Fig. 5, B) (Shen *et al.*, 2007). In addition in U-87 MG cells the two upper phosphorylated isoforms of Cx43 seem to be labeled at a higher density compared to U-251 MG which coincides with the RT-PCR experiment. Cx43 expression in transfected rat glioblastoma cell line is also higher compared to the two neoplastic cell lines (Fig. 5, B).

In order to confirm that the upper bands seen on the blots represented phosphorylated Cx43, cell extracts were treated with 1U/μg of calf intestinal alkaline phosphatase. As was expected the two upper bands almost completely disappeared following phosphatase treatment (Fig. 6). The lower band however also decreased following alkaline phosphatase treatment. This result was surprising since the lower band was believed to represent the non-phosphorylated isoform of Cx43. The data

however suggests that the lower, high intensity band represents another phosphorylated isoform signifying a visible absence of a non-phosphorylated band or expression at a level beyond the sensitivity of the technique. This result is not a complete surprise however, since astrocytoma cell lines are known to have constitutively activated signaling pathways, such as MAPK, which would result in a very high phosphorylation state of Cx43 (Reardon *et al.*, 2006). We can state that U-251 and U-87 cell lines express highly phosphorylated forms of Cx43.

Intercellular communication through gap junctions is not only dependent on the presence of connexin in the cell but also on the correct cellular sub-localization of the protein. In our cell models immunocytochemistry experiments show that Cx43 sub-localization is different between the two cell models (Fig. 5, C). U-251 MG cells show a complete lack of Cx43 on its plasma membrane whereas punctate structures indicative of connexon aggregation into plaques is observed in U-87 MG cells. This observation however does not necessarily mean that gap junctions in this cell model are functional since the connexons observed on the membrane may not be in an open conformation. A very important result in regards to Cx43 sub-localization in our cell models is the protein's presence in the nuclei of the cells in both cell lines (Fig. 5, C). There has been some reports of the C-terminal tail of Cx43 localizing in the nucleus (de Feijter *et al.*, 1996; Dang *et al.*, 2003); this has not been reported for human astrocytoma cells. The transfected rat cell line positive control shows much higher levels of Cx43 on the plasma membrane as well as around the nucleus. One can state that Cx43 in the studied cell lines are abnormally localized in the nuclei; this is the first demonstration of this phenomenon in malignant astrocytoma cell lines.

4.2 Phosphorylation of Cx43 in Astrocytoma

Phosphorylation is crucial to the translocation of Cx43 to the plasma membrane (Solan and Lampe, 2007). Since only the least malignant cell line, U-87 MG, exhibits Cx43 on its plasma membrane it is probable that phosphorylation is not identical between these two cell lines. Four phospho-specific Cx43 antibodies were used to decipher how the protein is being phosphorylated namely Ser-255 (MAPK), Ser-262 (PKC), Ser279/282 (MAPK) and Ser-368 (PKC).

When observing the blots an unexpected result was obtained: several bands below the expected molecular weight of 43 kDa were observed when using all four antibodies (Fig. 7, 8, 9, 10). These bands could represent fragmented Cx43 following degradation since it is known that the proteins must be hyperphosphorylated in order to be targeted for degradation (Leithe and Rivedal, 2004). These bands, ranging from 26 kDa to 34 kDa are much more decorated by the site specific phospho-antibodies present than the bands at 43-47 kDa. What is interesting to note is that the pattern of the fragmented bands as well as their intensity differs from one cell line to another depending on the phospho-antibody used to probe the blot. This suggests that the degradation pattern (ie which sites are associated with the degraded fragments) as well as the resulting size of the fragments differ between the two cell lines. When for example the Ser-255 blot is put side by side with an H-150 blot (Fig. 7, B) it is clear that the bands corresponding to the P1 and P2 isoforms of Cx43 are absent in the blot probed with the phospho-antibody; only a hyperphosphorylated band is seen which relates to Cx43 degradation (Berthoud *et al.*, 2004). Phosphorylations on other sites that were not studied (only four out of a dozen protein kinase phosphorylation consensus sites were used) could account for the

phosphorylated full-length Cx43 bands that were observed using the H-150 antibody (King and Lampe, 2005). It is important to note also that chemiluminescence was used in parallel for these experiments but only the strongest fragmented bands would appear while the rest would not be manifested on the blots (Fig. 7, 8, 9, 10). For this reason colorimetric Western Blotting was utilized in the study.

Immunocytochemistry experiments show a strong nuclear presence of Cx43 in both cell lines when the protein is phosphorylated on Ser-255 and Ser-262 (Fig. 7, C; 8, C) whereas Ser-279/282 and Ser-368 phosphorylated Cx43 is diffuse throughout the cells (Fig. 9, C; 10, C). As mentioned previously nuclear localization of Cx43 has already been documented (Dang *et al.*, 2003) but never in human astrocytoma cells. In order to confirm that indeed Ser-255 and Ser-262 phosphorylated Cx43 is nuclear, cross-sectional images of 1 micron were taken by confocal microscopy. Results showed that most of Ser-255 Cx43 was indeed nuclear since only a small proportion of the cells exhibited a ring-like structure characteristic of a perinuclear localization (Fig. 11). Ser-262 phosphorylation in both cell lines was entirely nuclear with no Cx43 detected in the nucleoli (Fig. 12). Finally as a last confirmation U-251 cells were separated into a nuclear-enriched and cytoplasmic fraction which showed a clear presence of Cx43 in the nuclear fraction (Fig. 13). These results taken together confirm the presence of Cx43 in the nuclei of the two cell lines. Since previous studies have shown that nuclear Cx43 had effects on cellular proliferation (Dank *et al.*, 2003) it is a strong possibility that the same can be observed in our cell models. It is possible that Cx43 in the nucleus can be involved in the control of transcription as suggested in the literature (Huang *et al.*, 2002; Mesnil *et al.*, 2005). As a matter of fact Cx43 has been shown to negatively regulate the

transcription of Cx32 in liver hepatoma cells (Zhang *et al.*, 2007). One can state that degradation fragments of Connexin43 that carry the phosphorylation sites Ser-255 and Ser-262 are aberrantly located inside the nuclei since the same sites are not recognized by the appropriate antibodies in the full length protein. This is also supportive of the occurrence of Cx43 degradation inside the cells and arguing against proteolytic degradation during protein extraction although a minor degradation can indeed be artefactual. This is a major finding in regard to the possibility that these fragments mediate transcriptional changes as proposed recently as a second role for connexins (Moore *et al.*, 2008).

4.3 Connexin43 Function in Astrocytoma

The presence of Cx43 on the plasma membrane does not necessarily signify functional intercellular gap junctional communication as the channels can be in their closed conformation. It was thus important to measure gap junctional communication in our cell models. Scrape loading experiments show a total lack of communication in U-251 MG cells, which is to be expected since no Cx43 is present on the membranes (Fig. 14). In U-87 MG cells however the cells show an incorporation of the Lucifer Yellow dye in all the cells. This would suggest the presence of functional connexons on the membrane taking part in either functional gap junctions or open hemichannels.

In recent years connexins have been shown to play a role in addition to the formation of gap junctions. Uncoupled connexons were shown to be in the open conformation as hemichannels and playing a role in cellular processes such as the transmission of death signals and ATP as well as NAD^+ signaling (Dbouk *et al.*, 2009).

When Lucifer Yellow dye was added to the cell monolayers without performing a scratch with a needle, U-87 MG cells incorporated the dye uniformly (Fig. 15). Flufenamic acid, a hemichannel inhibitor, confirmed the presence of hemichannels in U-87 MG cells (Fig. 16). Taken together these results confirm the presence of open hemichannels in U-87 MG cells. However since the dye would enter the cells regardless of the presence of a scratch or not it is impossible to tell if functional gap junctions are present just by utilizing the scrape loading technique. A more advanced method would have to be used using a micro-needle that injects the dye in one cell only and observe the diffusion to neighboring cells (Esen *et al.*, 2007). Since U-251 MG cells seem to completely lack any intercellular communication it would be worthwhile to try to find signaling pathways that would restore the normal membrane localization of Cx43. One can state that the punctuate highly phosphorylated connexin 43 protein observed on the plasma membrane of the less aggressive U-87 MG cells represent mainly functional hemichannels as demonstrated for the first time in this project. The function of the hemichannels in these cells, if confirmed *in vivo* in patient tumors, would shed light on the physio-pathology of the tumor.

4.4 Effect of Protein Kinase Inhibition on Cx43 Expression and Sub-localization in Astrocytoma

As discussed previously phosphorylation is a crucial event in the life cycle of Cx43 and the protein kinases responsible for these phosphorylations are important targets for connexin restoration. Three pathways were chosen for this study as they are known to be part of the main kinases responsible for the phoshorylation at the carboxyl end of

Cx43: PKC, PKA and ERK-MAPK (Solan and Lampe, 2009). Experimental data demonstrates that inhibition of the ERK-MAPK pathway using PD98059 was the only treatment which affected the full-length (43kDa) Cx43 expression and phosphorylation (P1 and P2) and then only in the U-87 MG cell line (Fig. 18). This suggests a difference in the signalosome of the two cell lines. It would be expected however that the inhibition of ERK-MAPK would decrease phosphorylation on Ser-255 and Ser-279/282 and that the inhibition of PKC would lower Ser-368 phosphorylation, since those sites are known to be targets by these kinases (Solan and Lampe, 2009). Our results do not show these decreases in phosphorylation. This could be attributed to other protein kinases which would phosphorylate these specific sites in our cell models since the explored sites can be phosphorylated by more than one kinase or kinase isoform. Yogo *et al.* (2006) have observed that in rat granulosa cells, PKA is implicated in the phosphorylation of Cx43 on Ser-368, which is usually a well studied PKC phosphorylation site. This may indicate that in U-251 MG and U-87 MG cells the four sites studied could be phosphorylated by other protein kinases that have not been investigated in this research.

Fragmentation of Cx43 however was shown to be affected by the various pathway inhibitions in both cell lines (Fig. 17-26). Shaghayegh Safakhoo, a Master's student in our laboratory, has demonstrated that a fragment of Cx43 can still be involved in metabolic responses (Safakhoo, 2007). She demonstrated that inhibition of PKC using BisI in N2A cells transfected with the C-terminal portion of Cx43 elicited a decrease in proliferation and an increase in apoptosis. These results are interesting since they offer a possible role of fragmented Cx43 in various metabolic phenomena. The sub-localization in the nuclei of transfectant cells expressing the carboxyl end of Cx43 in cell nuclei was

also reported (Dang *et al.*, 2003). In our research the changes in fragmented Cx43 is highly dependent on the treatment, the cell type as well as the specifically labeled site. It is interesting to note that in the case where U-251 MG cells were treated with PD98059 all Cx43 fragments increase (Fig. 17, A) whereas the full-length Cx43 remains unchanged. In U-87 MG cells, however, the opposite can be observed: while full-length Cx43 labeling increases no changes can be observed in the fragmented protein (Fig. 18, A). When U-251 MG cell blots were probed with Ser-255, PKA and ERK-MAPK inhibition resulted in a decrease of the 29-30 kDa fragments (Fig. 19, A). With the Ser-262 antibody an inhibition of PKC resulted in an increase of the 34 kDa Cx43 fragment (Fig. 21, A). No changes were observed in fragmented Cx43 when probed with Ser-279/282 (Fig. 23, A) however, treatment with PD98059 increased the 30-29 kDa fragment phosphorylated on Ser-368 (Fig. 25, A). In comparison, most of the phosphorylated Cx43 fragments were not affected by the treatments in U-87 MG cells. Ser-255 phosphorylated Cx43 fragments were affected by the treatments (Fig. 20, A), where all three treatments resulted in an increase of the 27-26 kDa doublet band. Ser-368 phosphorylated Cx43 fragments were also affected by the treatments (Fig. 26, A), where BisI and PD98059 treatment increased the 29.5 kDa band. These results are interesting as they seem to demonstrate that both cell lines possess very different degradation mechanisms. The modulation of PKC, PKA and ERK-MAPK had a much bigger effect on the Cx43 fragments in U-251 MG cells compared to the other cell line. Moreover, the results show that fragment size is associated with specific phosphorylation sites which was previously shown in other cell lines (Leithe and Rivedal, 2007).

While the inhibition of the three studied pathways showed specific effects on the fragmented bands, no alteration of the protein's sub-localization were observed. The only changes observed were an increase in immunocytochemistry staining in U-87 MG cells treated with PD98059 and probed with the H-150 antibody (Fig. 18, B), which corresponds to a matching increase seen on the Western blots (Fig. 18, A). Interestingly, when U-251 MG cells were treated with PD98059 and probed with the H-150 antibody, a shift of the Cx43 from its usual nuclear localization to the membrane is observed (Fig. 17, B; red arrows). One can state that the latter result is exciting since it suggests that ERK-MAPK inhibition in U-251 MG cells partially restored the normal membrane sub-localization of Cx43 that could potentially lead to functional gap junctions.

4.5 Effect of the Anti-cancer Flavanoid Morin on Cx43 Expression and Sub-localization in Astrocytoma

Flavanoids, natural compounds found mainly in fruits, have long been shown to act as anti-tumor agents (Birt and Bresnick, 1990). One such flavonoid, morin, has been shown to act as a chemopreventive agent against oral carcinoma (Brown *et al.*, 2003). Due to its anti-tumor properties morin was utilized as a treatment in our cell models and Cx43 expression/sub-localization was assessed. Interestingly, morin triggered an increase in Cx43 expression and phosphorylation on Ser-262 in U-251 MG cells (Fig. 28, A). Corresponding immunocytochemistry experiments show an increase in nuclear Cx43 using the H-150 antibody as well as an increase in cytoplasmic Cx43 phoshphorylated on Ser-262 (Fig. 28, D). No effects were observed in U-87 MG cells however (Fig. 29).

Again this demonstrates the differences in signaling pathways between those two cell lines in regards to Cx43 expression and cellular sub-localization.

In U-251 MG cells morin and PD98059 treatments have been shown to increase Cx43 phosphorylation as well as partially restoring plasma membrane localization respectively. Scrape loading experiments were performed to determine if the newly membrane-localized Cx43 forms functional gap junctions in U-251 MG cells. Neither morin nor PD98059 treatments alone or in combination, restored gap junctional intercellular communication (Fig. 30). This signifies that the increased Cx43 on the membrane does not form functional gap junctions. It may be that the channels are formed but remain in a closed conformation due to phosphorylation on the protein carboxyl end (Lampe and Lau, 2004). Further investigation into the pathway(s) responsible for this phosphorylation could help restore functional intercellular communication in this cell line. In addition, another explanation could be that the Cx43 observed on the membrane is not the full-length protein but a fragment of the protein. These fragments would not be able to form complete, functional channels with neighboring cells.

Morin, like most flavanoids, are effectors of several different signaling pathways (Spencer, 2008). Hsiang *et al.* (2005) have shown morin to be an inhibitor of the p38 MAPK pathway in Chang liver cells. In order to determine if this observation is occurring in our cell model we utilized SB203580, which is a p38 MAPK-specific inhibitor (Davies *et al.*, 2000). If SB203580 treatment could mimic the effects observed with morin it would then suggest a role of p38 MAPK in Cx43 phoshorylation in U-251 MG cells. As it turns out SB203580 treatment did increase Cx43 phoshorylation, more

specifically on Ser-262 (Fig. 31, A). Likewise, Cx43 increased in the nucleus when probed with the H-150 antibody as well as in the cytoplasm when phosphorylated on Ser-262 (Fig. 31, D). These data tend to indicate that in U-251 MG cells morin does negatively regulate the p38 MAPK pathway. It is interesting to point out that in some cell lines, such as oral carcinoma cells, morin was shown to have the opposite effect and activated p38 MAPK (Brown *et al.*, 2003). Morin's effects thus seem to be cell type dependent. In addition, morin has been shown to alter other signaling pathways such as PKB/AKT (Brown *et al.*, 2003), human protein kinase CK2 (Li *et al.*, 2009) and even protein phosphatases (Miranda *et al.,* 2006). It would thus be important in the future to try to decipher other signaling pathways affected by morin treatment. One can state that albeit the above reported results deserve more attention and in depth investigations, morin positively alter connexin expression or diminishes its turnover, an effect that can be reproduced by inhibition of the p38 MAPK. This result may be the first step in designing a therapeutic drug to the lethal glioblastoma multiforme targeted to the restoration of gap junction function.

4.6 Cx43 and Caveolae

In order for signaling molecules to compartmentalize at the plasma membrane, specific scaffolding and anchoring structures need to be present to assure the proper interactions between these molecules. Caveolae are such invaginations that permit the interaction between a variety of proteins and signaling molecules (Lajoie *et al.*, 2009). Caveolin-1 (cav-1), the main marker of caveolae, has been shown to decrease in highly malignant cell lines and also interact with Cx43 (Langlois *et al.*, 2008). Fractionation

experiments in both cell lines show the presence of cav-1 in the proper caveolae fractions (5 and 6) but to a higher degree in U-87 MG cells (Fig. 32). This supports previous report that cav-1 expression decreases malignancy: the more malignant the cell line, the lesser expression of Cav-1 (Burgermeister *et al.*, 2007). It is important to note the presence of cav-1 in fractions 9 through 13 as well, representing the proteins that have not yet localized to caveolae. Cx43 however did not localize to caveolae in both cell lines (Fig. 32). The result is not a surprise in U-251 MG cells since no Cx43 can be found on the membrane thus cannot be localized in caveolae. For U-87 MG cells however this signifies that the Cx43 proteins seen on the membrane (Fig. 5, C) are not located in the caveolae. If Cx43 does not interact with cav-1 this could explain why connexin sub-localization is not normal. As a confirmation, confocal microscopy was performed on U-251 MG cells to observe Cx43 and cav-1 cellular sub-localization. Results showed the absence of Cx43 on the membrane (as previously shown) whereas cav-1 was mainly localized to the membrane (Fig. 33). When those two images are seen side by side it is clear that Cx43 and cav-1 do not co-localize in the cell model. It is unknown however if the decrease in cav-1 in high-grade tumors plays a role in the abnormal localization of Cx43. It would be interesting to see if there was a way to try to restore cav-1 expression and if that in turn would affect Cx43 sub-localization.

5.0 CONCLUSIONS AND CLOSING REMARKS

The investigation of Cx43 expression, phosphorylation, cellular sub-localization and function was assessed in two human astrocytoma cell lines of different malignancies.

Cx43 was found to be present in both cell lines almost exclusively in its phosphorylated form, as determined with alkaline phosphatase treatment. Cx43 was shown to be phosphorylated on Ser-255, Ser-262, Ser-279-282 and Ser-368. Interestingly phosphorylated Cx43 was shown to be mainly nuclear, which was confirmed by confocal microscopy and nuclear extractions. The degradation pattern was constant for any one cell line but differed in the two cell lines. Importantly we showed that the fragments were produced intracellularly probably as a result of intense Cx43 turnover and moreover that some of the fragments were primarily located in the nuclei. This raises the question of their potential role (other than cell-cell communication) in effecting malignancy levels. The most malignant cell line showed a complete lack of intercellular communication whereas the least malignant cell line possesses open hemichannels on its plasma membranes.

Inhibition of the ERK-MAPK pathway in U-251 MG cells showed a partial transfer of the Cx43 to the membrane, thus restoring a normal localization. The same treatment triggered an increase in Cx43 expression and phosphorylation in U-87 MG cells. Also, the inhibition of PKC, PKA and ERK-MAPK affected Cx43 fragments in various ways dependent on the cell line and the phosphorylation site observed. This suggests a role of these pathways in the degradation of Cx43 in our cell models.

Furthermore, the flavanoid morin was shown to increase phosphorylation of Cx43 on Ser-262 in U-251 MG cells. This increase was attributed partly to the inhibition of the p38 MAPK pathway.

Finally, it was demonstrated that Cx43 does not co-localize with caveolin-1 inside caveolae structures at least in the astrocytoma cell lines. This absence of interaction could be associated with the aberrant Cx43 localization in our cell models.

Taken together, these results show interesting possibilities in regards to Cx43 restoration of function in human astrocytoma. Whether it is by increasing Cx43 expression or restoring normal membrane localization, drugs could be targeted to achieve these results in human astrocytoma in an effort to possibly revert to a more normal phenotype. More detailed studies based on our findings are needed in order to assess and complete our results.

6.0 REFERENCES

Ahmad, S., Mineta, T., Martuza, R.L. and Glazer, R.I. (1994) Antisense expression of protein kinase Cα inhibits the growth and tumorigenicity of human glioblastoma cells. Neurosurgery. 35, 904-908.

Ahmad, S., Diez, J.A., George, C.H. and Evans, W.H. (1999) Synthesis and assembly of connexins *in vitro* into homomeric and heteromeric functional gap junction hemichannels. Biochem. J. 339, 247-253.

Andrade-Rozental, A.F., Rozental, R., Hopperstad, M.G., Wu, J.K., Vrionis, F.D. and Spray, D.C. (2000) Gap junctions: the "kiss of death" and the "kiss of life". Brain Research Reviews. 32, 308-315.

Arnold, J.M., Phipps, M.W., Chen, J. and Phipps, J. (2005) Cellular sublocalization of Cx43 and the establishment of functional coupling in IMR-32 neuroblastoma cells. Molecular Carcinogenesis. 42, 159-169.

Atkinson, M.M., Lampe, P.D., Lin, H.H., Kollander, R., Li, X-R. And Kiang, D.T. (1995) Cyclic AMP modifies the cellular distribution of connexin43 and induces a persistent increase in the junctional permeability of mouse mammary tumor cells. J. Cell Sci. 108, 3079-3090.

Beardslee, M.A., Laing, J.G., Beyer, E.C. and Saffitz, J.E. (1998) Rapid turnover of connexin43 in the adult rat heart. Circ. Res. 83, 629-635.

Bennett, M.V.L. (1994) Connexins in disease. Nature. 368, 18-19.

Berthoud, V.M., Beyer, E.C. and Seul, K.H. (2000) Peptide inhibitors of intercellular communication. Am. J. Physiol. Lung Mol. Physiol. 279, L619-622.

Berthoud, V.M., Minogue, P.J., Laing, J.G. and Beyer, E.C. (2003) Pathways for degradation of connexins and gap junctions. Cardiocascular Reasearch. 62, 256-267.

Besson, A. and Yong, V.W. (2001) Mitogenic signaling and the relationship to cell cycle regulation in astrocytomas. Journal of Neuro-oncology. 51, 245-264.

Birt, D.F. and Bresnick, E. (1990) Chemoprevention by non-nutrient components of vegetables and fruits. Cancer and Nutrition. 7, 221-260.

Breitkreutz, D., Braiman-Wiksman, L., Daum, N., Denning, M.F. and Tennenbaum, T. (2007) Protein Kinase C family: on the crossroads of cell signaling in skin and tumor epithelium. J. Cancer Res. Clin. Oncol. 133, 793-808.

Brissette, J.L., Kumar, N.M., Gilula, N.B. and Dotto, G.P. (1991) The tumor promotor 12-O-tetradecanoylphorbol-13-acetate and the *ras* oncogene modulate expression and phosphorylation of gap junction proteins. Molecular and Cellular Biology. 11, 5364-5371.

Britz-Cunningham, S.H., Shah, M.M., Zuppan, C.W. and Fletcher, W.H. (1995) Mutations of the connexin43 gap junction gene in patients with heart malformations and defects of laterality. New England Journal of Medicine. 33, 1323-1329.

Brown, J., O'Prey, J. and Harrison, P.R. (2003) Enhanced sensitivity of human oral tumours to the flavanol, morin, during cancer progression: involvement of the Akt and stress kinase pathways. Carcinogenesis. 24, 171-177.

Burgermeister, E., Xing, X., Röcken, C., Juhasz, M., Chen, J., Hiber, M., Mair, K., Shatz, M., Liscovitch, M., Schmid, R.M. and Ebert, M.P. (2007) Differential expression and function of caveolin-1 in human gastric cancer progression. Cancer Research. 67, 8519-8526.

Cesen-Cummings, K., Fernesto, M.J., Malkinson, A.M. and Ruch, R.J. (1998) Frequent reduction of gap junctional intercellular communication and connexin43 expression in human and mouse lung carcinoma cells. Carcinogenesis. 19, 61-67.

Chipman, J.K., Mally, A. and Edwards, G.O. (2002) Disruption of gap junctions in toxicity and carcinogenicity. Toxological Sciences. 71, 146-153.

Chu, F-F. and Doyle, D. (1985) Turnover of plasma membrane proteins in rap hepatoma cells and primary cultures of rat hepatocytes. J. Cell Biol. 260, 3097-3107.

Crow, D.S., Beyer, E.C., Paul, D.L., Kobe, S.S. and Lau, A.F. (1990) Phosphorylation of connexin43 gap junction protein in uninfected and Rous sarcoma virus-tranformed mammalian fibroblasts. Mol. Cell. Biol. 10, 1754-1763.

Cruciani, V. and Mikalsen, S-O. (2002) Connexins, gap junctional intercellular communication and kinases. Biology of the Cell. 94, 433-443.

Czyz, J. (2008) The stage-specific function of gap junctions during tumourigenesis. Cell. Mol. Biol. Lett. 13, 92-102.

Dang, X., Doble, B.W. and Kardami, E. (2003) The carboxy-tail of connexion-43 localizes to the nucleus and inhibits cell growth. Mol. Cell. Biochem. 242, 35-38.

Darrow, B.J., Fast, V.G., Kleber, A.G., Beyer, E.C. and Saffitz, J.E. (1996) Functional and structural assessment of intercellular communication. Increased conduction velocity and enhanced connexin expression in dibutyryl cAMP-treated cultured cardiac myocytes. Circ. Res. 79, 174-183.

Davies, S.P., Reddy, H., Caivano, M. and Cohen, P. (2000) Specificity and mechanism of action of some commonly used protein kinase inhibitors. Biochem. J. 351, 95-105.

Dbouk, H.A., Mroue, R.M., El-Sabban, M.E. and Talhouk, R.S. (2009) Connexins: a myriad of functions extending beyond assembly of gap junction channels. Cell Cummun Signal. 7, 1-17.

Deschenes, S.M., Walcott, J.L., Wexler, T.L., Scherer, S.S. and Fishbeck, K.H. (1997) Altered trafficking of mutant Cx32. J. Neurosci. 17, 9077-9084.

Desplantez, T., Dupont, E., Severs, N.J. and Weingart, R. (2007) Gap junction channels and cardiac impulse propagation. J. Membr. Biol. 218, 13-28.

Diez, J.A., Ahmad, S. and Evans, W.H. (1999) Assembly of heteromeric connexons into guinea-pig liver en route to the Golgi apparatus, plasma membrane and gap junctions. Eur. J. Biochem. 262, 142-148.

Dunham, B., Liu, S., Taffet, S., Trabka-Janik, E., Delmar, M., Petryshyn, R., Zheng, S. and Vallano, M. (1992) Immunolocalization and expression of functional and nonfunctional cell-to-cell channels from wild-type and mutant rat heart connexin43 cDNA. Circ. Res. 70, 1233-1243.

Esen, N., Shuffield, D., Syed, M.M. and Kielian, T. (2007) Modulation of connexin expression and gap junction communication in astrocytes by the gram-positive bacterium S. aureus. Glia. 55, 104-117.

Evans, W.H. and Boitano, S. (2001) Connexin mimetic peptides: specific inhibitors of gap-junctional intercellular communication. Biochmical Society Transactions. 29, 606-612.

Evans, W.H., De Vuyst, E. And Leybaert, L. (2006) The gap junction cellular internet: connexin hemichannels enter the signaling limelight. Biochem. J. 397, 1-14.

Falk, M.M. (2000) Biosynthesis and structural composition of gap junction intercellular channels. European Journal of Cell Biology. 79, 584-574.

Falk, M.M., Kumar, N.M. and Gilula, N.B. (1994) Membrane insertion of gap junction connexins: polytopic channel forming membrane proteins. Journal of Cell Biology. 127, 343-355.

de Feijter, A.W., Matesic, D.F., Ruch, R.J., Guan, X., Chang, C.C. and Trosko, J.E. (1996) Localization and function of the connexin 43 gap-junction protein in normal and various oncogene-expressing rat liver epithelial cells. Mol. Carcinog. 16, 203-212.

Fishman, G.I., Moreno, A.P., Spray, D.C. and Leinwand, L.A. (1991) Functional analysis of human cardiac gap junction channel mutants. Proc. Natl. Acad. Sci. USA. 88, 3525-3529.

George, C.H., Kendall, J.M., Campbell, A.K. and Evans, W.H. (1998) Connexin-aqueorin chimerase report cytoplasmic calcium environments along trafficking pathways leading to gap junction biogenesis in living COS-7 cells. J. Biol. Chem. 273, 29822-29829.

George, C.H., Kendall, J.M. and Evans, W.H. (1999) Intracellular trafficking pathways in the assembly of connexins into gap junctions. J. Biol. Chem. 274, 8678-8685.

Goldberg, G.S., Beachberger, J.F., tajima, Y., Merritt, M., Omori, Y., Gawinowica, M.A., Narayanan, R., Tan, Y., Sanai, Y., Yamasaki, H., Naus, C., Tsuda, H.- and-Nicholson, B.J. (2000) Connexin43 suppresses MFG-E8 while inducting contact growth inhibition of glioma cells. Cancer Research. 60, 6018-6026.

Goodenough, D.A. and Paul, D.L. (2003) Beyond the gap: functions of unpaired connexon channels. Nature Reviews in Molecular Cell Biology. 4, 1-10.

Gurney, J.G. and Kadan-Lottick, N. (2001) Brain and other central nervous system tumors: rates, trends, and epidemiology. Curr. Opin. Oncol. 13, 160-166.

Gutcher, I., Webb, P.R. and Anderson, N.G. (2003) The isoform-specific regulation of apoptosis by protein kinase C. Cell Mol. Life Sci. 60, 1061-1070.

Hossain, M.Z., Ao, P. and Boynton, A.L. (1998) Platelet-derived growth factor-induced disruption of gap junctional communication and phosphorylation of connexin43 involves protein kinase C and mitogen-activated protein kinase. J. Cell. Physiol. 174, 66-77.

Hossain, M.Z., Jagdale, A.B., Ao, P. And Boynton, A.L. (1999a) Mitogen-activated protein kinase and phosphorylation of connexin43 are not sufficient for the disruption of gap junctional communication by platelet-derived growth factor and tetradecanoylphorbol acetate. J. Cell. Physiol. 179, 87-96.

Hossain, M.Z., Jagdale, A.B., Ao, P., Kazlauskas, A. and Boynton, A.L. (1999b) Disruption of gap junctional communication by the platelet-derived growth factor is mediated via multiple pathways. J. Biol. Chem. 274, 10489-10496.

Hossain, M.Z. and Boynton, A.L. (2000) Regulation of cx43 gap junctions: the gatekeeper and the password. Science's STKE. 54, PE1-5.

Hsiang, C-Y., Wu, S-L. and Ho, T-Y. (2005) Morin inhibits 12-*O*-tetradecanoylphorbol-13-acetate induced hepatocellular transformation via activator protein 1 signaling pathway and cell cycle progression. Biochemical Pharmacology. 69, 1603-1611.

Huang, R-P., Hossain, M.Z., Huang, R., Gano, J., Fan, Y. And Boynton, A.I. (2001) Connexin 43 (CX43) enhances chemotherapy-induced apoptosis in human glioblastoma cells. Int. J. Cancer. 92, 130-138.

Huang, R., Lin, Y., Wang, C.C., Gano, J., Lin, B., Shi, Q., Boynton, A., Burke, J. and Huang, R-P. (2002) Connexin 43 Suppresses Human Glioblastoma Cell Growth by Down-Regulation of Monocyte Chemotactic Protein 1, as Discovered Using Protein Array Technology. Cancer Research. 62, 2806-2812.

Hulleman, E. and Helin, K. (2005) Molecular machanisms in gliomagenesis. Advances in cancer research. 1-27.

Jagannathan, J., Prevedello, D.M., Dumont, A.S. and Laws, E.R. (2006) Cellular signaling molecules as therapeutic targets in glioblastoma multiforme. Neurosurg. Focus. 20, 1-7.

Jongsma, H.J., van Rijen, H.M.V., Kwak, B.R. and Chanson, M. (2000) Phosphorylation of connexins: consequences for permeability, conductance, and kinetics of gap junction channels. Current topics in Membranes. 49, 131-143.

Jordan, K., Solan, J.L., Dominguez, M., Sia, M., Hand, A., Lampe, P.D. and Laird, D.W. (1999) Trafficking, assembly, and function of a connexin43-green fluorescent protein chimera in live mammalian cells. Molecular Biology. 10, 2033-2050.

Kanemitsu, M.Y. and Lau, A.F. (1993) Epidermal growth factor stimulates the disruption of gap junctional communication and connexin43 phosphorylation independent of 12-tetradecanoylphorbol-13-acetate-sensitive protein kinase C: the possible involvement of mitogen-activated protein kinase. Mol. Biol. Cell. 4, 837-848.

Kanemitsu, M.Y., Loo, L.W.M., Simon, S., Lau, A.F. and Eckhart, W. (1997) Tyrosine phosphorylation of connexin43 by v-Src is mediated by SH2 and SH3 domain interactions. J. Biol. Chem. 272, 22825-22831.

Kelseel, D.P., Dunlop, J. and Hodgins, M.B. (2001) Human diseases: clues to cracking the connexin code? Trends in Cell Biology. 11, 2-6.

Kim, D.Y., Kam, Y., Koo, S.K. and Joe, C.O. (1999) Gating connexin 43 channels reconstituted in lipid vesicles by mitogen-activated protein kinase phosphorylation. J. Biol. Chem. 274, 5581-5587.

King, T.J. and Lampe, P.D. (2005) Temporal regulation of connexin phosphorylation in embryonic and adult tissues. Biochim. Biophys. Acta. 1719, 24-35.

Knight, M.M., McGlashan, S.R., Garcia, M., Jensen, C.G. and Poole, C.A. (2009) Articular chondrocytes express connexin 43 hemichannels and P2 receptors - a putative mechanoreceptor complex involving the primary cilium? J. Anat. 214, 275-283.

Krajewska, W.M. and Maslowska, I. (2004) Caveolins: structure and function in signal transduction. Cellular and molecular biology letters. 9, 195-220.

Kumar, N.M. and Gilula, N.B. (1996) The gap junction communication channel. Cell. 84, 381-388.

Laing, J.G. and Beyer, E.C. (1995) The gap junction protein connexin43 is degraded via the ubiquitin proteasome pathway. J. Biol. Chem. 270, 26399-26403.

Laing, J.G., Tadros, P.N., Westphale, E. and Beyer, E.C. (1997) Degradation of connexin43 gap junctions involves both the proeasome and the lysosome. Experimental Cell Research. 236, 482-492.

Laird, D.W. (2006) Life cycle of connexins in health and disease. Biochem. J. 394, 527-543.

Laird, D.W. (2005) Connexin phosphorylation as a regulatory event linked to gap junction internalization and degradation. Biochimica et Biocphysica Acta. 1711, 172-182.

Laird, D.W. (1996) The life cycle of connexin: gap junction formation, removal, and degradation. Journal of Bioenergetics and Biomembranes. 28, 311-318.

Laird, D.W., Castillo, M. and Kasprzak, L. (1995) Gap junction turnover, intracellular trafficking, and phosphorylation of connexin43 in brefeldin A-treated rat mammary tumor cells. J. Cell Biol. 131, 1193-1203.

Lajoie, P., Goetz, J.G., Dennis, J.W. and Nabi, I.R. (2009) Lattices, rafts, and scaffolds: domain regulation of receptor signaling at the plasma membrane. J Cell Biol. 185, 381-385.

Lampe, P.D. and Lau, A.F. (2000) Regulation of gap junctions by phosphorylation of connexins. Archives of Biochemistry and Biophysics. 384, 205-215.

Lampe, P.D., TenBroek, E.M., Burt, J.M., Kurata, W.E., Johnson, R.G. and Lau, A.F. (2000) Phosphorylation of connexin43 on serine-368 by protein kinase C regulates gap jucntional communication. J. Cell Biol. 149, 1503-1512.

Lampe, P.D. and Lau, A.F (2004) The effects of connexin phosphorylation on gap jucntional communication. The International Journal of Biochemistry and Cell Biology. 36, 1171-1186.

Langlois, S., Cowan, K.N., Shao, Q., Cowan, B.J. and Laird, D.W. (2008) Caveolin-1 and -2 interact with connexin43 and regulate gap junctional intercellular communication in keratinocytes. Mol Biol Cell. 19, 912-928.

Lau, A.F., Warn-Cramer, B. and Lin, R. (2000) Regulation of connexin43 by tyrosine protein kinases. Current Topics in Membranes. 49, 315-341.

Lauf, U., Giepmans, B.N.G., Lopez, P., Braconnot, S., Chen, S-C. and Falk, M.M. (2002) Dynamic trafficking and delivery of connexons to the plasma membrane and accretion to gap junctions in living cells. PNAS. 99, 10446-10451.

Leithe, E. and Rivedal, E. (2004) Epidermal growth factor regulates ubiquitination, internalization and proteasome-dependent degradation of connexin43. Journal of Cell Science. 117, 1211-1220.

Leithe, E. and Rivedal, E. (2007) Ubiquitination of gap junction proteins. J. Membr. Biol. 217, 43-51.

Levin, M. (2007) Gap junctional communication in morphogenesis. Progress in Biophysics and Molecular Biology. 94, 186-206.

Li, C., Liu, X., Lin, X. and Chen, X. (2009) Structure-activity relationship of 7 flavonoids on recombinant human protein kinase CK2 holoenzyme. Zhong Nan Da Xue Xue Bao Yi Xue Ban. 34, 20-26.

Lin, D., Zhou, J., Zelenka, P.S. and Takemoto, D.J. (2003) Protein kinase Cγ regulation of gap junction activity through caveolin-1-containing lipid rafts. Investigative Ophtamology and Visual Science. 44, 5259-5268.

Lissandron, V. and Zaccolo, M. (2006) Compartmentalized cAMP/PKA signaling regulates cardiac excitation-contraction coupling. J. Muscle Res. Cell Motil. 27, 399-403.

Loewenstein, W.R. (1966) Permeability of membrane junctions. N.Y. Acad. Sci. 137, 441-472.

Loewenstein, W.R. and Rose, B. (1992) The cell-cell channel in the control of growth. Semin. Cell Biol. 3, 59-79.

Lokker, N.A., Sullivan, C.M., Hollenbach, S.J., Israel, M.A. and Giese, N.A. (2002) Platelet-derived growth factor (PDGF) autocrine signaling regulates survival and mitogenic pathways in glioblastoma cells: evidence that the novel PDGF-C and PDGF-D ligands may play a role in the development of brain tumors. Cancer Research. 62, 3729-3735.

Mackay, H.G. and Twelves, C.G. (2007) Targeting the Protein Kinase C family: are we there yet? Nature Reviews in Cancer. 7, 554-562.

Maher, E.A., Furnari, F.B., Bachoo, R.M., Rowitch, D.H., Louis, D.N., Cavence, W.K. and DePinho, R.A. (2001) Malignant gliomas: genetics and biology of a grave matter. Genes Dev. 15, 1311-1333.

Martin, P.E.M., Mambetisaeva, E.T., Archer, D.A., George, C.H. and Evans, W.H. (2000) Analysis of gap junction assembly using mutated connexins detected in Charcot-Marie-Tooth X-linked disease. Journal of Neurochemistry. 74, 711-720.

Martin, P.E.M., Blundell, G., Ahmad, S., Errington, R.J. and Evans, W.H. (2001) Multiple pathways in the trafficking and assembly of connexin26, 32 and 43 into gap junction intercellular communication channels. Journal of Cell Science. 114, 3845-3855.

Martin P.E.M. and Evans, W.H. (2004) Incorporation of connexins into plasma membranes and gap junctions. Cardiovascular Research. 62, 378-387.

Mellor, H. and Parker, P.J. (1998) The extended protein kinase C family. Biochem. J. 332, 281-292.
Mese G., Richard, G. and White, T.W. (2007) Gap junctions: basic structure and function. Journal of Investigative Dermatology. 127, 2516-2524.

Mesnil, M. (2002) Connexins and cancer. Biology of the Cell. 94, 493-500.

Mesnil, M. (2004) Jonctions communicantes et cancer: implications et perspectives. Medecine/sciences. 20, 197-206.

Mesnil, M., Crespin, S., Avanzo, J-L. and Zaidan-Dagli, M-L. (2005) Defective gap junctional intercellular communication in the carcinogenic process. Biochimica et Biophysica Acta. 1719, 125-145.

Miranda, M.A., Okamoto, A.K., Ferreira, C.V., Silva, T.L., Granjeiro, J.M. and Aoyama, H. (2006) Differential effects of flavonoids on bovine kidney low molecular mass protein tyrosine phosphatase. J. Enzyme Inhib. Med. Chem. 21, 419-425.

Moorby, C. and Patel, M. (2001) Dual functions of connexins: Cx43 regulates growth independently of gap junction formation. Experimental Cell Research. 271, 238-248.

Moore, J.C., Tsang, S.Y., Rushing, S.N., Lin, D., Tse, H.F., Chan, C.W. and Li, R.A. (2008) Functional consequences of overexpressing the gap junction Cx43 in the cardiogenic potential of pluripotent human embryonic stem cells. Biochem Biophys Res Commun. 377, 46-51.

Moreno, A.P., Saez, J.C., Fishman, G.I. and Spray, D.C. (1994) Human connexin43 gap junction channels. Regulation of unitary conductances by phosphorylation. Circ. Res. 74, 1050-1057.

Moreno, A.P. (2005) Connexin phosphorylation as a regulatory event linked to channl gating. Biochimica et Biophysica Acta. 1711, 164-171.

Musil, L.S. and Goodenough, D.A. (1991) Biochemical analysis of connexin43 intracellular transport, pohsphorylation, and assembly into gap junction plaques. J. Cell Biol. 115, 1357-1374.

Musil, L.S. and Goodenough, D.A. (1993) Multisubunit assembly of an integral plasma membrane channel protein, gap junction connexin43, occurs after exit from the ER. Cell. 74, 1065-1077.

Musil, L.S., Le, A-C.N., VanSlyke, J.K. and Roberts, L.M. (2000) Regulation of connexin degradation as a mechanism to increase gap junction assembly and function. J. Biol. Chem. 275, 25207-25215.

Nakase, T. and Naus, C.C.G. (2004) Gap junctions and neurological disorders of the central nervous system. Biochimica et Biophysica Acta. 1662, 149-158.

Naus, C.C.G., Elisecich, K., Zhou, D., Beliveau, D.J. and Del Maestro, R.F. (1992) In vivo growth of C6 glioma cells transfected with connexin43 cDAN. Cancer Research. 52, 4208-4213.

Phipps M., Phipps J., Whitfield J.F., Ally A. and Narang R.L. (1990) Carcinogenesis implications of the neighbourhood coherence principle (NCP). Medical hypothesis. 31, 289-301.

Phipps M., Daroszewski J. and Phipps J. (1997) How the neighbourhood coherence principle (NCP) can give rise to tissue homeostasis: a cellular automation approach. Journal of theoretical biology. 185, 475-485.

Plotkin, L.I., Manolagas, S.C. and Bellido, T. (2002) Transduction of cell survival signals by connexin-43 hemichannels. Journal of Biological Chemistry. 277, 8648-8657.

Pu, P., Xia, Z., Yu, S. and Huang, Q. (2004) Altered expression of Cx43 in astrocytic tumors. Clinical Neurology and Neurosurgery. 107, 49-54.

Qin, H., Shao, Q., Curtist, H., Galipeau, J., Belliveau, D.J., Wang, T., Alaoui-Jamali, M.A. and Laird, D.W. (2002) Retroviral delivery of connexin genes to human breast tumor cells inhibits *in vivo* tumor growth by a mechanism that is independent of significant gap junctional intercellular communication. Journal of Biological chemistry. 277, 29132-29138.

Qin, H., Shao, Q., Igdouras, S.A., Moulay, A.A-J. and Laird, D.W. (2003) Lysosomal and proteasomal degradation play distinct roles in the life cycle of Cx43 in gap junctional intercellular communication-deficient and –competent breast tumor cells. The Journal of Biological Chemistry. 278, 30005-30014.

Quist, A.P., Rhee, S.K., Lin, H. and Lal, R. (2000) Physiological role of gap-junctional hemichannels: extracellular calcium-dependent isosmotic volume regulation. Journal of Cell Biology. 148, 1063-1074.

Rabadan-Diehl, C., Dahl, G. and Werner, R. (1994) A connexin-32 mutation associated with Charcot-Marie-Tooth disease does not affect channel formation in oocytes. FEBS Lett. 351, 90-94.

Reardon, D.A., Rich, J.N., Friedman, H.S. and Bigner, D.d. (2006) Recent advances in the treatment of malignant astrocytoma. Journal of Clinical oncology. 24, 1253-1265.

Roger, C., Mograbi, B., Chevalier, D., Michiels, J.F., Tanaka, H., Segretain, D., Points, G. And Fenichel, P. (2004) Disrupted traffic of connexin 43 in human testicular seminoma cells: overexpression of Cx43 induces membrane location and cell proliferation decrease. J. Pahtol. 202, 241-246.

Rahman, S., Carlir, G. and Evans, W.H. (1993) Assembly of hepatic gap junctions. J. Biol. Chem. 268, 1260-1265.

Rose, B., Mehta, P.P. and Loewenstein, W.R. (1993) Gap junction protein gene suppresses tumorigenicity. Carcinogenesis. 14, 1073-1075.

Saez, J.C., Nairm, A.C., Czernik, A.J., Fishman, G.I., Spray D.C. and Hertzberg, E.L. (1997) Phosphorylation of connexin43 and the regulation of neonatal rat cardiac myocyte gap junctions. J, Mol. Cell Cardiol. 29, 2131-2145.

Saffitz, J.E., Laing, J.G. and Yamada, K.A. (2000) Connexin expression and turnover. Circ. Res. 86, 723-728.

Sanchez-Alvarez, R., Tabernero, A., Sanchez-Abarca, L.I., Orfao, A., Giaume, C. and Medina, A. (2001) Proliferation of C6 glioma cells is blunted by the increase in gap junction communication caused by tolbutamide. FEBS Letters, 509, 202-206.

Reddy, C.S. (2005) Alterations in Protein Kinase A signaling and cleft palate: a review. Human and Experimental Toxicology. 24, 235-242.

Rivedal, E. and Opsahl, H. (2001) Role of PKC and MAP kinase in EGF- and TPA-induced connexin43 phosphorylation and inhibition of gap junction intercellular communication in rat liver epithelial cells. Carcinogenesis. 22, 1543-1550.

Roberts, P.J. and Der, C.J. (2007) Targeting the Raf-MEK-ERK mitogen-activated protein kinase cascade for the treatment of cancer. Oncogene. 26, 3291-3310.

Safakhoo, S. (2007) Sous-localisation de la connexin 43 dans les cellules de neuroblastomes: les mécanismes responsables. M. Sc. thesis submitted at the Institut Armand-Frappier, Université du Québec.

Salameh, A. and Dhein, S. (2005) Pharmacology of gap junctions. New pharmacological targets for treatment of arrhythmia, seizure and cancer. Biochimica et Biophysica Acta. 1719, 36-58.

Santos, A., Calvet, L., Terrier-Lacombe, M-J., Larsen, A., Bénard, J., Pondarré, C., Aubert, G., Morizet, J., Lavelle, F. and Vassal, G. (2004) *In Vivo* Treatment with CPT-11 Leads to Differentiation of Neuroblastoma Xenografts and Topoisomerase I Alterations . Cancer Research. 64, 3223-3229.

Schubert, A-L., Schubert, W., Spray, D.C. and Lisanti, M.P. (2002) Connexin family members target to lipid raft domains and interact with caveolin-1. Biochmistry. 41, 5754-5764.

Schulze, A., Nicke, B., Warne, P.H., Tomlinson, S. and Downward, J. (2004) The transcriptional response to Raf activation is almost completely dependent on mitogen-activated protein kinase kinase activity and shows a major autocrine component. Mol. Biol. Cell. 15, 3450-3463.

Schweizer, A., Fransen, J.A., Matter, K., Kreis, T.F., Ginsel, L. and Hauri, H.P. (1990) Identification of an intermediate compartment involved in protein transport from endoplasmic reticulum to Golgi apparatus. Eur. J. Cell. Biol. 53, 185-196.

Seino, S. and Shibasaki, T. (2005) PKA-dependent and PKA-independent pathaways for cAMP-regulated exocytosis. Physiol. Rev. 85, 1303-1342.

Segretain, D.and Falk, M.M. (2004) Regulation of connexin biosynthesis, assembly, gap junction formation, and removal. Biochimica et Biophysica Acta. 1662, 3-21.

Severs, N.J., Shovel, K.S., Slade, A.M., Powell, T., Twist, V.W. and Green, C.R. (1989) Fate of gap junctions in isolated adult mammalian cardiomyocytes. Circ. Res. 65, 22-42.

Shen, Y., Khusial, P.R., Li, X., Ichikawa, H., Moreno, A.P. and Goldberg, G.S. (2007) Src utilizes cas to block gap junctional communication mediated by connexin43. J. Boil. Chem. 282, 18914-18921.

Shinoura, N., Chen, L., Wani, M.A., Kim, Y.G., Larson, J.J., Warnick, R.E., Simon, M., Menon, A.G., Bi, W.L. and Stambrook, P.J. (1996) Protein and messenger RNA expression of connexin43 in astrocytomas: implications in brain tumor gene therapy. J. Neurosurg. 84, 839-846.

Smart, E.J., Ying, Y-S., Mineo, C. And Anderson, R.G.W. (1995) A detergent-free method for purifying caveolae membrane from tissue culture cells. Proc. Natl. Acad. Sci. USA. 92, 10104-10108.

Solan, J.L. and Lampe, P.D. (2005) Connexin phosphorylation as a regulatory event linked to gap junction channel assembly. Biochimica et Biophysica Acta. 1711, 154-163.

Solan, J.L. and Lampe, P.D. (2007) Key Connexin 43 Phosphorylation Events Regulate the Gap Junction Life Cycle. J Membrane Biol. 217, 35-41.

Solan, J.L. and Lampe, P.D. (2009) Connexin43 phosphorylation: structural changes and biological effects. Biochem. J. 419, 261-272.

Sorgen, P.L., Duffy, H.S., Sahoo, P., Coombs, W., Delmari, M. and Spray, D.C. (2004) Structural changes in the carboxyl terminus of the gap junction protein connexin43 indicates signaling between binding domains for c-src and zonula occludens-1. The Journal of Biological Chemistry. 279, 54695-54701.

Soroceanu, L., Manning Jr, T.G. and Sontheimer, H. (2001) Reduced expression of connexin-43 and functional gap junction coupling in human gliomas. Glia. 33, 107-117.

Spencer, J.P. (2008) Flavonoids: modulators of brain function? Br J Nutr. 99, ES60-77.

Spray, D.C., Moreno, A.P., Kessler, J.A. and Dermietzel, R. (1991) Characterization of gpa junctions between cultured leptomeningeal cells. Brain Res. 568, 1-14.

Stout, C., Goodenough, D.A. and Paul, D.L. (2004) Connexins: functions withoug junctions. Current opinion in cell biology. 16, 507-512.

Tagliaferri, F., Teodori, L., Valente, M.G., Stipa, F., Cucina, A., Göhde, W., Coletti, D., Alo, P. and Stipa, S. (1999) In vitro proliferation and in vivo malignancy of cell lines simultaneously derived from a chemically-induced heterogeneous rat mammary tumor. In Vitro Cellular and Developmental Biology-Animal. 36, 163-166.

TenBroek, E.M., Lampe, P.D., Solan, J.L., Reynhout, J.K. and Johnson, R.G. (2001) Ser364 of connexin43 and the upregulation of gap junction assembly by cAMP. J. Cell Biol. 155, 1307-1318.

Thomas, M.A., Huang, S., Cokoja, A., Riccio, O., Staub, O., Suter, S. and Chanson, M. (2002) Interaction of connexins with protein partners in the control of channel turnover and gating. Biology of the Cell. 94, 445-456.

Traub, O., Look, J., Paul, D. and Willecke, K. (1987) Cyclic adenosine monophosphate stimulates biosynthesis and phosphorylation of the 26 kDa gap junction protein in cultured mouse hepatocytes. J. Cell Biol. 43, 48-54.

Trosko, J.E. and Ruch, R.J. (1998) Cell-cell communication in carcinogenesis. Frontiers in Bioscience. 3, d208-236.

Unger, V.M., Kumar, N.M., Gilula, N.B. and Yeager, M. (1999) Three-dimensional structure of a recombinant gap junction membrane channel. Science. 283, 1176-1180.

Warn-Cramer, B.J., Lampe, P.D., Kurata, W.E., Kanemistu, M.Y., Loo, L.W.M., Eckhart, W. and Lau, A.F. (1996) Characterization of the mitogen-activated protein kinase phosphorylation sites on the connexin43 gap junction protein. J. Biol. Chem. 271, 3779-3786.

Warn-Cramer, B.J., Cottrel, G.T., Burt, J.M. and Lau, A.F. (1998) Regulation of connexin-43 gap junctional intercellular communication by mitogen-activated protein kinase. J. Biol. Chem. 273, 9188-9196.

Warn-Cramer, B.J. and Lau, A.F. (2004) Regulation of gap junction by tyrosine kinases. Biochimica et Biophysica Acta. 1662, 81-95.

Yamasaki, H. (1990) Gap junctional intercellular communication and carcinogenesis. Carcinogenesis. 11, 1051-1058.

Yogo, K., Ogawa, T., Akiyama, M., Ishida-Kitagawa, N., Sasada, H., Sato, E. and Takeya, T. (2006) PKA implicated in the phosphorylation of Cx43 induced by stimulation with FSH in rat granulosa cells. Journal of Reproduction and Development. 52, 321-328.

Zhang, D., Kaneda, M., Nakahama, N-I., Arii, S. and Morita, I. (2007) Connexin 43 expression promotes malignancy of HuH7 hepatocellular carcinoma cells via the inhibition of cell–cell communication. Cancer Letters. 252, 208-215.

Zhang, H., Links, P.H., Ngsee, J.K., Tran, K., Cui, Z., Ko, K.W.S. and Yao, Z. (2004) Localization of low density lipoprotein receptor-related protein 1 to caveolae in 3T3-L1 adipocytes in response to insulin treatment. The Journal of Biological Chemistry. 279, 2221-2230.

Zhang, Y-W., Kaneda, M. And Morita, I. (2003a) The gap junction-independent tumor-suppressing effect of connexin-43. The Journal of Biological Chemistry. 278, 44852-44856.

Zhang, Y-W., Nakayama, K., akayama, K-I. And Morita, I. (2003b) A novel route for Connexin 43 to inhibit cell proliferation: negative regulation of S-phase kinase-associated protein (Skp2). Cancer Research. 63, 1623-1630.

Zhang, Q., Furukawa, K., Chen, H.H., Fujinawa, R., Kozutsumi, Y., Suzuki, A. and Urano, T. (2006) Down-regulation of caveolin-1 in mouse Lewis lung cancer P29 is a causal factor for the malignant properties in a high-metastatic subline. Oncol. Rep. 16, 289-294.

Zhu, D., Cavaney, S., Kidder, G.M. and Naus, C.C.G. (1991) Transfection of C6 glioma cells with connexin43 cDNA: analysis of expression, intercellular coupling, and cell proliferation. Proc. Natl. Acad. Sci. USA. 88, 1883-1887.

Zschocke, J., Bayatti, N. and Behl, C. (2004) Caveolin and GLT-1 gene expression is reciprocally regulated in primary astrocytes: Association of GLT-1 with non-caveolar lipid rafts. Glia. 49, 275-287.

APPENDIX

Figure 34. Nonspecific binding of alkaline phosphatase-conjugated secondary antibody.

U-251 MG and U-87 MG proteins were electrophoretically separated on 10% SDS-PAGE and transferred to a nitrocellulose membrane, as described in the Materials and Methods. The membrane was probed with an alkaline phosphatase-conjugated anti-rabbit secondary antibody in the absence of any primary antibody. The only band present is a doublet at 24 kDa which is more visible in the U-251 than the U-87 cells.

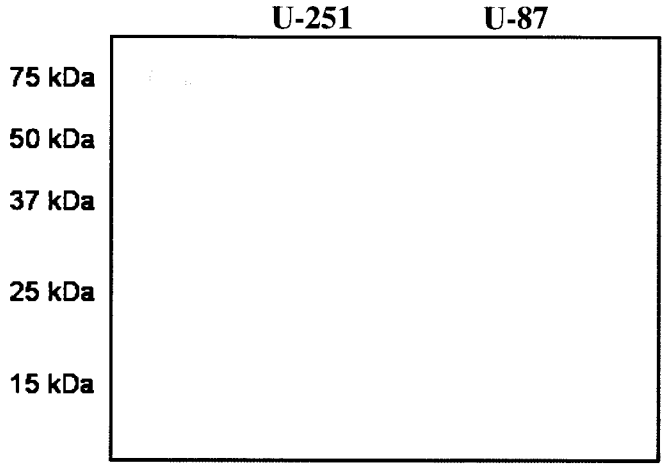
U-251
U-87
75 kDa
50 kDa
37 kDa
25 kDa
15 kDa

Figure 35. Nonspecific binding of secondary antibodies, AlexaFluor 488nm and 647 nm.

U-251 cells were fixed in 4% paraformaldehyde, permeabilized with 0.1% Triton X-100, and probed with AlexaFluor 488nm anti-rabbit and AlexaFluor 647nm anti-mouse in the absence of any primary antibodies. Reverse phase images also shown. Images were taken at 10x magnification.

	Secondary Antibody only	Reverse Phase
AlexaFluor 488nm (anti-rabbit)		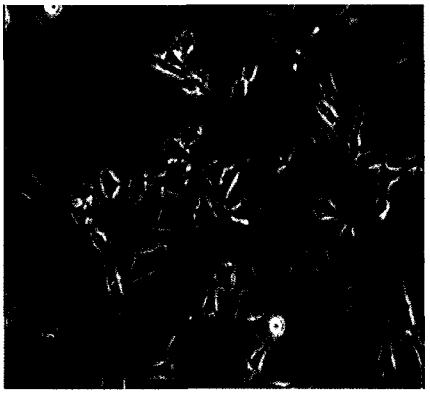
AlexaFluor 647nm (anti-mouse)